The Pennsylvania State University
The Graduate School
Eberly College of Science

SYNCHRONIZATION OF CHAOTIC SYSTEMS

A Thesis in
Mathematics
by
Krešimir Josić

Submitted in Partial Fulfillment
of the Requirements
for the Degree of

Doctor of Philosophy

August 1999

We approve the thesis of Krešimir Josić.

Date of Signature

Nigel Higson
Professor of Mathematics
Co-Chair of Committee

C. Eugene Wayne
Professor of Mathematics
Co-Chair of Committee
Thesis Adviser

Yakov B. Pesin
Professor of Mathematics

Andrew G. Clark
Professor of Biology

Gary L. Mullen
Professor of Mathematics
Head of Department of Mathematics

Abstract

Synchronization of chaotic systems has been actively studied since 1990 due to its intrinsic interest, and its applicablity in biology, physics, engineering, control theory and safe communications. Despite the extensive research in this area, a mathematical framework within which the phenomenon could be described and analyzed has not been fully developed. The goal of the first part of the present work is to use the theory of invariant manifolds to create such a framework. This approach allows us to analyze in a unified way synchronization schemes that have been treated distinctly in the literature, to show which quantities can be used to determine the onset and stability of synchronization, and to prove the local equivalence of unidirectionally and bidirectionally coupled synchronized systems.

The emergence of coherent structures in networks of coupled chaotic systems may also be viewed as a type of synchronization. Numerical observations of breathers, traveling pulses, waves, and other coherent structures have been made in such systems. Many analytic results for networks imply that the coupling strength necessary for synchronization increases as a power of the size of the system. This implies that synchronization may not be physically important, since in physical systems the coupling strengths can not vary more than a few orders of magnitude. In the second part of the present work it is shown rigorously that periodic, stable fixed states exist in arbitrarily long chains of chaotic systems for a fixed coupling strength. Thus coherent behavior in networks of chaotic systems may not require an increase in coupling strength with the increase in the size of the network, as earlier results suggest.

Contents

List of Figures

Chapter 1

Introduction

In the last decade the surprising phenomenon of synchronization between coupled chaotic systems has generated much interest. The phenomenon was first observed numerically in a lattice of diffusively coupled chaotic systems by Fujisaka and Yamada in 1984 [2]. The first observations of chaotic synchronization in physical systems, as well as the first steps towards a mathematical description and analysis of the phenomenon were carried out in 1986 by Afraimovich, Verichev, and Rabinovich [1]. It is interesting to note that the this research was carried out at the Institute for Applied Physics in Nizhniy Novgorod, the same place that Andronov and Witt did some of their seminal work on synchronization properties of systems with stabel periodic solutions.

The study of chaotic synchronization became popular in the West after the discovery of master-slave synchronization by Pecora and Carroll in 1990 [4]. The applications of chaotic synchronization in secure communications, which were demonstrated experimentally in 1991, engaged the interest of the physics and engineering communities, and it has been an active area of research since. Many different aspects and incarnations of chaotic synchronization were studied: system-subsystem synchronization [4],[20], synchronization in unidirectionally and bidirectionally coupled systems [9],[10], anti-phase synchronization [10],[11], partial synchronization [3] and generalized synchronization [7],[8]. The phenomenon has been observed in many physical systems, for instance mechanical and electrical systems [1],[12], laser systems [13], biological systems [14] and Josephson junctions [15]. Chaotic synchronization has also found a number of applications in control theory [19], parameter estimation from time series [17], and the stabilization of unstable periodic orbits in chaotic attractors [18]. A good review of developments in the experimental study of synchronized chaotic systems is given in [21].

Despite the active interest, until recently a satisfactory mathematical framework within which the various aspects of chaotic synchronization could be discussed and examined was lacking. Different aspects of the problem were studied by a number of mathematicians. Afraimovich was the first to develop analytic tools to study chaotic synchronization in lattices of diffusively coupled oscillators, and this work was continued in collaboration with Hale and Chow [73], [74], [9]. Similar work was done by Pecora, Carroll and Heagy [32], with more emphasis on numerical techniques. Tresser, Worfolk and Bass proposed a framework for system-subsystem synchronization in [31], while the problem of generalized synchronization was addressed by Hunt, Grebogi and Ott [61]. Ashwin, Buescu and Stewart studied the bifurcations by which synchronization between systems may break down, and relations with riddled basins of attraction [50], [51].

The goal of the next chapter is to develop a framework within which many types of synchronization can be discussed in terms of r-hyperbolic invariant manifolds. For synchronization to be physically observable, it needs to persist under small perturbations. The present description will lead to necessary and sufficient conditions for such persistence and will illuminate relations between what appear to be different types of synchronization mechanisms. Although the idea that persistent invariant manifolds provide a natural way to describe synchronization is implicit in many of the works already mentioned, it has first been carefully examined in [46] and [47].

The definitions and examples presented here will mostly concern flows in $\mathbb{R}^n$. The case of discrete dynamical systems or dynamical systems on more general manifolds involves only minor modifications and will be discussed briefly.

The more difficult problem of coherent behavior in networks of chaotic systems is considered in the last chapter. It has recently been reported that networks of locally coupled chaotically bursting neurons can exhibit coherent behavior for a fixed coupling strength regardless of the size of the network [16]. We consider a model network comprised of locally coupled identical Lorenz systems. Motivated by the standard approach in the study of partial differential equations, first the fixed states of the system are examined. It is shown that for many types of local couplings an infinite number of fixed states can be expected. Furthermore, in particular cases spatially periodic fixed states are found to persist at a fixed coupling strength in networks of arbitrary sizes. This result proves that some stable, coherent behavior persists regardless of the size of the network.

1.1 Some Examples

The phenomenon of chaotic synchronization was first noted independently by Fujisaka and Yamada [2], Afraimovich, Verichev, and Rabinovich [1] and Pecora and Carroll [4]. In this section several typical examples of synchronization in networks of chaotic oscillators are presented. A framework within which these examples can be described and analyzed will be given in the next chapter.

Example 1.1.1 Afraimovich, Verichev, and Rabinovich [1] considered the following coupled pair of forced nonlinear oscillators.

$$
\begin{aligned}
x_1' &= y_1 \\
y_1' &= -ky_1 - x_1(1 + q\cos\theta + x_1^2) - c(y_1 - y_2) \\
x_2' &= y_2 \\
y_2' &= -ky_2 - x_2(1 + q\cos\theta + x_2^2) - c(y_2 - y_1) \\
\theta' &= \Omega
\end{aligned}
\tag{1.1}
$$

From previous observations it was known that for a range of values of the parameters k, q and Ω the uncoupled systems oscillate chaotically.

In numerical experiments it was observed that above a critical coupling value c_*, $|x_1 - x_2| \to 0$ and $|y_1 - y_2| \to 0$ as $t \to \infty$, i.e. the two systems synchronized. This is demonstrated in figure 1.1.1. In the same paper the authors gave an analytic explanation of the phenomenon. It was also observed that the synchronization persisted if the parameters of the two systems differed by a small amount. The observation was verified experimentally with a couple of electrical circuits which are modeled well by the equations 1.1.

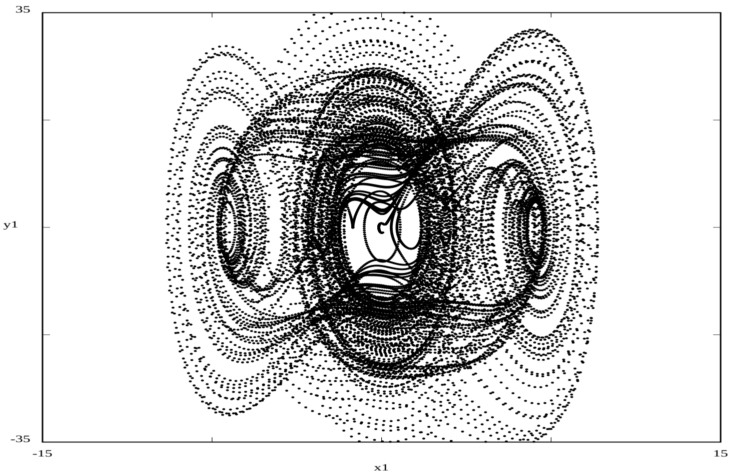

Figure 1.1: A typical trajectory of system (1.1) for parameter values $q = 50$, $\Omega = 2$, and $k = .46$

Example 1.1.2 (System-subsystem synchronization) In the previous example synchronization was a result of a diffusive coupling between two chaotic oscillators. Pecora and Carroll introduced a different type of coupling that leads to synchronization [4]. Given a differential equation $x' = f(x)$, we can think of the variable x as $x = (u, v) \in \mathbb{R}^n = \mathbb{R}^{n-m} \times \mathbb{R}^m$. The system $x' = f(x)$ with $x = (x_1, ..., x_n)$ is split into two parts $u = (x_1, ..., x_{(n-m)})$, $v = (x_{(n-m+1)}, ..., x_n)$, Using this notation the following pair of coupled systems can be defined:

$$\begin{aligned} u' &= f(u, v) \\ v' &= g_1(u, v) \qquad \hat{v}' = g_2(u, \hat{v}) \end{aligned} \tag{1.2}$$

In particular, Pecora and Carroll studied the following pair obtained from the Lorenz equations in this way:

$$\begin{aligned} x' &= \sigma(y - x) \\ y' &= \rho x - y - xz \quad \hat{y}' = \rho x - \hat{y} - x\hat{z} \\ z' &= -\beta z + xy \qquad \hat{z}' = -\beta\hat{z} + x\hat{y} \end{aligned} \tag{1.3}$$

Numerical investigations have shown that $|y(t) - \hat{y}(t)| \to 0$ and $|z(t) - \hat{z}(t)| \to 0$ as $t \to \infty$, so that the two systems synchronize. In this case it is easy to construct a Lyapunov function to show that the solution $y(t) = \hat{y}(t), z(t) = \hat{z}(t)$ is an exponentially stable state. Conditional Lyapunov exponents, the Lyapunov exponents of the linearization of the system around the synchronous state, were proposed as quantities that determine the stability of the synchronized solution [5]. It was later observed that the conditional Lyapunov exponents were inadequate for this purpose [6].

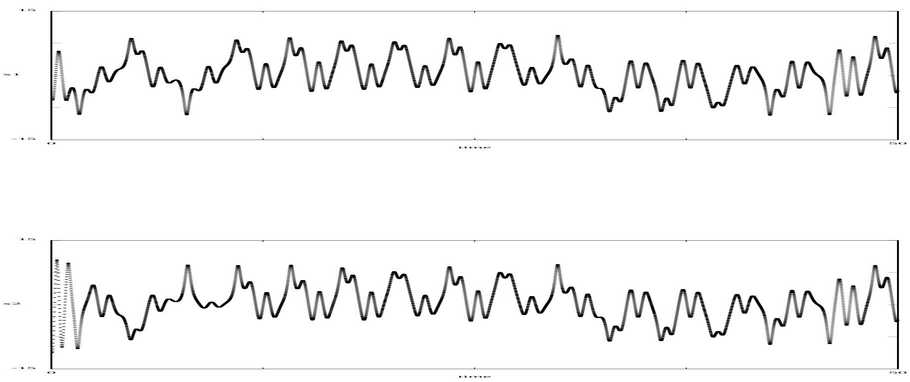

Figure 1.2: Timeseries for $x_1(t)$ and $x_2(t)$ in system (1.1). The coupling constant c was chosen above the threshold necessary for synchronization. After transients die down, the two systems synchronize perfectly.

Chaotic synchronization was first applied in the field of safe communications. There has been much research in this area, however the basic idea is the following: Thesystem (1.3) can also be synchronized if we use y as a driving variable, and create a subsystem using the x and z variables. In other words, a second response system may be defined as

$$\begin{aligned} \hat{\hat{x}}' &= \sigma(y - \hat{\hat{x}}) \\ \hat{\hat{z}}' &= -\beta\hat{\hat{z}} + \hat{\hat{x}}y. \end{aligned} \tag{1.4}$$

with the property that

$$\lim_{t\to\infty} |x(t) - \hat{\hat{x}}(t)| = \lim_{t\to\infty} |z(t) - \hat{\hat{z}}(t)| = 0 \tag{1.5}$$

Since y and $\hat{y}$ in system (1.3) are synchronized, $\hat{y}$ can be used to drive the system (1.4) so that (1.5) still holds.

Assume that the system (x, y, z) is now part of a transmitter, while the systems $(\hat{y}, \hat{z})$, and $(\hat{\hat{x}}, \hat{\hat{z}})$ are part of the receiver. If the synchronization is stable, an information bearing signal i of small amplitude may be added to the driving signal $x(t)$ without affecting the synchronization. If $x(t) + i(t)$ is used to drive subsystem $(\hat{y}, \hat{z})$, then $\hat{y}(t) \approx y(t)$ can be used to drive system (1.4). According to (1.5), it follows that $x(t) + i(t) - \hat{\hat{x}}(t) \approx i(t)$, so that the information bearing signal may be recovered by the receiver. Since a typical chaotic signal $x(t)$ has broadband spectrum, the transmitted signal $x(t) + i(t)$ is both masked, and hard to discern from noise.

K.M. Short has shown that this scheme is not completely secure [22]. If the signal $x(t) + i(t)$ is intercepted and recognized as a deterministic signal, methods of time series analysis can be used to recover the signal $x(t)$, and thus break the encryption.

Example 1.1.3 (Generalized Synchronization) Two dynamical systems are said to be synchronized in a generalized sense if there is a continuous function ϕ from the phase space of the first to the

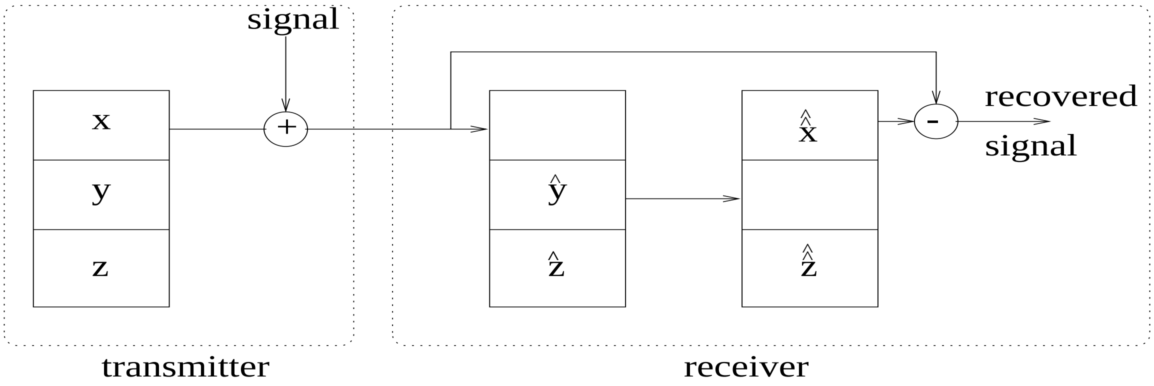

Figure 1.3: A schematic representation of safe communications via chaos synchronization. The information bearing signal is masked using the chaotic output $x(t)$ of a chaotic circuit in the transmitter.

phase space of the second taking orbits of the first system to orbits of the second. It was observed in [8],[7] that two uni-directionally coupled dynamical systems can synchronize in this more general sense. A particular network in which such synchronization can be observed is a Rössler system driving a Lorenz system:

$$\begin{aligned} x_1' &= -y_1 - z_1 & x_2' &= \sigma(y_2 - x_2) - k(x_2 - x_1) \\ y_1' &= x_1 + 0.2y_1 & y_2' &= \rho x_2 - y_2 - x_2 z_2 \\ z_1' &= 0.2 + z_1(x_1 - \mu) & z_2' &= -\beta z_2 + x_2 y_2. \end{aligned} \tag{1.6}$$

Abarbanel, Rulkov, and Suschik [7] have proposed the *auxiliary system approach* to detect generalized synchronization in the case of uni-directionally coupled systems. In this approach two identical response systems are driven by a single driving system. If the two response systems synchronize, it may easily be shown that a synchronization function ϕ exists. The continuity or smoothness of this function cannot be deduced directly.

Example 1.1.4 (Synchronization in networks of oscillators) It is natural to ask if synchronization occurs in larger networks of chaotic oscillators. This question has been studied extensively by Afraimovich [1],[72], [73], [76]. Several examples of this type of synchronization are given in [9]. In particular consider the following diffusively coupled chain of Duffing Oscillators diffusively coupled to their nearest neighbors

$$z_i'' + \beta z_i' - k\Delta z_i - \alpha z_i + \gamma z_i^3 = (B \cos \omega t) \tag{1.7}$$

where $\Delta z_i = z_{i-1} - 2z_i + z_{i+1}$ is a discrete Laplacian, and we have periodic or von Neumann boundary conditions. For a sufficiently strong coupling, a Lyapunov function for the submanifold $z_1 = z_2 = \cdots = z_n$ can be found, and therefore the oscillators synchronize. In general the coupling strength necessary for synchronization depends on the number of oscillators in the chain.

Example 1.1.5 ($n : m$ synchronization of chaotic oscillators) $n : m$ synchronization of weakly coupled phase oscillators is a phenomenon that has already been observed by Huygens, and has been

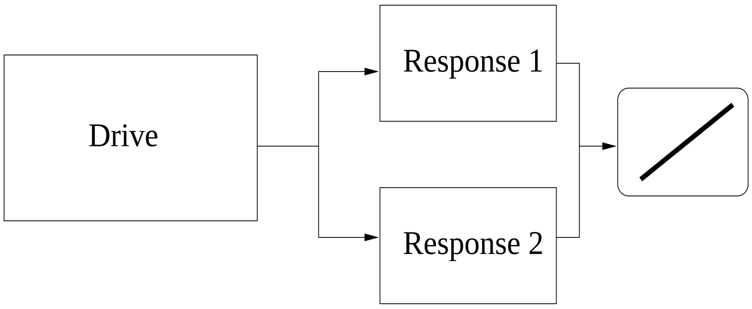

Figure 1.4: A schematic diagram of the auxiliary system method of detection of generalized synchronization.

studied extensively, see for instance [23], [24]. This phenomenon can be explained by the theory of perturbed rotations of S^1. In particular, the attractor of two uncoupled periodically oscillating systems is $\mathbb{T}^2$. If the two oscillators are exponentially stable then this manifold is stable under small perturbations and will thus persists for small couplings. By taking a Poincaré section, the flow on the torus can be reduced to a map of the circle. For the uncoupled system, this map will be conjugate to a pure rotation, and the results outlined in [25] show that a generic perturbation of such a map will have attracting periodic orbits whose basins of attraction contain all but a finite number of repelling points in S^1. Since a weak coupling corresponds to a small perturbation of the flow on the torus, and thus a perturbation of the map of the circle induced by the Poincaré section, it follows that all but finitely many orbits will asymptotically approach a periodic orbit on the torus. These stable periodic orbits correspond to phase locked states.

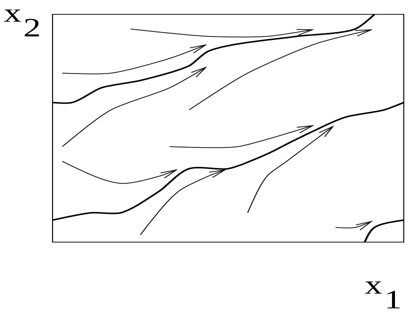

Figure 1.5: 2:1 synchronization between two phase oscillators.

A generalized form of $n : m$ synchronization was observed in [26], [27]. It was observed that the unstable periodic orbits imbedded in each of the attractors of the coupled systems were $n : m$ phase locked. A similar type of synchronization was observed when a phase coherent attractor was driven at approximately twice its fundamental frequency. Not all forms of chaotic $n : m$ synchronization fit in the framework presented in the next chapter.

Example 1.1.6 (Partial Synchronization in Networks) In [3] and [48] it was shown that a network of dynamical systems can be desynchronized, while a subset of the systems comprising the network is identically synchronized. In [48] a system of three lasers is considered, in which two of the lasers are synchronized perfectly, while the third is never synchronized to the other two. In general several subsets of the systems comprising the network may exhibit synchronous behavior, while not synchronized with each other. This type of synchronization may be important in biological systems, for instance the olfactory bulb.

Example 1.1.7 (Synchronization of Chaotically Bursting Neurons) Partial and full synchronization in a pair of electrically coupled, chaotically bursting neurons from the pyloric central pattern generator of the lobster stomatogastric ganglion was reported in [30]. The neurons were coupled electrically through gap junctions. This type of coupling is equivalent to the diffusive couplings introduced in examples 1.1.1, and 1.1.4. The strength of the natural coupling was controlled by introducing an artificial electrical synapse connecting the soma of the two neurons.

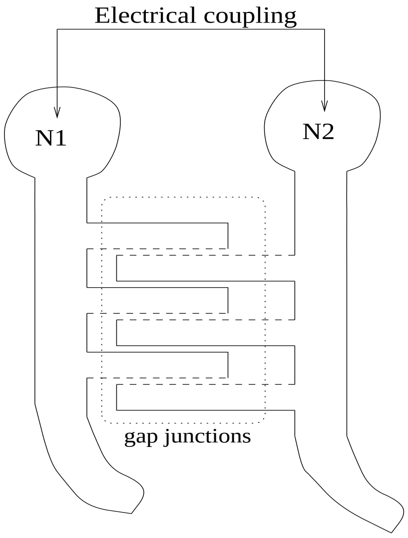

Figure 1.6: Two biological neurons with natural gap junction coupling, and artificial coupling.

If there there is no artificial coupling between the neurons, the chaotic bursts occur synchronously, while the individual spikes in the bursts remain unsynchronized. This means that the slow currents which carry the bursts are synchronized, while the fast currents which are responsible for the spikes are desynchronized, and so there is only partial synchronization between the two systems. When the artificial diffusive coupling is increased past a certain threshold, the spikes within the bursts also synchronize and full synchronization occurs.

Very similar behavior can be observed in numerical simulations in coupled chaotically bursting Rose-Hindmarsch neurons, as reported in [29].

Example 1.1.8 (Networks of Rose-Hindmarsch neurons) A lattice of 100×100 diffusively coupled, chaotically bursting neurons modeled by the Rose-Hindmarsch equations was considered in [16]. The system is described by the following equations

$$\begin{aligned} x'_{i,j} &= y_{i,j} + 3x^2_{i,j} -^3_{i,j} + I_{i,j} - \epsilon(4x_{i,j} - x_{i+1,j} - x_{i-1,j} - x_{i,j+1} - x_{i,j-1}) \\ y'_{i,j} &= 1 - 5x^2_{i,j} - y_{i,j} \\ z'_{i,j} &= 0.0021(4x_{i,j} - z_{i,j} + 6.4) \end{aligned} \tag{1.8}$$

where $I_{i,j} = 3.281 \pm 0.05$ is the applied current which varies throughout the lattice, and periodic boundary conditions are assumed. Each of the systems in the networks bursts chaotically when decoupled from the others. A typical timeseries is shown in figure 1.1.8

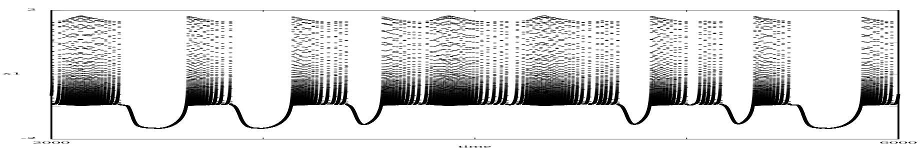

Figure 1.7: A typical timeseries for the x variable in the Rose-Hindmarsch equations (1.8)

.

For sufficiently large values of the coupling parameter ϵ, all systems in the network synchronize identically. The coupling strenght necessary to achieve full synchrony increases with the size of the network. For smaller values of ϵ *bursting synchronization* takes place: the neurons burst synchronously across the network, while the individual spikes in the burst remain desynchronized. For even smaller values of ϵ the network breaks into burst synchronized islands. All neurons within the island are burst synchronized, but the islands are not synchronized with each other. This type of behavior coexists with bursting synchronization, and this regime is thus called bistable. If ϵ is decreased further, the network becomes desynchronized.

Interestingly, the bifurcation value of ϵ at which the system enters the bistable region does not seem to depend on the size of the lattice. This is important from a physiological perspective, since it indicates that this type of coherent behavior can be expected in large neural networks at physiolocially feasable coupling strenghts. Since patterns similar to ones appearing in this model have been observed in *vivo* in experiments with turtles, hallucinations, and models of cortical tissues, it is important to examine states which remain stable at a fixed coupling regardless of the size of the system.

Chapter 2

Invariant Manifolds and Synchronization

2.1 Motivation and Basic Definitions

In this section the basic definitions are motivated and given. These definitions are made rigorous in the next section.

Roughly speaking, synchronization between the two systems

$$x_1' = f(x_1, x_2) \quad x_2' = g(x_1, x_2) \quad f, g : \mathbb{R}^{2n} \to \mathbb{R}^n \tag{2.1}$$

means that there exists a smooth and invertible map ϕ which carries trajectories on the attractor of the first system to trajectories on the attractor of the second. This map should have the property that if an orbit of the first system approaches a trajectory $x_1(t)$ on the attractor of the first system, then the corresponding orbit of the second system approaches the trajectory $x_2(t) = \phi(x_1(t))$. Thus, once transients have died away, a knowledge of the state of the first system allows one to predict the state of the second.

Remark 2.1.1 *It is important to note that we can still formally speak about individual systems when they are coupled as in equation (2.1). However, even if the uncoupled systems are autonomous the individual coupled systems will be non-autonomous.*

The following discussion recasts these ideas in terms of invariant manifolds. First we need to make sense of the idea of the attractor for each of the two subsystems after they are coupled. A priori, the phase space of the coupled system will be the product of the phase spaces of the subsystems, and if the coupled system has an attractor at all, it may be of much higher dimension than the attractors of the original subsystems. One way to insure that we can still speak of the attractors of the two n-dimensional subsystems is to require that the invariant manifold be the graph of a diffeomorphism $\phi : \Omega \subset \mathbb{R}^n \to \mathbb{R}^n$. Such an n-manifold with boundary will be referred to as "*diagonal-like*". If Π^1 and Π^2 are the projections from the phase space of the coupled system onto the phase spaces of the first and second subsystems respectively, and Ω is the attractor of the coupled system which lies inside an invariant *diagonal-like* manifold M, then the requirement that M is diagonal-like implies that there exists a smooth map between the sets $\Pi^1(\Omega)$ and $\Pi^2(\Omega)$ in the phase space of the system $x_1(t)$ and $x_2(t)$ respectively.

Secondly we need to require that solutions in some non-trivial region of phase space synchronize. In other words the manifold under consideration should not only be invariant under the flow, but trajectories in some neighborhood should also be attracted to it. Such manifolds will be called "*locally attracting*". One way to insure that an invariant manifold is locally attracting is to require it to be normally hyperbolic [35], [36] with trivial unstable normal bundle.

Finally, in order to avoid some pathologies, like trajectories leaving the region under consideration, we require the invariant manifolds to be compact and inflowing. An "*inflowing*" manifold is a compact manifold with boundary, such that on the boundary the vector-field is directed into the interior of the manifold.

Definition 2.1.2 *The systems x_1 and x_2 in (2.1) are* synchronized *if there exists a compact, diagonal-like, smooth n-manifold M with boundary which is invariant under the flow, inflowing and locally attracting. M will be referred to as the* synchronization manifold.

Remark 2.1.3 When the synchronization manifold M is a subset of the diagonal $D = \{(x_1, x_2) \in \mathbb{R}^{2n} : x_1 = x_2\}$ then the two systems are synchronized identically. In all other cases the conditions of definition 2.1.2 imply to *generalized synchronization* as defined in [29]. A similar definition of chaotic synchronization was introduced in [46].

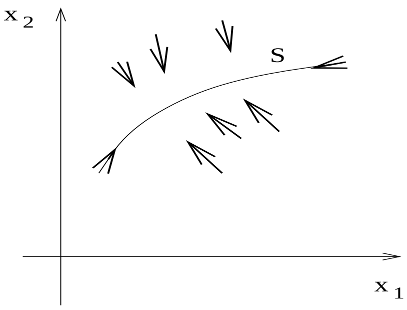

Figure 2.1: A schematic representation of synchronization

In particular the synchronization manifold M can be viewed as the graph of the function ϕ defined above, and so the existence of the manifold M implies the existence of the function ϕ. In addition, in order for such synchronization to be of physical interest, it should persist under small perturbations of either the coupling, or the two subsystems.

The dynamics on the synchronization manifold can (and in general will) be quite complicated. In particular, it may have both positive and negative Lyapunov exponents. In order to insure that synchronization persists under perturbation of the system, we require that the rate at which trajectories are attracted toward the manifold is greater than the rates of contraction within the manifold. If the rate of attraction is exponentially r times greater than the contraction rates within the manifold, the synchronization manifold is called *normally k-hyperbolic.* Precise definitions and a discussion of this notion will be given in the next section.

Definition 2.1.4 *The synchronization of x_1 and x_2 is called* stable *if the synchronization manifold M is normally k-hyperbolic for some $k \geq 1$.*

Notice that the qualitative behavior of each of the coupled systems may change under small perturbations, in particular if the parameters of either are close to a bifurcation value. If the synchronization manifold persists, the two systems will remain synchronized.

Remark 2.1.5 This definition of stable synchronization is close to the one given in [46]. The main difference is that the present definition does not require an invariant splitting of the tangent space and is thus better suited for practical applications. Moreover, the requirement that the invariant manifold is compact and inflowing is made explicit in our consideration. The case of noncompact synchronization manifolds is more subtle and will not be addressed here.

Example 2.1.6 Consider the case of two coupled Lorenz systems:

$$\begin{aligned} x_i' &= \sigma_i(y_i - x_i) + c_i(x_2 - x_1) \\ y_i' &= \rho_i x_i - y_i - x_i z_i + c_i(y_2 - y_1) \\ z_i' &= -\beta_i z_i + x_i y_i + c_i(z_2 - z_1) \end{aligned}$$

where $i = 1, 2$ and $c_1 = -c_2$. When the coefficients σ_i, ρ_i, and β_i of the two systems agree then it is immediate that the diagonal $D \in \mathbb{R}^6$ (i.e. the set defined by $x_1 = x_2$, $y_1 = y_2$, and $z_1 = z_2$) is an invariant set. Using an extension of the argument given in [33] it is possible to show that there is an invariant inflowing ellipsoid E around the origin in $\mathbb{R}^6$.

Therefore all solutions of the coupled systems remain bounded and we may take $M = D \cap E$ as a compact, inflowing, invariant 3-manifold. To show that M is in fact attracting consider the difference variables $\xi_1 = x_1 - x_2$, $\xi_2 = y_1 - y_2$, and $\xi_3 = z_1 - z_2$, so that:

$$\begin{aligned} \xi_1' &= \sigma(\xi_2 - \xi_1) - 2c_1\xi_1 \\ \xi_2' &= \rho\xi_1 - (1 + 2c_1)\xi_2 - x_2\xi_3 - z_1\xi_1 \\ \xi_3' &= -(\beta + 2c_1)\xi_3 + y_1\xi_1 + x_2\xi_2 \end{aligned}$$

The synchronization manifold M corresponds to $(\xi_1, \xi_2, \xi_3) = (0, 0, 0)$ and these coordinates are taken in a direction orthogonal to M. Therefore showing that the synchronization manifold is stable is equivalent to showing that the origin in ξ space is attracting for all values of (x_1, x_2, x_3). For a sufficiently strong coupling c it can be shown that:

$$V = -\frac{g}{2}(\xi_1^2 + \xi_2^2 + \xi_3^2)$$

is a Lyapunov functional for the ξ variables. The stronger the coupling, the larger the constant g that can be chosen in the expression for V. Since the Lyapunov functional is quadratic, this implies that trajectories nearby M are attracted exponentially, and an appropriate choice of coupling constant will make M k-hyperbolic. For strong coupling the synchronization between the two systems is stable. In particular, it is not necessary that σ_i, ρ_i, and β_i be equal – even two nonidentical systems which are close in the C^1 topology will be nearly synchronized.

2.2 r-Normal Hyperbolicity and Generalized Lyapunov Numbers

Early in the study of invariant manifolds it was observed that even if they are exponentially stable they may lose their smoothness, and even disappear under small perturbations [43]. A sufficient condition for the persistence of smooth manifolds is r-normal hyperbolicity which has its origins in the work of Sacker [42], and was precisely formulated by Fenichel [38]. Mañe has subsequently shown that r-hyperbolicity is also a necessary condition for smooth persistence [44]. The following discussion is based on Fenichel's original presentation.

Let X be a C^1 vector field on $\mathbb{R}^n$ with flow F^t and let M be a compact, connected manifold with boundary which is overflowing and invariant under the flow F^t. Consider the usual metric on $\mathbb{R}^n$ so that the tangent space of M decomposes as $T\mathbb{R}^n|_M = TM \oplus N$, where N is the normal bundle of M. Let $\pi : T\mathbb{R}^n|_M \to N$ be the orthogonal projection. Define the linearization A^t of the flow parallel to the manifold, and B^t normal to the manifold as

$$A^t(m) = D(F^{-t}|_M)(m) \quad A^t(m) : T_m M \to T_{F^{-t}} M \tag{2.2}$$
$$B^t(m) = \pi DF^t(F^{-t}(m)) \quad B^t(m) : N_{F^{-t}(m)} \to N_m \tag{2.3}$$

The generalized Lyapunov numbers are defined as follows

$$\nu_X(m) = \inf\{a : \frac{\|B^t(m)\|}{a^t} \to 0 \text{ as } t \to \infty\} = \limsup_{t\to\infty} \|B^t(m)\|^{\frac{1}{t}} \tag{2.4}$$

and if $\nu_X(m) < 1$

$$\sigma_X(m) = \inf\{s : \|A^t(m)\| \, \|B^t(m)\|^s \to 0 \text{ as } t \to \infty\} = \limsup_{t\to\infty} \frac{\log \|A^t(m)\|}{-\log \|B^t(m)\|} \tag{2.5}$$

The rate of contraction in the direction normal to the manifold is measured by $\nu(m)$, while $\sigma(m)$ measures is the ratio of the exponential rate of contraction in the normal direction, and the exponential rate of contraction in M. Both $\nu(m)$ and $\sigma(m)$ are constant on orbits and depend only on the flow near the α set of m.

The following theorem will be used to provide conditions for persistent synchronization.

Theorem 2.2.1 (Fenichel, 1971) *Let X be a C^r vector field on $\mathbb{R}^n$ with an invariant, overflowing, compact, connected manifold with boundary $\bar{M} = M \cup \partial M$, properly embedded in $\mathbb{R}^n$. If $\nu_X(m) < 1$ and $\sigma_X(m) < 1/r$ for all $m \in M$ then for any C^r vector field Y in some C^1 neighborhood of X there is a manifold $\bar{M}_Y$ overflowing invariant under Y and C^r diffeomorphic to $\bar{M}$.*

There is a technical difficulty in applying this result to justify the definitions of the preceding section since the synchronization manifold is required to be stable and inflowing invariant. The definitions of the generalized Lyapunov numbers do not make sense in this case. The problem is resolved by the following construction:

Let X denote a vector field with flow F^t which leaves a manifold M invariant. Define $\phi : N \to \mathbb{R}^n$ by $\phi(m, v) = m + \exp_m v$. By a standard result of differential geometry [37] there exists a $\delta > 0$ such that ϕ maps $N^\delta = \{v \in N : |v| < \delta\}$ diffeomorphically onto a neighborhood of M.

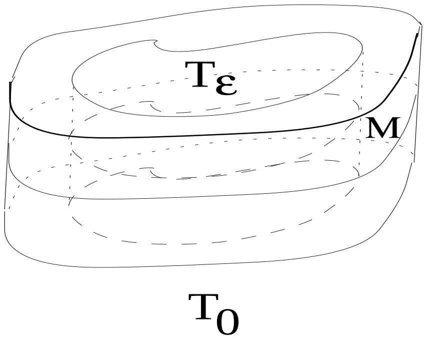

Figure 2.2: T_0 is a tubular neighborhood of the manifold M. T_0 contains T_ϵ, which is a tubular neighborhood of M_ϵ.

Since the manifold M is inflowing invariant, we may define $M_\epsilon = F^\epsilon(M) \subset M$ so that M_ϵ is inflowing invariant. To each of the corresponding subsets of the normal bundle $N^{\delta,\epsilon} = \{(m,v) \in N_p^\delta : p \in M_\epsilon\}$ we can associate a neighborhood $T_\epsilon = \phi(N^{\delta,\epsilon})$.

Clearly $T_\epsilon \subset T_{\epsilon/2} \subset T_0$, and thus we can define a smooth function Φ on T_0 such that

$$\Phi(x) = \begin{cases} 0 & \text{if } x \in T_\epsilon, \\ 1 & \text{if } x \in T_0 - T_{\epsilon/2}. \end{cases}$$

We will consider the vector field

$$\mathcal{X} = X + 2\Phi \cdot (kV - X) \tag{2.6}$$

where the vector field V is defined by $V_{\phi(m,v)} = -v$ and k is a constant which will be determined subsequently. Note that if $\tilde{X}$ is a small perturbation of X in T_0, then

$$\tilde{\mathcal{X}} = \tilde{X} + 2\Phi \cdot (kV - \tilde{X}) \tag{2.7}$$

is a small perturbation of $\mathcal{X}$. By construction, the manifold M is an overflowing invariant manifold under the flow induced by $\mathcal{X}$.

Let $\mathcal{T} = \{x \in T_0 : \Phi(x) > \frac{1}{4}\}$. Notice that the rate of contraction in the direction normal to M can be adjusted in $\mathcal{T}$ by changing the value of the constant k.

The vector field X points in on $\partial = \{x \in M : \phi(x) = \frac{1}{4}\}$. Also $\mathcal{X} = \frac{1}{2}X$ on ∂, so that by definition the vector filed $\mathcal{X}$ also points in on ∂. Therefore all orbits that leave M_ϵ in backwards time enter $\mathcal{T} \cap M$. Each $p \in \mathcal{T} \cap M$ has a coordinate neighborhood (x_i, y_i) inside $\mathcal{T} \cap M$ on which the vector field $\mathcal{X}$ can be expressed as

$$x_i' = f_i(x_i, y_i) \tag{2.8}$$
$$y_i' = g_i(x_i, y_i) - cy_i \tag{2.9}$$

where $c > \frac{k}{4}$. The exponential contraction in the direction normal to the manifold may be bounded below by K, where

$$K = \sup_{(x_i, y_i) \in \mathcal{T}} g_i(x_i, y_i) - \frac{1}{4}k \tag{2.10}$$

Since k is an arbitrary constant, this implies that $\sigma(m)$, and $\nu(m)$ can be controlled for any m on orbits that leave the submanifold M_ϵ in backwards time.

If $\nu_X(m) < 1$ and $\sigma_X(m) < 1/r$ for all m on orbits that do not leave M_ϵ in backwards time, then the manifold M is r-hyperbolic and overflowing under the flow of $\mathcal{X}$ for sufficiently large values of k. Now if $\tilde{X}$ is a small perturbation of the X, then $\tilde{\mathcal{X}}$ as defined by equation (2.7) is a small perturbation of $\mathcal{X}$. Since M is r-hyperbolic, there is a manifold $\tilde{M}$ which is inflowing invariant under the flow of $\tilde{\mathcal{X}}$. Since $\tilde{M}$ is close to M and $\tilde{\mathcal{X}} = \tilde{X}$ in T_ϵ, the manifold $\tilde{M} \cap T_\epsilon$ is an inflowing invariant manifold under the flow of the vector field $\tilde{X}$. Thus we have proved the following

Proposition 2.2.2 *If $\nu_X(m) < 1$ and $\sigma_X(m) < 1/r$ for all m on orbits that do not leave M in backwards time then an inflowing submanifold of M containing an attractor of the flow F^t persists as an inflowing manifold under small perturbations.*

For an inflowing manifold it is more natural to calculate the generalized Lyapunov numbers in the direction of forward time. In particular $\nu(m)$ defined in (2.4) may be replaced by

$$\nu_X^*(m) = \limsup_{t \to \infty} \|\pi DF^t(m)|_N\|^{\frac{1}{t}} \tag{2.11}$$

measuring the contraction rate of the flow of a field X in forward time. This fact follows from Fenichel's Uniformity Lemma which will also prove useful in further considerations.

Lemma 2.2.3 (Fenichel's Uniformity Lemma, 1971) *Let B be a compact, backward invariant subset of M. If $\|B^t(m)\|/a^t = \|\pi DF^t(F^{-t}(m))\|/a^t \to 0$ as $t \to \infty$ for all $m \in B$, then there are constants $\hat{a} < a$, and c such that $\|\pi DF^t(F^{-t}(m))\| < c\hat{a}^t$ for all $m \in B$, and $t \geq 0$. Similarly if B is forward invariant and $\|\pi DF^t(m)\|/a^t \to 0$ as $t \to \infty$ for all $m \in B$, then there are constants $\hat{a} < a$, and c such that $\|\pi DF^t(m)\| < c\hat{a}^t$ for all $m \in B$, and $t \geq 0$. Moreover ν and ν^* achieve their suprema on B.*

We can use the Uniformity Lemma to prove the following.

Proposition 2.2.4 *Let X and $\mathcal{X}$ be the vector fields constructed in the proof of proposition 2.2.2 and $\nu_{\mathcal{X}}(m) < 1$ and $\nu_X^*(m) < 1$ for all $m \in M$. Then for a sufficiently large k*

$$\sup_{m \in M} \nu_{\mathcal{X}}(m) = \sup_{m \in M} \nu_X^*(m) \tag{2.12}$$

Proof: This is a consequence of Fenichel's Uniformity Lemma 2.2.3 which holds for both $\nu_{\mathcal{X}}(m)$ and $\nu_X^*(m)$. If $\nu(m) < a < 1$ for all $m \in M$ then by the Uniformity Lemma there exists a constant C such that $\|\pi DF^t(F^{-t}(m))|_N\| < Ca^t$. Since $\|\pi DF^t(m)|_N\| = \|\pi DF^t(F^{-t}(F^t(m)))|_N\|$, we can conclude that $\sup_{m \in M} \nu_{\mathcal{X}}(m) \geq \sup_{m \in M} \nu_X^*(m)$ when $m \in M_\epsilon$. But since $\nu_X^*(m)$ is constant on orbits, and any point in M enters M_ϵ this inequality must hold on all of M.

Consider $m \in M$ which do not leave M_ϵ in backwards time, so that there exists an n such that $F^{-t}(n) = m$. Applying the Uniformity Lemma to $\nu^*_X(m) < a < 1$ we can conclude that $\|\pi DF^t(F^{-t}(m))|_N\| = \|\pi DF^t(n)|_N < Ca^t$. By choosing a sufficiently large k we can assume that there exists a point $p \in M_\epsilon$ which does not leave M_ϵ in backwards time such that $\nu_{\mathcal{X}}(p) > \nu_{\mathcal{X}}(m)$ for all $m \in M - M_\epsilon$. Therefore $\sup_{m\in M} \nu_{\mathcal{X}}(m) \leq \sup_{m \in M} \nu^*_X(m)$. $\diamondsuit$

In some applications it is important the the normal bundle N is invariant under the flow of X. If we start with a bundle N with this property, it will remain invariant under the vector field constructed in the proof of proposition 2.2.2.

Proposition 2.2.5 *Let ϕ^t_X and $\phi^t_{\mathcal{X}}$ be the flows of X and $\mathcal{X}$ respectively. If $D\phi^t_X|_M$ preserves the normal bundle N, then so does $D\phi^t_{\mathcal{X}}|_M$.*

Proof: The proof will be carried out in a local coordinate system (x, y) naturally defined by N in the vicinity of M so that $\{(x, y)|y = 0\} \subset M$. Since both ϕ^t_X and $\phi^t_{\mathcal{X}}$ have M as an invariant manifold by construction, in these coordinates both flows can be described by:

$$\phi^t_X \begin{bmatrix} x \\ 0 \end{bmatrix} = \begin{bmatrix} \Theta^t(x,0) \\ 0 \end{bmatrix} \qquad \phi^t_{\mathcal{X}} \begin{bmatrix} x \\ 0 \end{bmatrix} = \begin{bmatrix} \Psi^t(x,0) \\ 0 \end{bmatrix} \tag{2.13}$$

Given any initial point p we can choose t small enough so that $\phi^t_{\mathcal{X}}(p)$ is in the same coordinate patch as p. Therefore we can work in a coordinate patch without loss of generality. Since the normal bundle is invariant it follows that in the vicinity of the invariant manifold the vector field X can be written in local coordinates as

$$\begin{bmatrix} x' \\ y' \end{bmatrix} = \begin{bmatrix} f(x) + \mathcal{O}(y^2) + \mathcal{O}(xy) \\ q(x)y + \mathcal{O}(y^2) \end{bmatrix} \tag{2.14}$$

so that in the vicinity of M the vector field $\mathcal{X}$ has by definition the form

$$\begin{bmatrix} x' \\ y' \end{bmatrix} = \begin{bmatrix} (1-\kappa(x))f(x) + \mathcal{O}(y^2) + \mathcal{O}(xy) \\ (-\lambda + q(x))y + \mathcal{O}(y^2) \end{bmatrix} \tag{2.15}$$

For small y we can write the flow as

$$\phi^t_{\mathcal{X}} \begin{bmatrix} x \\ y \end{bmatrix} = \begin{bmatrix} \Psi^t(x,0) + \delta\Psi^t(x,y) \\ \delta\eta^t(x,y) \end{bmatrix}. \tag{2.16}$$

The small order terms then satisfy

$$\begin{aligned} &\frac{\mathrm{d}}{\mathrm{d}t} \begin{bmatrix} \delta\Psi^t(x,y) \\ \delta\eta^t(x,y) \end{bmatrix} \\ &= \begin{bmatrix} (1-\kappa(\Psi^t_0 + \delta\Psi^t))(f(\Psi^t_0 + \delta\Psi^t)) - (1-\kappa(\Psi^t_0))f(\Psi^t_0) + \mathcal{O}((\delta\eta^t)^2) + \mathcal{O}(\delta\eta^t\delta\Psi^t) \\ (-\lambda + q(\Psi^t_0 + \delta\Psi^t))\delta\eta^t + \mathcal{O}((\delta\eta^t)^2) \end{bmatrix} \end{aligned} \tag{2.17}$$

where $\Psi^t_0 = \Psi^t(x, 0)$, and the remaining dependences on initial conditions were dropped for notational convenience. To first order in $\delta\Psi^t(x, y)$ and $\delta\eta^t(x, y)$ we have

$$\frac{\mathrm{d}}{\mathrm{d}t} \begin{bmatrix} \delta\Psi^t(x,y) \\ \delta\eta^t(x,y) \end{bmatrix} = \begin{bmatrix} [(1-\kappa(\Psi^t_0))f'(\Psi^t_0) - \kappa'(\Psi^t_0))f(\Psi^t_0)]\delta\Psi^t \\ (-\lambda + q(\Psi^t_0)\ \delta\eta^t(x,y) \end{bmatrix}. \tag{2.18}$$

This may be viewed as a linear equation in $\delta\Psi^t(x,y)$ and $\delta\eta^t(x,y)$ with fundamental solution

$$S^t(x) = \begin{bmatrix} S_1^t(x) & 0 \\ 0 & S_2^t(x) \end{bmatrix}. \tag{2.19}$$

The fundamental solution depends on x only, since $\delta\Psi^t(x,y)$ and $\delta\eta^t(x,y)$ were treated as variables, and $\Psi_0^t = \Psi^t(x,0)$ depends only on x. The solutions of (2.17) can be expressed in terms of this fundamental solution as

$$\begin{bmatrix} \delta\Psi^t(x,y) \\ \delta\eta^t(x,y) \end{bmatrix} = S^t(x)\begin{bmatrix} x \\ y \end{bmatrix} + S^t(x)\int_0^t (S^r)^{-1}(x)h(r)\mathrm{d}r \tag{2.20}$$

where $h(t)$ consists of the nonlinear terms that were ignored in (2.18)

$$h(t) = \begin{bmatrix} \mathcal{O}((\delta\eta^t)^2) + \mathcal{O}((\delta\Psi^t)^2) + \mathcal{O}(\delta\eta^t\delta\Psi^t) \\ \mathcal{O}((\delta\eta^t)^2) + \mathcal{O}(\delta\eta^t\delta\Psi^t) \end{bmatrix}. \tag{2.21}$$

Since the flow of the vector field $\mathcal{X}$ is given by equation (2.16) we get

$$D\phi_{\mathcal{X}}^t(x,0) = \begin{bmatrix} \frac{\partial}{\partial x}\Psi^t(x,0) & 0 \\ 0 & 0 \end{bmatrix} + \begin{bmatrix} \frac{\partial}{\partial x}\delta\Psi^t(x,0) & \frac{\partial}{\partial y}\delta\Psi^t(x,0) \\ \frac{\partial}{\partial x}\delta\eta^t(x,0) & \frac{\partial}{\partial y}\delta\eta^t(x,0) \end{bmatrix} \tag{2.22}$$

However $\frac{\partial}{\partial y}\delta\Psi^t(x,0) = 0$ because the the right hand side of equation (2.20) depends on $\delta\Psi^t(x,y)$ only through terms of higher order, and $\delta\Psi^t(x,0) = \delta\eta^t(x,0) = 0$. Since $y = 0$ is invariant, $\frac{\partial}{\partial x}\delta\eta^t(x,y) = 0$. Therefore $D\phi_{\mathcal{X}}^t(x,0)$ is a block diagonal matrix, and preserves the normal bundle. $\diamondsuit$

2.3 The Relation Between Conditional Lyapunov Exponents and Generalized Lyapunov Numbers

The original papers of Pecora and Carroll [4] and Fujisaka and Yamada introduced conditional Lyapunov exponents, also known as sub-Lyapunov exponents, and normal or transversal Lyapunov exponents to measure the stability of the invariant manifold. The negativity of these numbers was used in many investigations as a criterion for the stability of an invariant manifold for the coupled system. It was shown theoretically [50], and in numerical and physical experiments [51], [57] that a simple calculation of these quantities is insufficient for the prediction of synchronization.

To explain the relation between the transversal Lyapunov exponents and the generalized Lyapunov numbers ν and σ we will assume that the coupled system has an attractor A contained in the synchronization manifold and that A is topologically transitive. The tangential and normal Lyapunov exponents can be defined as

$$\lambda_{\perp}(m,v) = \lim_{t\to\infty}\frac{1}{t}\log\|\pi_N DF^t(m)v\| \tag{2.23}$$

$$\lambda_{\|}(m,v) = \lim_{t\to\infty}\frac{1}{t}\log\|DF^t(m)w\| \tag{2.24}$$

when the limits exist and where $v \in N$ and $w \in TM$.

In [50] it is shown that both of these exponents exist μ-almost everywhere for any invariant measure supported on A. Moreover for each m, $\lambda_\perp(m,v)$ takes on one of the values $\lambda_\perp^1(m) \leq \ldots \leq \lambda_\perp^{s(m)}(m)$, and there is a related filtration of N_p equivalent to the case of ordinary Lyapunov exponents.

Let $SA = \{(p,v) : p \in A, v \in N \text{ and } \|v\| = 1\}$ denote the normal unit sphere bundle of the attractor A, and $\text{Erg}_{F^t}(A)$ the set of all invariant probability measures supported on an attractor A.

Proposition 2.3.1 *Let M be an inflowing, invariant manifold for the flow of a vector field X satisfying the conditions of proposition 2.2.2 and containing a single topologically transitive attractor A of the flow. Moreover assume that $A = \cap_{t\in\mathbb{R}^+} F^t(M)$, that is M is a fundamental neighborhood of A. If $\sup_{\mu\in Erg_{F^t}(A)} \lambda_\perp^s(\mu) < 0$, or $\sup_{m\in M} \log \nu_X^*(m) < 0$ then*

$$\sup_{(m,v)\in SN} \limsup_{t\to\infty} \frac{1}{t} \log \|\pi DF^t(m)v\| = \sup_{\mu\in Erg_{F^t}(A)} \lambda_\perp^s(\mu) = \sup_{m\in M} \log \nu_X^*(m) \tag{2.25}$$

Equivalently, $\sup_{\mu\in Erg_{F^t}(A)} \lambda_\perp^s(\mu) \geq 0$ if, and only if $\sup_{m\in M} \log \nu_X^*(m) \geq 0$.

Proof: The first equality is contained in Theorem 2.8 of [51].

In the proof of proposition 2.2.2 it was shown that $\sup_{m\in M} \nu_{\mathcal{X}}(m)$ is achieved on orbits that do not leave M_ϵ. Since $A = \cap_{t\in\mathbb{R}^+} F^t(M_\epsilon)$ it follows that $\sup_{m\in M} \nu_{\mathcal{X}}(m)$ is achieved on A. By proposition 2.2.4 this implies that $\sup_{m\in M} \nu_X^* = \sup_{m\in A} \nu_{\mathcal{X}}$.

Let $B = A$ in the Uniformity Lemma 2.2.3. If $\nu_{\mathcal{X}} < a$ for all $m \in A$, then

$$\|\pi DF^t(F^{-t}(m))\| < Ca^t \tag{2.26}$$

for all $m \in A$, and hence $\|\pi DF^t(m)\| < Ca^t$, so that $\nu_X^* < a$ for all $m \in A$. Similarly, if $\nu_X^* < a$ for all $m \in A$, then

$$\|\pi DF^t(m)\| < Ca^t \tag{2.27}$$

for all $m \in A$, and hence $\|\pi DF^t(F^{-t}(m))\| < Ca^t$, so that $\nu_X^* < a$ for all $m \in A$. These inequalities imply $\sup_{m\in A} \nu_X^*(m) = \sup_{m\in A} \nu_{\mathcal{X}}(m)$.

It follows that

$$\sup_{m\in M} \nu_X^*(m) = \sup_{m\in A} \nu_{\mathcal{X}}(m) = \sup_{m\in A} \nu_{\mathcal{X}}(m) = \sup_{(m,v)\in SN} \limsup_{t\to\infty} \|\pi DF^t(m)v\|^{\frac{1}{t}}. \tag{2.28}$$

$\diamond$

From this proposition it follows that the transversal Lyapunov exponents $\lambda_\perp(\mu)$ need to be negative for all invariant measures supported on the attractor A. Even if the Lyapunov numbers of typical orbits in A are negative, it is possible that there are points $p \in A$ such that $\lambda_\perp(p) > 0$. In such cases the manifold M will not be Lyapunov stable, and may not persist under perturbations. This situation is discussed further in the next section.

2.4 Comments on Generalized Lyapunov Numbers

Since the synchronization manifold M defined in 2.1.2 is assumed to be smooth, it follows that the map ϕ, which satisfies graph$(\phi) = M$ providing the relation between the coupled systems is required to be differentiable. This definition is equivalent to what is referred to as *differentiable generalized synchronization* or DGS in the literature. It is motivated by the fact that if the function ϕ were required to be only continuous, then the attractor A of one system may have lower Lyapunov dimension than the attractor $\phi(A)$ of the second system. In this case a small error in measurement of the state variables of the first system would be amplified by the function ϕ, rendering our definition of generalized synchronization irrelevant for physical applications.

By theorem 2.2.1, it is the suprema of both generalized Lyapunov numbers ν and σ on the synchronization manifold that determine whether it will persist as a smooth manifold under small perturbations. In this section we discuss these quantities and how they relate to the loss of synchronization between coupled systems. There have been frequent misconceptions about the correct measures for stable chaotic synchronization, and some cautionary examples are provided below.

2.4.1 The First Generalized Lyapunov Number ν

By theorem 2.12 in [50] the transversal Lyapunov exponents for *all* invariant measures on an attractor A have to be negative for the synchronization manifold to be locally attracting. Proposition 2.3.1 implies that this is equivalent to requiring $\nu^*(p) < 1$ for all points p in the synchronization manifold. Generally there are infinitely many ergodic invariant measures on the attractor A, which makes it difficult to directly calculate these quantities using numerical techniques. Fortunately the work of Hunt and Ott [52], [53], [54] suggests that the transversal Lyapunov exponents achieve their supremum on periodic orbits of low period imbedded in A. This gives some hope for computational estimates of the range of stability of synchronization manifolds.

Consider a pair of diffusively coupled systems, for instance the system considered in example 2.1.6. Typically, we expect the transition to desynchronization to begin by a change of transversal stability of a periodic orbit in the attractor A, perhaps as a result of a saddle-node bifurcation. As the coupling strength between the two systems is decreased the number of transversally unstable orbits in A is expected to increase. Moreover, if the transversal Lyapunov exponents are positive on a set that is dense in A, then A has a locally riddled basin[1].

In the case of diffusively coupled systems it frequently happens that the unstable manifold of an orbit in A doubles back, asymptotically approaching A in forward time. A trajectory following this unstable manifold would therefore get re-injected into the vicinity of the synchronization manifold M. This is manifested as an intermittent loss of synchronization. The frequency of these intermittent bursts will increase with the increase of transversally unstable orbits. Any amount of noise can increase this effect since it may push any orbit into the unstable region. An increase in the frequency and time of intermittent desynchronization is typically observed in physical and numerical simulations of diffusively coupled systems as the coupling strength is decreased [55], [56].

Remark 2.4.1 This type of bifurcation may occur in the case of general types of synchronization discussed in section 2.5, or generally when a system has an attractor contained in a normally hyperbolic invariant manifold. For instance see [56].

Remark 2.4.2 Due to the finite precision of numerical calculations, two identical coupled systems starting at different points of phase space may become identically synchronized in finite time. This

[1] Let V be an open neighborhood of a Milnor attractor A, and define $U(V)$ to be the set of all points that remain in V in forward time. A has a locally riddled basin if there exists a neighborhood V of A such that $l(B_\delta(x) \cap U(V)^c) > 0$ for all $x \in A$ and $\delta > 0$. This means the Lebesgue measure of points in any neighborhood $x \in A$ leaving V is positive.

is because the exponentially decaying distance between them will eventually be smaller than the numerical precision at which the calculations are carried out, and hence approximated by 0. This is referred to as *hard locking*, and is a purely numerical artifact. It is possible that a true orbit intermittently leaves the synchronization manifold, which will not be observed if hard-locking occurs. In numerical simulations in which intermittent desynchronization is expected to occur, we can either add a small amount of noise to the system, or introduce a small difference between the two systems to prevent numerical hard locking.

Notice that hard locking will not typically occur in the case of generalized synchronization, since a computed orbit can not land and remain exactly on a generic synchronization manifold. This is again due to the finite precision of the calculations. Hard locking is therefore expected only in the case of identically synchronized systems.

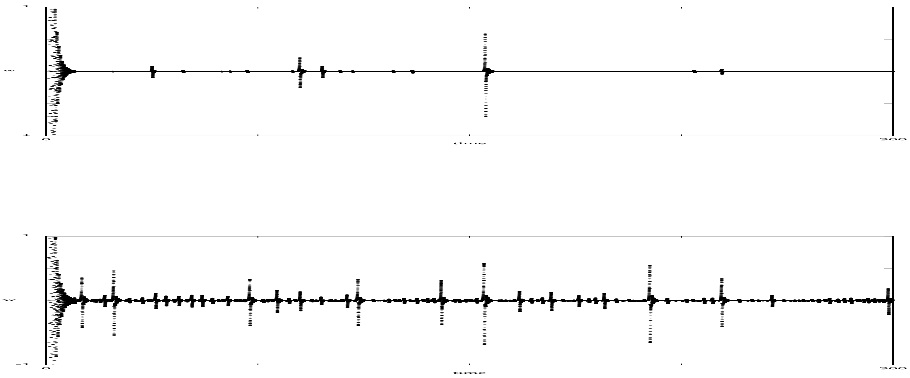

Figure 2.3: The two figures represent the timeseries of $x_1(t)-x_2(t)$ in example 2.1.6. As the coupling strength c is decreased, the frequency of intermittent desynchronization increases.

Several methods for determining the asymptotic stability of the synchronization manifold have been based on the assumption that the asymptotic stability of the origin in the linearization of the equations describing the dynamics transversal to the manifold implies the transversal stability of the manifold itself. In general this is true only for coupled autonomous systems for which the network has bounded orbits. This result will follow as a corollary to a theorem about linear extensions.

Definition 2.4.3 *Let (X, p, B) be a vector bundle over a compact metric space B, and π^t and ρ^t be flows on X and B respectively. Then π^t is an* extension *of ρ^t if the following diagram commutes*

$$\begin{tikzcd} X \arrow[r, "\pi^t"] \arrow[d, "p"'] & X \arrow[d, "p"] \\ E \arrow[r, "\rho^t"] & E \end{tikzcd}$$

If $\pi^t : X_q \to X_{\rho^t(q)}$ is linear for all $t \in \mathbb{R}$, and $q \in B$, then π^t is a linear extension *of ρ^t.*

If $X = X_s \oplus X_u$ for some invariant vector subbundles X_s and X_u and

$$\begin{aligned} \|\pi^t(x)\| &\leq d\|x\|e^{-\alpha t} & x \in X_s, t > 0 \\ \|\pi^{-t}(x)\| &\leq d\|x\|e^{-\alpha t} & x \in X_u, t > 0 \end{aligned} \tag{2.29}$$

then the extension is hyperbolic.

The following theorem is a weaker version of theorem III.3.4 in [35]

Theorem 2.4.4 *If $X = \{x \in X : \lim_{t\to\infty} \|\pi^t(x)\| = 0\}$, then the extension π^t of ρ^t is hyperbolic.*

Corollary 2.4.5 *Consider the coupled differential equations*

$$x' = f(x) \tag{2.30}$$

$$y' = A(x)y \tag{2.31}$$

where $A(x)$ is a matrix depending only on x. If $y = 0$ is asymptotically stable, and there exists a compact, inflowing manifold B for the flow of $x' = f(x)$, then (2.31) is uniformly asymptotically stable for all initial conditions $(x_0, y_0) \in B \times \mathbb{R}^n$

Proof: The flow on the entire space is a linear extension of the flow of the equation $x' = f(x)$, and hence we are in a position to use theorem 2.4.4. The only problem is that the set B is only positively invariant, while the theorem assumes that B is invariant. This can be circumvented by creating a boundaryless double of the manifold B. Since B is compact and inflowing, it can be extended by a uniform amount in a backwards direction to $B_{-\epsilon} \supset B$. A copy of B_ϵ can be glued to B_ϵ along the boundary to create its boundaryless double D, which is a compact manifold without boundary [45]. We can leave the vector field unchanged in B, and use the same idea as in section 2.2 to extend it to a flow on D. We can now define a linear extension of the flow on D in an arbitrary way, as long as all points approach D in forward time, and it agrees with the original extension on $B \subset D$. The manifold D is compact and invariant, so that the extension is hyperbolic by theorem 2.4.4. It follows directly from the definition of hyperblic linear extensions that the system (2.31) is uniformly asymptotically stable. $\diamondsuit$

Corollary 2.4.6 *Assume that there is a coordinate system in a neighborhood of a compact, inflowing manifold M in which the equations of motion take the form*

$$x' = f(x) \tag{2.32}$$

$$y' = g(x, y) \tag{2.33}$$

where $g(x, 0) = 0$, so that M corresponds to the set $y = 0$. If the linearization of these equations around M

$$y' = D_y(x, 0)y \tag{2.34}$$

has $y = 0$ as an asymptotically stable point for any orbit in the manifold M, then the manifold M is uniformly asymptotically stable under the flow of (2.33).

Proof: This is a direct consequence of proposition 2.4.5, and the fact that the uniformly asymptotic stability of the origin in (2.34) implies the uniform asymptotic stability of the non-autonomous equation (2.33) as shown in theorem III.2.3 of [59]. $\diamondsuit$

It is not possible to conclude the stability of the synchronization manifold using this approach in general. The following is a counterexample to a method developed in [58] based on such an assumption:

Example 2.4.7 For the coupled pair of systems

$$\begin{aligned} x' &= F(x,t) \\ y' &= F(y,t) + E(x-y) \end{aligned} \tag{2.35}$$

with $E(0) = 0$, the diagonal $\Delta = \{x, y \in \mathbb{R}^{2n} : x = y\}$ is an invariant manifold. If we let $w = x - y$, then the dynamics in the direction transversal to Δ are governed by

$$w' = F(x,t) - F(y,t) - E(x-y) \tag{2.36}$$

This equation can be linearized around Δ to

$$w' = [D_x F(x,t) + DE(0)]w \tag{2.37}$$

In [58] it is assumed that the asymptotic stability of the origin in (2.37) implies the asymptotic stability of the origin of (2.36). As mentioned in the proof of corollary 2.4.6, it needs to be assumed that the system (2.37) is *uniformly asymptotically stable* for this statement to hold.

The following counterexample is an adaptation of example III.2.14 in [59]. Consider the following pair of coupled systems:

$$\begin{aligned} x_1' &= -ax_1 \\ x_2' &= (-2a + \sin(\ln t) + \cos(\ln t))x_2 \\ y_1' &= -ay_1 \\ y_2' &= (-2a + \sin(\ln t) + \cos(\ln t))y_2 - (x_1 - y_1)^2 \end{aligned} \tag{2.38}$$

with $a > \frac{1}{2}$. In this case the linearized system (2.37) takes the form

$$\begin{aligned} w_1' &= -aw_1 \\ w_2' &= (-2a + \sin(\ln t) + \cos(\ln t))w_2. \end{aligned} \tag{2.39}$$

The independent solutions to these equations are:

$$\begin{aligned} w_1(t) &= \exp(-2at) \\ w_2(t) &= \exp(-2at + t\sin(\ln t)). \end{aligned} \tag{2.40}$$

Therefore the linearized system (2.37) has the origin as an asymptotically stable point. The solutions of the equations describing the driving system (x_1, x_2) have the same solutions, so that we can choose an $\epsilon > 0$ and $\Delta_\epsilon = \{(x,y) \in \Delta : |x| < \epsilon\}$ as a candidate for the synchronization manifold.

Notice that the origin is not uniformly asymptotically stable for equations (2.40). The full equations describing the motion transversal to the synchronization manifold in this case take the form

$$\begin{aligned} w_1' &= -aw_1 \\ w_2' &= (-2a + \sin(\ln t) + \cos(\ln t))w_2 + w_1^2. \end{aligned} \tag{2.41}$$

It can be shown that these equations have the origin as an unstable fixed point [59]. It follows that the response system y will not synchronize to the drive x despite the asymptotic stability of the linearized system.

By the Uniformity Lemma 2.2.3, if $a > \sup_{m \in M} \log \nu_X^*(m)$, then there are constants $\hat{a} < a$ and c such that $\|\pi DF^t(m)|_N\| < c\hat{a}^t$ for all $m \in M_\epsilon$, and $t \geq 0$. Therefore despite the fact that ν^* depends on the asymptotics of the dynamics, it also provides an *uniform* estimate on the rate of contraction normal to the synchronization manifold.

The normal Lyapunov exponents and $\nu^*(m)$ only determine the stability of the manifold in an infinitesimal neighborhood. In pathological situations it is possible that the basin of attraction is very small in the normal direction, so that a small amount of noise may desynchronize the systems.

Blakely, et. al. [60] also provide an example of two phase locked periodically oscillating systems coupled in such a way that the stable eigenvectors of the fixed point of the Poincaré section are non-normal. In this situation the ϵ-spectrum of the return matrix is large, and hence small perturbations of the system have a large influence on its stability. Experimental observation indicate that two physical systems of this type are very difficult to synchronize. The authors propose to use the distance from the synchronization manifold in the normal direction $(d(x(t), M))^2$ as a quadratic Lyapunov function for the system. It is not clear whether this example is relevant to a wide class of couplings and systems. It is also unclear when desynchronization in chaotic systems is due to non-normality, to positive normal Lyapunov exponentes, or to both.

2.4.2 The Second Generalized Lyapunov Number σ

Mañe has shown that the conditions of theorem 2.2.1 are also necessary for a manifold M to persist as a smooth manifold under perturbations [44]. In particular the second Lyapunov number must satisfy $\sigma(p) < 1/r$ for all $p \in M$, that is the attraction in the normal direction must be r times exponentially stronger then the attraction inside the manifold.

The importance of this condition is demonstrated by Hunt, Ott and Yorke [61]. The results of this paper imply that in the case of unidirectionally coupled system if $\sigma(p) > 1$ for any point on the synchronization manifold M, the manifold will generically persist only as a non-differentiable, Hölder continuous manifold under perturbations. Moreover, the Hölder exponent of the synchronization manifold also depends on the strength of the coupling between the systems. These results will be discussed further in section 2.5. A similar example of an attracting torus which is not normally hyperbolic and bifurcates into an attractor which is not even a topological manifold is provided in [62].

Remark 2.4.8 Examples in [46] suggest that if for a synchronization manifold $\sup_{p \in M} \nu(p) < 1$, but the condition $\sup_{p \in M} \sigma(p) < 1$ is not satisfied, then a small perturbation of the system may result in intermittent desynchronization. Considering the results discussed in this section, it is more likely that this is a consequence of $\nu(p)$ being greater than 1 for some p on the perturbed manifold.

The fact that $\sup_{p \in M} \sigma(p) < 1$ would more likely result in the non-differentiability of the perturbed manifold.

2.5 Extensions

The definitions of the previous section can be directly extended to cover more complex situations in larger networks of systems.

Consider a network of coupled systems $x_1, x_2, \ldots, x_N$ where $x_i \in \mathbb{R}^{n_i}$. The entire system evolves in $\mathbb{R}^K$, where $K = \sum_{i=1}^{N} n_i$. We can consider the natural projections $\Pi_i : \mathbb{R}^{Nn} \to \mathbb{R}^{n_i}$ onto the phase space of the networks i-th system. Assume that the evolution of the system is determined by

$$x_i' = f_i(x_1, \ldots x_N) \qquad f_i : \mathbb{R}^K \to \mathbb{R}^{n_i}. \tag{2.42}$$

More general types of synchronization may occur in such extended networks. If only a subset of the systems comprising the network are synchronized, as illustrated in example 1.1.6, we can talk about partial synchronization. In the following definition partial synchronization is defined in terms of the existence of a diffeomorphism from the neighborhood of the attractor of one system in the network to the attractor of another, i.e. knowledge of the state of x_j is sufficient to predict the state of x_i. In particular we want such a diffeomorphism to exist regardless in what state the remainder of the network is. For this purpose we introduce the following "section" of $\mathbb{R}^K$: let $c \in \mathbb{R}^{K-n_i+n_j}$ and define

$$S_{i,j}(c) = \{(x_1, x_2, \ldots, x_N) \in \mathbb{R}^K : (x_1, \ldots, \hat{x}_i, \ldots, \hat{x}_j, \ldots, x_N) = c\}$$

where $\hat{x}_i$ means that the i-th vector is omitted.

Definition 2.5.1 *The system i is synchronized to the system j in the network (2.42) if there exists a compact, smooth synchronization manifold M with boundary which is invariant under the flow, inflowing, locally attracting, and such that the projection Π_j of $M \cap S_{i,j}(c)$ is smooth and one-to-one for all $c \in \mathbb{R}^{K-n_i+n_j}$. The synchronization is stable if M is r-normally hyperbolic for $k \geq 1$. A network for which these conditions hold for a subset of L systems where $L < N$ is called* partially synchronized.

This definition is rather weak. It only requires that there exists a smooth map from system i to system j, regardless in what state the remainder of the network is. Thus many coherent states of the system are covered by this definition, in particular stable fixed and phase locked states. The following example shows that this relation is not necessarily reflexive.

Example 2.5.2 Consider the following system

$$x' = g(x), \qquad x \in \mathbb{R}^n, \qquad n > 1 \tag{2.43}$$

$$y' = -ky + \epsilon\, c(x), \qquad y \in \mathbb{R} \tag{2.44}$$

where g and c are C^1 and the unit ball $B_1 \subset \mathbb{R}^n$ is inflowing invariant for equation (2.44). For small ϵ and sufficiently large k the manifold $M = B_1 \times \{0\}$ persists as an invariant manifold of the coupled system, and moreover its projection onto the phase space of x is smooth and one-to-one. However the projection onto the one-dimensional phase space of y will not be even finite-to-one. Therefore for small ϵ, y will be synchronized to x, but x will not be synchronized to y.

As this example indicates, we cannot expect mutual synchronization given two coupled systems which require a different number of variables to be fully described.

Example 2.5.3 System-subsystem synchronization may be viewed as synchronization in the sense of definition 2.5.1. In particular the systems (u, v) and $\hat{v}$ in equation (1.2) are synchronized if there is a compact submanifold M of the graph of the function $\Phi : \mathbb{R}^n \to \mathbb{R}^m$ defined by $\Phi(u, v) = v$ which is a synchronization manifold.

If $L = N$ so that all projections Π_i are smooth and one-to-one then the entire network is synchronized. Knowledge of the behavior of each system determines the behavior of the rest of the network. In the case $L < N$, only a subset consisting of L systems is synchronized. The behavior of each system in this subset can be used to predict the behavior of other systems in the synchronized group.

The most direct way of showing existence of invariant manifolds is applicable to networks with certain symmetries. Let Γ be a group acting on the phase space of the entire network $\mathbb{R}^K$ so that the induced action on the tangent space leaves the vector field defined by (2.42) invariant. If $\text{Fix}(\Gamma) = \{x \in \mathbb{R}^K : \Gamma x = x\}$ is a manifold then it will be invariant under the flow of the equations (2.42). For $\text{Fix}(\Gamma)$ to be a synchronization manifold it needs to satisfy the remaining conditions given in 2.5.1.

The simplest example of such an action is the group $\Gamma = \{\text{Id}, x \to y\}$ acting on the coupled pair of systems

$$x' = f(x, y) + c(x, y) \quad y' = f(y, x) + c(x, y) \quad x, y \in \mathbb{R}^n \tag{2.45}$$

where $c(x, y) = c(y, x)$. In this case $\text{Fix}(\Gamma) = \{(x, y) \in \mathbb{R}^{2n} : x = y\}$.

Notice that if Γ has a subgroup S, then $\text{Fix}(S) \supset \text{Fix}(\Gamma)$. It can happen that as parameters are changed, the manifold $\text{Fix}(\Gamma)$ looses stability, while $\text{Fix}(S)$ remains stable. This occurs when $\text{Fix}(\Gamma)$ looses stability in $\text{Fix}(S)$, but not in the direction normal to $\text{Fix}(S)$. In this case synchronization in large clusters of oscillators breaks down to synchronization of smaller clusters. In particular, if Γ has many subgroups $S_1, \dots S_n$, the subgroups of smaller order can correspond to invariant manifolds of higher dimensions, and therefore to smaller synchronization clusters. This situation was examined recently by Ashwin and Terry [49].

The following is a physically relevant example of strict partial synchronization:

Example 2.5.4 In [48] a system of three lasers modeled by equations of the following was analyzed

$$\begin{aligned} x_1' &= f(x_1, x_2) \\ x_2' &= g(x_1, x_2, x_3) \qquad\qquad x_1, x_2, x_3 \in \mathbb{R}^n \\ x_3' &= f(x_3, x_2) \end{aligned} \tag{2.46}$$

where $g(x_1, x_2, x_3) = g(x_3, x_2, x_1)$. The system is invariant under the transformation $\mu(x_1, x_2, x_3) = (x_3, x_2, x_1)$ so that the manifold $N = \text{Fix}(\mu) = \{(x_1, x_2, x_3) \in \mathbb{R}^{3n} : x_1 = x_3\}$ is invariant. If N contains an inflowing attracting submanifold M, the conditions of definition 2.5.1 are satisfied. It is clear that in this case M is the graph of the identity map between the phase spaces of system x_1 and x_3.

On M the equations reduce to

$$x_1' = f(x_1, x_2) \quad x_2' = g(x_1, x_2, x_1) \tag{2.47}$$

and without further assumptions this system does not have any further invariant manifolds. In the particular case considered in [48] it is shown that in particular $\{(x_1, x_2, x_3) \in \mathbb{R}^{3n} : x_1 = x_2 = x_3\}$ is not an invariant manifold, and hence synchronization of all three lasers is not possible.

Numerically it is observed that the two outer lasers x_1 and x_3, are synchronized, while they do not synchronize with x_2. From a physical viewpoint this might seem peculiar since x_1 and x_3 are not coupled to each other directly, but only indirectly through the middle laser x_2.

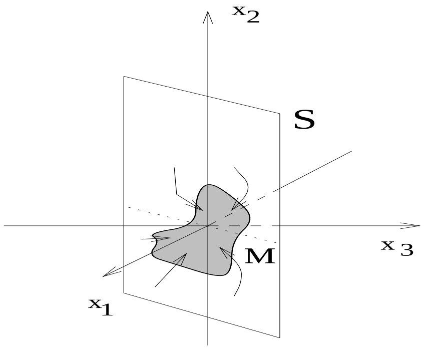

Figure 2.4: A schematic representation of the situation in example 2.5.4. The shaded area corresponds to the synchronization manifold.

Another similar example of partial synchronization in a network of three discrete dynamical systems is given in [3].

Example 2.5.5 Consider the two coupled Lorenz systems of example 2.1.6 with a coupling sufficiently strong to put them in a synchronization regime. This small network can now be expanded by adding more systems. If the connections are sufficiently weak, the small interactions will not destroy the synchronization manifold, oscillators 1 and 2 will remain synchronized, and thus the network will be partially synchronized while the remainder of the network will be desynchronized.

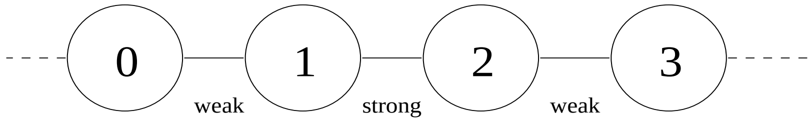

Figure 2.5: A schematic diagram of the extended network in example 2.5.5

Remark 2.5.6 Partial sub-synchronization of two systems can be defined similarly. For instance we could talk about partial synchrony of $x = (x_1, x_2, \ldots, x_n)$ and $y = (y_1, y_2, \ldots, y_m)$ if a subset of the variables of each system are synchronized to each other. System-subsystem synchronization may be understood in this context. In the notation of example 1.1.2, the variables y and $\hat{y}$, and z and $\hat{z}$ of the Lorenz equations are synchronized. There are also examples of systems in which the slow variables are approximately synchronized, while the fast variables are not [29].

The condition that the projections Π_i are one-to-one can be further weakened.

Definition 2.5.7 *If the projection Π_j of $M \cap S_{i,j}(c)$ in definition 2.5.1 is smooth and n-to-one for all $c \in \mathbb{R}^{K-n_i+n_j}$ then system i is* partially phase locked *to system j. If, moreover, the projections Π_i of $M \cap S_{i,j}(c)$ is smooth and m-to-one for all $c \in \mathbb{R}^{K-n_i+n_j}$ then the systems i and j are $n : m$* phase locked.

In this case the manifold M is only locally a graph of a smooth map from system i to j. A simple example is the $n : m$ phase locking of phase oscillators. In [26], the auxiliary method was used to show that a chaotically driven chaotic circuit synchronizes to the driving signal. In one case, the projection of the synchronization manifold onto the phase space of the driven system is 2:1. In more general instances of phase locking of chaotic systems such as the ones examined in [27] and [28], a synchronization manifold may not exist. In this case the above definitions cannot be used directly. The case of $n : m$ synchronization between uni-directionally coupled systems is discussed further in section 2.7.

Remark 2.5.8 These definitions apply only to autonomous systems, so that example 1 is not covered directly. In this case we may think of the system as evolving in $S^1 \times \mathbb{R}^2 \times \mathbb{R}^2$, and the role of the synchronization manifold is played by $M = S^1 \times D$, where $D = \{x_1, x_2, y_1, y_2 | x_1 = x_2, y_1 = y_2\}$. In general a network of N periodically or quasi-periodically driven systems evolves in $\mathbb{T}^{mN} \times \mathbb{R}^K$ for some integer M. This network will be (partially) synchronized if there exists a submanifold $M = \mathbb{T}^N \times N$ where N satisfies the conditions of definition 2.5.1 or 2.5.7. The synchronization will again be stable if M is r-normally hyperbolic.

The case of more general non-autonomous systems is more problematic. For instance, given coupled non-autonomous systems

$$x' = f(x, y, t) \quad y' = g(x, y, t) \tag{2.48}$$

the synchronization manifold needs to be defined as $\mathbb{R} \times N$ where N again satisfies definitions 2.5.1 or 2.5.7. However, this manifold is not compact, and thus the results from [38] do not carry over directly. Extensions of the theory to non-compact invariant manifolds do exist, but some further uniformity in the vector field and the invariant manifold need to be assumed [63].

2.6 Equivalence of Unidirectional and Bidirectionally Coupled Synchronized Systems

In this section it will be assumed that the normal bundle N of the synchronization manifold M is invariant. This means that $DF^t(N_p) \subset N_{F^t(p)}$ in the notation of section 2.2.

Example 2.6.1 Consider the case of two identical, symmetrically coupled systems

$$\begin{aligned} x' &= f(x) + c(x, y) \\ y' &= f(y) + c(y, x) \qquad x, y \in \mathbb{R}^n \end{aligned} \tag{2.49}$$

where $c(x, y) = -c(y, x)$. The diagonal $\Delta = \{(x, y) \in \mathbb{R}^{2n} : x = y\}$ is invariant since it is fixed under the involution $I(x, y) = (y, x)$ which leaves the system invariant. Define a change of coordinates

$\chi = x - y$ and $\eta = x + y$, for which equations (2.49) become

$$\begin{aligned} \chi' &= f(\frac{\chi+\eta}{2}) - f(\frac{\eta-\chi}{2}) + 2c(x,y) \\ \eta' &= f(\frac{\chi+\eta}{2}) + f(\frac{\eta-\chi}{2}). \end{aligned} \tag{2.50}$$

By assumption $c(x,x) = 0$, so that close to the diagonal $c(x,y) = c_x(x,x)\chi + \text{h.o.t.}$ Therefore the linearization of the system around $\chi = 0$, along a trajectory $(0, \eta_0(t)$ takes the form

$$\begin{aligned} \chi' &= [Df(\eta_0(t)) + kc_x(\eta_0(t), \eta_0(t))]\ \chi \\ \eta' &= Df(\eta_0(t))\ \eta \end{aligned} \tag{2.51}$$

These equations leave invariant the normal bundle $\tilde{N}$ with basis vectors $\frac{\partial}{\partial \eta_i}$. Therefore there is an invariant splitting of the tangent space of Δ defined by $T\mathbb{R}^{2n}|_\Delta = T\Delta + N$, where N has basis vectors $\frac{\partial}{\partial x_i} + \frac{\partial}{\partial y_i}$.

Remark 2.6.2 The normal bundle of the synchronization manifold can not always be chosen to be invariant. Sufficient conditions for the existence of an invariant normal bundle are investigated in [38].

Normal r-hyperbolicity of the overflowing synchronization manifold M implies other useful properties of the dynamics in the vicinity of M. In particular if $p \in M$, there is a manifold $W^s(p)$ such that if $x \in W^s(p)$ then $d(F^t(x), F^t(p)) \le Ce^{-\nu^*(p)t}$ as $t \to \infty$ where $\nu^*(p)$ is the normal Lyapunov exponent defined in section 2.2. Here we will consider only the case in which $W^s(p)$ depend smoothly on the base point p and fiber the stable manifold of M.

Let us define

$$v^t = DF^t(m)v_0 \tag{2.52}$$

$$\hat{v}^t = DF^t(m)\hat{v}_0 \tag{2.53}$$

$$w^t = \pi DF^t(m)w_0 \tag{2.54}$$

where π again denotes the projection of a vector in TM onto the normal bundle N, we define:

$$\begin{aligned} \rho(m) &= \inf\{\rho > 0 : [|w^t|/|v^t|]/\rho^t \to 0 \ \text{ as } \ t \to \infty \ \text{ for all } \ w_0 \in N, v_0 \in TM\} = \\ &= \limsup_{t\to\infty} \|DF^{-t}|_{TM}(F^t(m))\|^{\frac{1}{t}} \|\pi DF^t(m)|_N\|^{\frac{1}{t}} \end{aligned} \tag{2.55}$$

$$\tau(m) = \inf\{\tau > 1 : [|w^t|/|v^t|]^\tau/|\hat{v}^t| \to 0 \text{ as } t \to \infty \text{ for all } w_0 \in N, \text{ and } v_0, \hat{v}_0 \in TM\} \tag{2.56}$$

If $\nu^*(m) < 1$ and $\rho(m) < 1$ for all $m \in M$ the manifold M is called a manifold with *contracting structure*[2]. The following theorem from [39], [40] relates the generalized Lyapunov numbers $\rho(m)$ and $\tau(m)$ and the existence and smoothness of the fibers $W^s(p)$.

Theorem 2.6.3 (Fenichel 1974,1977) *Let M be a C^r manifold with boundary, inflowing invariant with contracting structure under the flow of a C^r vector field X, where $r \ge 2$. Then there exist a unique invariant family $\mathcal{W} = \{W^s(p) : p \in M\}$ of C^r manifolds such that each $W^s(p)$ is tangent to N_p at p. If moreover $\tau(p) < 1/r'$ for all $p \in M$, where $1 \le r' \le r-1$ then the dependence of the family $\mathcal{W}$ on the base point p is $C^{r'}$.*

[2] An overflowing manifold with expanding structure was considered in [39], [40]. By reversing the direction of the flow we can use the theory developed in these articles.

In this context uniqueness means that if $\tilde{\mathcal{W}} = \{\tilde{W}^s(p) : p \in M\}$ is another family of invariant manifolds that fiber the stable manifold of M in some neighborhood of M, then $\tilde{\mathcal{W}} \cap \mathcal{W} = \{\tilde{W}^s(p) \cap W^s(p) : p \in M\}$ is an invariant family with the same properties.

Proof: The only part of the theorem which is not proved explicitly in [39], [40] is the uniqueness of the foliation. It is a consequence of the fact that the contraction within each fiber is faster than the contraction in the manifold. In particular, if $q \in W^s(p)$ and $q' \in W^s(p')$ then

$$\frac{||F^t(q) - F^t(p)||}{||F^t(q') - F^t(p)||} \to 0 \qquad \text{as} \qquad t \to \infty \tag{2.57}$$

If there exists another foliation $\tilde{W}^s$ of the stable manifold of the synchronization manifold in a neighborhood of M containing q and p with the properties given in the theorem, then there exist $p, p' \in M$, and q, q' such that $q \in W^s(p)$, $q \notin \tilde{W}^s(p)$ $q' \in \tilde{W}^s(p)$, and $q' \in W^s(p')$. Considering the new foliation, we obtain the equivalent of (2.57):

$$\frac{||F^t(q') - F^t(p)||}{||F^t(q) - F^t(p)||} \to 0 \qquad \text{as} \qquad t \to \infty \tag{2.58}$$

However (2.57) and (2.58) can not hold simultaneously. $\diamondsuit$

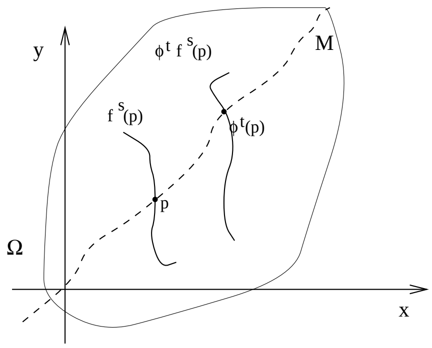

Figure 2.6: A schematic representation of the invariant foliation

Let us again consider a pair of coupled systems described by

$$x' = f(x, y) \quad y' = g(x, y) \tag{2.59}$$

The coupling between the two systems is *unidirectional* if one of the equations is independent of the other, i.e. either $f(x, y) = f(x)$, or $g(x, y) = g(y)$. The coupling can be unidirectional in only part of the phase space. Physically this would mean that in part of the phase space the behavior of one system has no influence on the behavior of the other. An example of this situation is provided by two electrical circuits coupled through a diode: only if the voltage difference between the circuits remains below a certain threshold may the coupling be viewed as unidirectional. The following definition makes this notion precise

Definition 2.6.4 *The two systems in (2.59) are said to be unidirectionally coupled on $\Omega \subset \mathbb{R}^n \times \mathbb{R}^n$ if $g(x, y)$ is independent of x for each $y \in \Pi^2(\Omega)$ or if $f(x, y)$ is independent of y for each $x \in \Pi^1(\Omega)$.*

In this situation manifolds $W^s(p)$ which are pieces of affine spaces will be of particular importance.

Definition 2.6.5 *If there exists an open set $\Omega \subset \mathbb{R}^{2n}$ such that $W^s(p) = \{p\} \times \mathbb{R}^n \cap \Omega$ or $W^s(p) = \mathbb{R}^n \times \{p\} \cap \Omega$ then the fiber $W^s(p)$ is called* straight on Ω.

Straight fibers are directly related to unidirectional synchronization as the statement of the following lemma shows.

Lemma 2.6.6 *Assume the two systems in (2.59) are stably synchronized so that the synchronization manifold M has contracting structure. The fibers $W^s(p)$ are straight in an open set Ω such that $\Omega \cap M = M$ if, and only if the coupling is unidirectional.*

Proof: Assume that $f(x, y)$ depends on y in any open set Ω intersecting M. This means that there exists a point $p = (x_0, y_0) \in M$ and points $(x_0, y_1), (x_0, y_2)$ such that the x components of the vector field at (x_0, y_1) and (x_0, y_2) are different. If these two points belong to $W^s(p)$ then $F^t((x_0, y_i)) \in W^s(F^t(p))$ for $i = 1, 2$. Since the x components of the points in this fiber evolve as $x(t) = x(0) + f(x(0), y_i(0))t + \mathcal{O}(t^2)$, it follows that after some small time t, $\Pi_x F^t(x_0, y_1) \neq \Pi_x F^t(x_0, y_2)$, where Π_x denotes projection on the first coordinate. Therefore $F^t(W^s(p))$ is not straight.

On the other hand, if the coupling is unidirectional in a set $\tilde{\Omega}$ satisfying the assumptions, then the system is described by

$$x' = f(x) \quad y' = g(x, y) \tag{2.60}$$

in the vicinity of M. Therefore the sets $\{p\} \times \mathbb{R}^n$ are an invariant, straight fibration of a neighborhood $\Omega \subset \tilde{\Omega}$ of the synchronization manifold. Since the invariant fibration is unique under the standing assumptions, it follows that this is in fact the only invariant fibration. This proves the converse. $\diamondsuit$

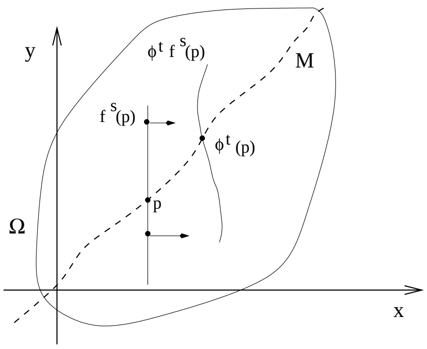

Figure 2.7: If the x component of the vector field is not constant along a fiber $W^s(p)$, then the fiber will not be mapped to a straight fiber under the flow.

This lemma is the essential step in the proof of the following theorem:

Theorem 2.6.7 *Suppose that the conditions of lemma 2.6.6 are satisfied, and that the fibers $W^s(p)$ depend smoothly on $p \in M$, then there exists a smooth change of coordinates in some neighborhood Ω of M which take the original bidirectionally coupled system into a unidirectionally coupled system.*

Proof: Since the fibers $W^s(p)$ are smooth and by the hypothesis of the theorem depend smoothly on $p \in M$, they give a coordinate system in the neighborhood of M in a natural way. The problematic case in which $\{p\} \times \mathbb{R}^n$ is tangent to M resulting in a singularity is ruled out since each $W^s(p)$ is tangent to N_p at p. The fibers $W^s(p)$ are straight in this coordinate system by definition, and so by the previous lemma the coupling is unidirectional. $\diamondsuit$

Remark 2.6.8 Unidirectionally and bidirectionally coupled systems are treated separately in the physical literature. This result shows that if the systems are synchronized, from an abstract viewpoint there is no difference between these two types of couplings.

Example 2.6.9 Consider a unidirectionally coupled system $x_1' = f(x_1)$ and $x_2' = g(x_1, x_2)$, where $x_1, x_2 \in \mathbb{R}^n$. Define a linear change of coordinates by

$$(y_1, y_2) = (\frac{1}{2r}(r+1)x_1 + (r-1)x_2, \frac{1}{2r}(r-1)x_1 + (r+1)x_2 = \xi^{-1} \circ \eta \circ \xi(x_1, x_2)$$

where $\xi(x_1, x_2) = (x_1 - x_2, x_1 + x_2)$ rotates the space so that the diagonal D goes to $\xi_1 = 0$, and $\eta(\xi_1, \xi_2) = (\frac{1}{r}\xi_1, \xi_2)$. The straight fibers go to lines that are at an angle with the ξ_1 axis. The transformation $\eta(\xi_1, \xi_2) = (\xi_1, 2\xi_2)$ tilts the fibers so that they are not straight any longer after we go back by ξ^{-1}. In the new coordinates (y_1, y_2) the fibers will still be pieces of affine spaces, however the angle at which they intersect the diagonal can be controlled by changing r.

In general it is not possible to obtain an explicit description of the manifolds $W^s(p)$ of a bidirectionally coupled system, however this theorem shows that under certain conditions it is sufficient to study unidirectionally coupled systems to obtain some information about bidirectionally coupled systems.

2.7 Unidirectionally Coupled Systems as Extensions

In the preceding section it was shown that frequently bidirectional coupling and unidirectinal coupling are equivalent. In the next two sections we will examine unidirectional couplings with the understanding that under appropriate conditions these results can be carried over to more general situations. In the case of unidirectional coupling the existence of a synchronization manifold can be proved as a direct consequence of results on extensions of flows which can be found in [64] and [35]. Let X be a C^r manifold, and (E, p, X) a vector bundle of class C^r over X. The flow Φ^t on E is an extension of a flow Ψ^t on X if the following diagram commutes

$$\begin{tikzcd} E \arrow[r, "\Phi^t"] \arrow[d, "p"'] & E \arrow[d, "p"] \\ X \arrow[r, "\Psi^t"] & X \end{tikzcd}$$

Consider the unidirectionally coupled system

$$x' = f(x) \qquad y' = g(x,y) \qquad x \in \mathbb{R}^n, y \in \mathbb{R}^m \tag{2.61}$$

Denote by Φ^t the flow of the entire system on $\mathbb{R}^{n+m}$, and by Ψ^t the flow of the driving system x on $\mathbb{R}^n$. If $\mathbb{R}^{n+m}$ is viewed as a trivial vector bundle over $\mathbb{R}^n$, then it is immediate that the above diagram commutes and Φ^t is an extension of Ψ^t.

Using this notation and Theorem 3.1 in [64] we immediately have the following result giving sufficient conditions for the system y to be synchronized to the system x.

Theorem 2.7.1 *If there exists an invariant, inflowing, compact manifold Ω for the flow Ψ^t in $\mathbb{R}^n$, a $T_0 > 0$ and $K < 1$ such that for every $x \in \Omega$ and y_1, y_2*

$$|\Phi^{T_0}(x,y_1) - \Phi^{T_0}(x,y_2)| < K|y_1 - y_2| \tag{2.62}$$

then there exists a unique continuous invariant section $\sigma : \Omega \to \Omega \times \mathbb{R}^m$

In other words, if the conditions of the theorem are satisfied there exists a continuous function Σ with graph σ taking orbits of system x to orbits of system y.

Let $I_c = \{x \in \mathbb{R}^m : |x| < c\}$ and assume that the box $\Omega \times I_c$ is inflowing under the flow of the full system (2.61). If $\lim_{t\to\infty} |\Phi^t(x,y_1) - \Phi^t(x,y_2)| = 0$ for all $x \in \Omega$ and $|y_1|, |y_2| < c$ then we call the system *asymptotically stable* in $\Omega \times I_c$ with respect to the projection p.

Corollary 2.7.2 *Assume that the system (2.61) has an attractor A, is asymptotically stable in $\Omega \times I_c$ with respect to p, and there exists a T_0 such that condition (2.62) is satisfied on set $\Omega \times I_c$. Then there exists a continuous function $F : \mathbb{R}^n \to \mathbb{R}^m$ taking the orbits of system x in the neighborhood of $p(A)$ to the orbits of system y.*

Remark 2.7.3 There is some confusion in the literature about the properties of the function F. In [8] it is claimed that if the system is asymptotically stable on $\Omega \times I_c$ without necessarily satisfying condition (2.62) then an invariant, possibly discontinuous section of the normal bundle exists. In general this may not be true since the function F may be multivalued [67]. Asymptotic stability is in general weaker than condition (2.62). If the system is assumed to be only asymptotically stable in a compact, positively invariant set $B \subset E$, the situation is more complicated, and will be addressed in the next section.

Theorem 2.7.1 does not imply that the map F is smooth, and hence its graph will not necessarily be a synchronization manifold as defined in section 2.1. As discussed in section 2.3, this can be undesirable. Our next task is therefore to introduce conditions that will guarantee the smoothness of this map. We will see that, roughly speaking, the larger the contraction within the fibers, the higher the regularity of the map F, and the synchronization manifold $M = graph(F)$.

Let Ω be an open subset of $\mathbb{R}^n$ with compact closure, overflowing invariant under Ψ^t.

Definition 2.7.4 *The flow Ψ^t is k-*contracting *over Ω if there exist numbers $c > 0$ and $0 < \mu < 1$ such that for $s = 0, 1, \ldots, k$ the following relation holds*

$$\sup_{x\in\Omega}(\|D\Psi^{-t}(x)\|^s \|D\Phi^t|_{T_{\Psi^{-t}(x)}}\|) \leq c\mu^t \;\; \textit{for all} \;\; t > 0 \tag{2.63}$$

where

$$\|D\Phi^t|_{T_{\Psi^{-t}(x)}}\| = \sup\{\|D\Phi^t(w)\| : w \in T_\nu p^{-1}(x) \textit{ where } \nu \in p^{-1}(x), \textit{ and } \|w\| < 1\}. \tag{2.64}$$

This definition simply says that the flow Ψ^t is k-contracting if the rate of contraction within the fibers is k times *exponentially* stronger than the rate of contraction of the flow in the base Ω. The following theorem shows that this is a sufficient condition for the synchronization manifold M to be smooth.

Theorem 2.7.5 (Hirsch, Pugh, Shub 1977) *If the flow Ψ^t is k-contracting over Ω, then there exists a unique C^k smooth Ψ^t invariant section $F : \mathbb{R}^n \to \mathbb{R}^{n+m}$. In other words system y is synchronized to system x, and the synchronization manifold is graph(F).*

Remark 2.7.6 Here we again encounter the same technical difficulty that we encountered in section 2.2, since the manifold Ω is assumed to be overflowing. To apply these results to the case where Ω contains an attractor of the first system we can apply the collaring construction used in section 2.2. This shows that if Ω is inflowing, condition (2.63) needs to be satisfied only on orbits that do not leave Ω in backwards time for theorem 2.7.5 to imply the existence of a unique synchronization manifold $M = \text{graph}(F)$.

If the map F is not differentiable, we can use its Hölder exponent as a measure of regularity. Roughly speaking, the higher the Hölder exponent of the map, the more F looks like a smooth map. One such result can be found in theorem 3.8 of [64]. More useful in the present context is the following theorem announced in [61]. Let $-h_r$ be the least negative past-history Lyapunov exponent of the response system y. Assume that the driving system has $n-1$ positive, and one negative past-history Lyapunov exponent $-h_d$

Theorem 2.7.7 *If $h_r < h_d$ then for a typical systems the Hölder exponent of the map F is equal to $h_r(x)/h_d(x)$.*

A numerical example of a discrete dynamical system in which the map F becomes more regular as the contraction rate is increased is also provided in [61].

Example 2.7.8 A direct method of determining generalized synchronization in physical systems, and numerical models is the auxiliary method introduced in [7]. The method is essentially an application of the theory outlined above.

Given a unidirectionally coupled system $x' = f(x)$, $y' = f(x,y)$, the idea is to consider the auxiliary system $z' = f(x,z)$. It is difficult to experimentally determine whether the systems x, and y are synchronized in a generalized sense. However if the systems y and z synchronize identically, we may conclude that $\lim_{t\to\infty} |\phi^t(x,y_0) - \phi^t(x,z_0)| = 0$, since the flow of the systems (x,y) and (x,z) is the same. If the system x has an attractor, the orbits of the extended system remain uniformly bounded, then there exists a map F taking the attractor of system x to an attractor of system y. If the contraction rate is uniform in the sense of equation (2.62), then the conditions of corollary 2.7.2 are satisfied, and F is continuous.

The regularity of the map F can then be checked using theorems 2.7.5 and 2.7.7. In particular the exponential decay of $|\phi^t(x,y_0) - \phi^t(x,z_0)|$ can be compared to the contraction rates within the attractor $p(A)$ of the driving system. As discussed in section 2.4, non-typical orbits of the attractor of system x may play an important role in such comparisons. In particular the contraction rates would have to be compared for all orbits in the attractor to obtain a true bound on the regularity. This will typically be impossible to do numerically, and analytic techniques, or results similar to those announced in [53] and [54] need to be used.

Also note that for diffusive couplings, an increase in coupling strength is going to result in a higher regularity of the synchronization manifold. For instance consider the following equations

$$x' = f(x) \quad y' = g(y) + K(x-y) \quad z' = g(z) + K(x-z) \tag{2.65}$$

where z plays the role of an auxiliary system, and the driving system has an attractor A. Let $\eta = x - y$ so that

$$\eta' = f(x) - g(y) - K\eta. \tag{2.66}$$

Let $\bar{\Omega}$ be a compact set containing A, and choose $c > 0$ so that $c > \sup\{|x| : x \in \bar{\Omega}\}$.

We want the set $\bar{\Omega} \times I_c$ to be inflowing under the flow of this dynamical system. By compactness K can be defined so that

$$K > \sup_{|y|=c, x\in\Omega} \left[\frac{|f(x) - g(y)|}{|x-y|} \right] \tag{2.67}$$

then η in equation (2.66) will be decreasing for all $|y| = c$ and $x \in \Omega$, which means that $\bar{\Omega} \times I_c$ is inflowing.

Let $\chi = y - z$, so that $\chi' = g(y) - g(z) - k\chi$. Expanding in a Taylor series around y gives

$$\chi' = [D_y g(y) - K]\chi + f(y,z) \tag{2.68}$$

Since $f(y,z) \to 0$ uniformly on the compact set $\bar{\Omega} \times I_c$, by theorem 2.4 of [59] it is sufficient to examine the linear part of equation (2.68). Let $\gamma = \sup_{y\in I_c} |D_y g(y)|$, so that

$$\int_0^t |D_y g(y(s))| \mathrm{d}s \leq \gamma t. \tag{2.69}$$

By Duhamel's formula

$$|\chi(t)| \leq e^{-Kt}|\chi(0)| + \int_0^t e^{-K(t-s)} |D_y g(y(s))||\chi(s)| \mathrm{d}s \tag{2.70}$$

Define $z(t) = e^{Kt}|\chi(0)|$ so that

$$z(t) \leq z(0) + \int_0^t |D_y g(y(s))| z(s) \mathrm{d}s \tag{2.71}$$

and by Gronwall's Inequality

$$z(t) \leq \exp[\int_0^t |D_y g(y(s))| \mathrm{d}s] z(0) \leq e^{\gamma t} z(0). \tag{2.72}$$

Equivalently $\chi(t) \leq e^{(\gamma - K)t}\chi(0)$. Therefore by choosing $K > \gamma$, we get exponential contraction in each of the fibers. Since this construction was independent of the base point of the fibers the rate of contraction within the fibers can be controlled uniformly throughout $\bar{\Omega} \times I_c$. Therefore system y can be synchronized to system x with a synchronization manifold of arbitrarily large smoothness by choosing a sufficiently high value of K.

As shown in the previous section, unidirectional and bidirectional coupling can frequently be thought as the same. Thus the results of this section can frequently be carried over to bidirectional systems.

Example 2.7.9 Consider the system

$$\begin{aligned} x' &= f(x) - \frac{1}{2}c(x,y) \\ y' &= f(y) + \frac{1}{2}c(x,y) \end{aligned} \tag{2.73}$$

where $c(x,x) = 0$. Let $u = y - x$, so that

$$u' = f(x+u) - f(x) + c(x, x+u) - c(x,x) + c(x,x) \tag{2.74}$$

In the vicinity of the diagonal, these equations are a perturbation of the following unidirectionally coupled system

$$\begin{aligned} u' &= Df(x)u + D_2c(x,x)u + c(x,x) \\ x' &= f(x) + c(x,x). \end{aligned} \tag{2.75}$$

In particular if system (2.7.9) has a compact submanifold in the vicinity of $\{(x,u) : u = 0\}$ as a synchronization manifold, then system (2.74) will also be synchronized.

2.8 $n : 1$ Synchronization in Unidirectionally Coupled Systems

Next we consider a unidirectionally coupled system for which the response is uniformly asymptotically stable in a set $B \subset E$. Under these assumptions, there may not exist a function F taking orbits from the drive to the response system, The existence of a more general correspondence will be proved under some mild restrictions. Some of these results are due to I. Bronshteyn [66].

Definition 2.8.1 *Let (E, p, X) be an vector bundle over X, and the flow Φ^t on E an extension of the flow Ψ^t on X. Let A be an attractor of the flow Ψ^t, $\bar{\Omega}$ a compact inflowing set containing A, and B a forward invariant subset of E such that $p(B) = \Omega$. Then B is* uniformly asymptotically stable *with respect to p if:*

1. *For every $\epsilon > 0$ there exists a $\delta > 0$ such that for every $a_1, a_2 \in B$ with $p(a_1) = p(a_2)$ and $d(a_1, a_2) < \delta$ we have $d(\Phi^t(a_1), \Phi^t(a_2)) < \epsilon$ for all $t > 0$.*
2. *For every $\epsilon > 0$, there exists a $\gamma > 0$ such that if $a_1, a_2 \in B$, $p(a_1) = p(a_2)$ and $d(a_1, a_2) < \gamma$, then $d(\Phi^t(a_1), \Phi^t(a_2)) < \epsilon$ for all t.*

These two conditions imply that $\lim_{t\to\infty} d(\Phi^t(a_1), \Phi^t(a_2)) = 0$.

In what follows it will be assumed that A is connected and contains negative semi-orbits that are dense in A. Let M be a minimal subset of A, so that for any $x \in \Omega$ the orbit $\{\Psi^t(x) : t \in \mathbb{R}\}$ is dense in M. Let $\tilde{A}$ be a connected attractor contained in B, and

$$\tilde{A}_0(M) = \tilde{A} \cap p^{-1}(M). \tag{2.76}$$

The following nontrivial lemma is proved in [65]

Lemma 2.8.2 *Under the assumptions of the preceding paragraphs, the map $p : \tilde{A}_0(M) \to M$ is a finite-to-one, local homeomorphism.*

In general, the map $p : \tilde{A}_0(M) \to M$ is not one-to-one. Consider, for instance, the case of a periodically driven phase oscillator which is 2:1 phase locked to the driving signal. The phase portrait of such a system is given in figure 2.8. If B is any closed set contained in the basin of the attracting orbit then the conditions of lemma 2.8.2 are satisfied. In this case the projection $p : \tilde{A}_0(M) \to M$ is two-to-one. In figure 2.8 the set B is represented by a shaded area.

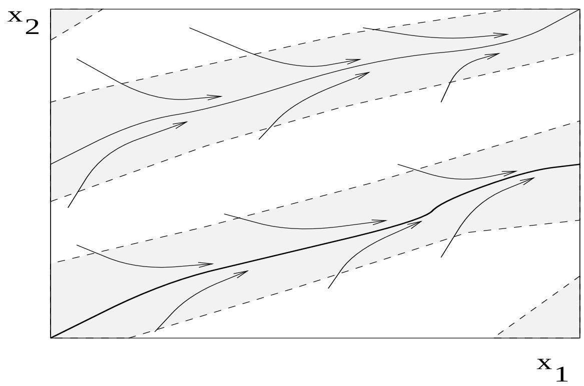

Figure 2.8: A phase portrait of a 2:1 phase locked system. The set B is is represented by the shaded area.

The following theorem uses lemma 2.8.2 to prove some properties of the projection from the attractor of the coupled system $\tilde{A}$ to the attractor of the driving system A.

Theorem 2.8.3 *For each point $a \in A$ the set $p^{-1}(a) \cap \tilde{A}$ consists of a finite number of points. Moreover, the function $a \to card[p^{-1}(a) \cap \tilde{A}]$ is constant on a residual subset of A.*

Proof: Note that for each two points $a_1, a_2 \in B$ such that $a_1 \neq a_2$, and $p(a_1) = p(a_2)$ there exists a $\delta(a_1, a_2)$ such that

$$\inf_{t<0} d(\Phi^t(a_1), \Phi^t(a_2)) \geq \delta(a_1, a_2). \tag{2.77}$$

We can prove this as follows: Let $\epsilon = d(a_1, a_2) > 0$, and δ be as in definition 2.8.1. Seeking a contradiction, assume that there exists a $t_0 < 0$ such that $d(\Phi^{t_0}(a_1), \Phi^{t_0}(a_2)) < \delta$. If we choose $b_1 = \Phi^{t_0}(a_1)$ and $b_2 = \Phi^{t_0}(a_2))$, then $p(b_1) = p(b_2)$ and $d(b_1, b_2) < \delta$. Therefore $d(\Phi^t(b_1), \Phi^t(b_2)) < \epsilon = d(a_1, a_2)$ for all $t > 0$. Choosing $t = -t_0$ gives a contradiction.

Let $x_1, x_2 \in A$ be two points whose negative semiorbits $\{\Psi^t(x_1) : t \leq 0\}$ and $\{\Psi^t(x_2) : t \leq 0\}$ are dense in A. There exists a sequence $\{-t_n\}_{n=0}^{\infty}$ such that $\lim_{n\to\infty} \Psi^{-t_n}(x_1) = x_2$. By compactness, there is a subsequence of the sequence of maps $\{\Phi^{-t_n} : B \to B\}_{n=0}^{\infty}$ which converges to a map $\chi : B \to B$. The map χ is not necessarily continuous. However since any two points $a_1, a_2 \in p^{-1}(x_1)$ remain a distance $\delta(a_1, a_2)$ apart along the backwards orbit, the restriction

$$\chi|_{p^{-1}(x_1)\cap\tilde{A}} : p^{-1}(x_1) \cap \tilde{A} \to p^{-1}(x_2) \cap \tilde{A} \tag{2.78}$$

is injective. Since the same argument can be carried out with x_2 in place of x_1 it follows that $p^{-1}(x_1) \cap \tilde{A}$ and $p^{-1}(x_2) \cap \tilde{A}$ have the same cardinality. Since it was assumed that A contains negative semi-orbits that are dense in A, the set of all orbits with negative orbits that are dense in A is residual in A.

The closure of the negative semiorbit of an arbitrary point $x \in A$ contains a minimal set M. By an argument identical to the one given in the preceding paragraph card$[p^{-1}(x) \cap \tilde{A}] <$ card$[p^{-1}(x_0) \cap \tilde{A}]$. However by lemma 2.8.2 card$[p^{-1}(x_0) \cap \tilde{A}]$ is finite. $\diamondsuit$

Remark 2.8.4 In a general situation we therefore expect that the response is $n : 1$ phase locked to the driving signal. An example of a response that is 2:1 phase locked to a chaotic driving signal is given in [26]. In general, theorem 2.8.3 might be the best possible. Examples in [67] show that even when the response is asymptotically stable, card$[p^{-1}(x) \cap \tilde{A}]$ may not be independent of x. Thus it is possible that the response system is $n(x) : 1$ phase locked to the drive, where $n(x)$ depends on $x \in A$.

Remark 2.8.5 Assume that the attractor A contains periodic orbits, $B = \bar{\Omega} \times I_c$, and B is uniformly asymptotically stable. Then for any $x \in A$ which lies on a periodic orbit card$[p^{-1}(x) \cap \tilde{A}] = 1$. This follows from the fact that I_c is connected, and thus definition 2.8.1 implies that for all $a_1, a_2 \in B$ with $p(a_1) = p(a_2)$ we have $\lim_{t \to \infty} d(\Phi^t(a_1), \Phi^t(a_2)) = 0$. However if card$[p^{-1}(x) \cap \tilde{A}] > 1$, and T_0 is the period of the orbit $\mathcal{O}(x)$, then $d(\Phi^{nT_0}(a_1), \Phi^{nT_0}(a_2)) = d(a_1, a_2) > 0$ for all $n \in \mathbb{Z}$.

By an argument identical to the one given in the proof of theorem 2.8.3, only points with no periodic orbit in the closure of their backwards orbits could have card$[p^{-1}(x) \cap \tilde{A}] > 1$. This fact seems to have been misinterpreted in some references.

2.9 Synchronization from the Viewpoint of Geometric Singular Perturbation Theory

It was pointed out in section 2.5 that invariant manifolds can be found in networks of coupled systems as the fixed spaces of groups of symmetries. A different approach is needed to show synchronization in networks without such symmetries. In this section it is shown that geometric singular perturbation theory can be applied to prove the existence of synchronization manifolds in diffusively coupled systems for large coupling coefficients.

Geometric singular perturbation theory applies to systems that have intrinsic slow and fast motions [88]. Frequently the equations governing the behavior of such a system can be written in the form

$$\begin{aligned} x' &= f(x, y, \epsilon) \\ y' &= \epsilon g(x, y, \epsilon). \end{aligned} \tag{2.79}$$

Under the change of timescale $t = \epsilon\tau$, these equations can be rewritten as

$$\begin{aligned} \epsilon\dot{x} &= f(x, y, \epsilon) \\ \dot{y} &= g(x, y, \epsilon) \end{aligned} \tag{2.80}$$

where $\dot{x}$ denotes differentiation with respect to the new time τ. The system (2.79) is usually referred to as the fast system, while (2.80) is called the slow system. The main idea of geometric singular perturbation theory is to look at both equation (2.79) as $\epsilon \to 0$ obtaining

$$\begin{aligned} x' &= f(x,y,0) \\ y' &= 0 \end{aligned} \tag{2.81}$$

and equation (2.80) as $\epsilon \to 0$ obtaining

$$\begin{aligned} 0 &= f(x,y,0) \\ \dot{y} &= g(x,y,0). \end{aligned} \tag{2.82}$$

Let M_0 be a bounded submanifold of the set $\{f(x,y,0) = 0\}$. Let l be the codimension of M_0 in the phase space of the entire system. M_0 is a normally hyperbolic manifold for the flow of (2.81) if the linearization of (2.81) around each critical point comprising the manifold M_0 has exactly l eigenvalues that do not lie on the imaginary axis. We can therefore use Fenichel's Theorem 2.2.1 to conclude that

Corollary 2.9.1 *If M_0 is a compact manifold with boundary which is normally hyperbolic at $\epsilon = 0$, then for a sufficiently small ϵ, there exists a manifold M_ϵ that lies within $\mathcal{O}(\epsilon)$ of M_0, is diffeomorphic to M_0, and is locally invariant under the flow of (2.79).*

Remark 2.9.2 This result does not follow directly from theorem 2.2.1 since M_0 is neither inflowing nor overflowing invariant. In [41] a trick similar to the collaring argument given in section 2.2 is used to show that theorem 2.2.1 can be applied to a subset of M_0.

M_0 is always locally a graph of a function $h^0(y)$ by the condition of normal hyperbolicity. We will assume that this is true globally, so that $M_0 = \{(x,y) : x = h^0(y)\}$, which will always be the case in the present case. By corollary 2.9.1 there exists a function h^ϵ such that the graph $M_\epsilon = \{(x,y) : x = h^\epsilon(y)\}$ is locally invariant under the flow of (2.79).

Using the function h^ϵ we may describe the slow motion on the invariant manifold M_ϵ by

$$\dot{y} = g(h^\epsilon(y), y, \epsilon) \tag{2.83}$$

and since $h^0(y) = h^\epsilon + \mathcal{O}(\epsilon)$ the original equation (2.79) can thus studied using regular perturbation techniques.

These ideas can be carried over to the case of diffusively coupled systems by perturbing from an infinitely strong coupling. Let us again consider a network of coupled systems. Following the notation of section 2.5 the network can be described by the equation systems $z_1, z_2, \ldots, z_N$ where $z_i \in \mathbb{R}^{n_i}$ with

$$z_i' = f_i(z_1, \ldots z_N) \qquad f_i : \mathbb{R}^K \to \mathbb{R}^{n_i}. \tag{2.84}$$

Following definition 2.5.1, let M_0 be a compact manifold with boundary such that Π_j of $M_0 \cap S_{i,j}(c)$ is smooth and one-to-one for all $c \in \mathbb{R}^{K-n_i+n_j}$ for at least one pair (i,j). Assume that there exists a change of coordinates around M_0 such that the equations (2.84) take the form

$$\begin{aligned} \dot{x} &= f(x,y) - ckx \\ \dot{y} &= g(x,y) \end{aligned} \tag{2.85}$$

where c is a parameter that controls the strength of the coupling, and k is a constant. Dividing by c gives

$$\begin{aligned} \epsilon\dot{x} &= \epsilon f(x,y) - kx \\ \dot{y} &= g(x,y) \end{aligned} \tag{2.86}$$

where $\epsilon = 1/c$. This is exactly the slow system to which singular perturbation theory can be applied. The corresponding fast system is

$$\begin{aligned} x' &= \epsilon f(x,y) - kx \\ y' &= \epsilon g(x,y) \end{aligned} \tag{2.87}$$

If we let $\epsilon \to 0$ from the fast system we obtain

$$\begin{aligned} x' &= -kx \\ y' &= 0 \end{aligned} \tag{2.88}$$

so that the condition of normal hyperbolicity is satisfied automatically. The slow system becomes

$$\begin{aligned} 0 &= x \\ \dot{y} &= g(x,y) \end{aligned} \tag{2.89}$$

which describes the motion on the slow manifold $x = 0$. The results of geometric singular perturbation theory can now be applied directly to conclude that for a sufficiently large coupling parameter c there exists a manifold M_ϵ which is $\mathcal{O}(\epsilon)$ close to M. If M_ϵ is inflowing, it satisfies all conditions of definition 2.5.1, and it can be concluded that system i is synchronized to system j. However if M is an inflowing manifold for (2.89), and remains inflowing under small perturbations, then we can conclude that M_ϵ is an inflowing manifold.

Although the conditions that were assumed on the coupling seem rather special, it will be shown that they cover many examples in the literature.

The same argument can be repeated for a more general case.

Proposition 2.9.3 *Assume that there is a change of coordinates such that in a compact neighborhood K of M_0, equation (2.84) can be written as*

$$\begin{aligned} \dot{x} &= f(x,y) - \Omega(x,y,c) \\ \dot{y} &= g(x,y). \end{aligned} \tag{2.90}$$

If there exists a C^1 monotonically increasing function $m(c)$, such that $\lim_{c\to\infty} = \infty$ and $\lim_{c\to\infty} \frac{\Omega(x,y,c)}{m(c)} = \omega(x,y)$ uniformly in the C^1 topology, and $\omega(0,y) = 0$. If $\omega_i(x,y) > 0$ for all components ω_i of ω and all $(x,y) \in K$, then for a sufficiently large coupling c, there exists a manifold M_ϵ locally invariant under the flow of (2.90).

Proof: We can again write

$$\begin{aligned} \epsilon\dot{x} &= \epsilon f(x,y) - \frac{\Omega(x,y,c)}{m(c)} \\ \dot{y} &= g(x,y). \end{aligned} \tag{2.91}$$

and by an argument equivalent to the one given above, we can view this as a perturbation problem from $\epsilon = 1/m(c) = 0$. Since in this limit the fast equations have the form

$$\dot{x} = -\omega(x,y) \qquad \dot{y} = 0 \tag{2.92}$$

the manifold $M_0 = \{(x,y) : x = 0\}$ is normally hyperbolic if $\omega_i(x,y) > 0$ for all components ω_i of ω and all $(x,y) \in K$. $\diamondsuit$

As will be shown in the following examples, this approach is very similar to the one adopted in [9] for systems with linear couplings. The main advantage of using geometric singular perturbation theory is that it is not necessary to assume that M_ϵ is an inflowing manifold, rather this can be concluded from the fact that M_0 is inflowing.

The following simple example demonstrates these ideas

Example 2.9.4 Consider a pair of coupled systems

$$\begin{aligned} x' &= f(x,y) - c(x-y) \\ y' &= g(x,y) - c(y-x) \qquad x, y \in \mathbb{R}^n \end{aligned} \tag{2.93}$$

Without any assumptions on f and g we can not use symmetry to prove the existence of an invariant manifold. However if we let $\eta = x - y$, and $\chi = x + y$, then the equations (2.93) can be written as

$$\begin{aligned} \epsilon\eta' &= \epsilon(\tilde{f}(\chi,\eta) - \tilde{g}(\chi,\eta)) - 2\eta \\ \chi' &= \tilde{f}(\chi,\eta) + \tilde{g}(\chi,\eta) \end{aligned} \tag{2.94}$$

where $\epsilon = 1/c$, and $\tilde{f}(\chi,\eta) = f(\frac{\chi+\eta}{2}, \frac{\chi-\eta}{2})$, and $\tilde{g}(\chi,\eta) = g(\frac{\chi+\eta}{2}, \frac{\chi-\eta}{2})$. Taking the limit $c \to \infty$, we get the pair of equations

$$\begin{aligned} \eta &= 0 \\ \chi' &= \tilde{f}(\chi,\eta) + \tilde{g}(\chi,\eta). \end{aligned} \tag{2.95}$$

In particular, if there is a compact inflowing submanifold for the flow of

$$\chi' = \tilde{f}(\chi,0) + \tilde{g}(\chi,0) \tag{2.96}$$

then it will persist as such under small perturbations. Since the invariant manifold described by $\eta = 0$ corresponds to $M_0 = \{(x,y) : x = y\}$, we can conclude that for large coupling strengths the two systems will be nearly synchronous.

The same argument can be repeated for large negative couplings, $c \to -\infty$. In this case we obtain the equations

$$\begin{aligned} \eta' &= \tilde{f}(\chi,\eta) - \tilde{g}(\chi,\eta) \\ \epsilon\chi' &= \epsilon(\tilde{f}(\chi,\eta) + \tilde{g}(\chi,\eta)) - 2\chi. \end{aligned} \tag{2.97}$$

If the flow of (2.9.4) has an inflowing, compact manifold for $\chi = 0$, then the two systems will be anti-synchronous[3] for large negative couplings.

[3] Anti-synchrony refers to the situation in which $x(t) = -y(t)$.

The more general situation of a network of linearly coupled systems

$$z' = A(c)z + f(z) \tag{2.98}$$

discussed in [9] can be handled similarly. Let c be the coupling parameter, $z = (z_1, z_2, \ldots, z_n)$, $z_j \in \mathbb{R}^N$,and $f = (f_1, f_2, \ldots, f_n) \in C^r(\mathbb{R}^{Nn}, \mathbb{R}^{Nn})$ for $r \geq 1$. Moreover, we assume that for all c, $A(c)$ is self-adjoint, and has 0 as a simple eigenvalue with a corresponding eigenvector $E = (I, I, \ldots, I)^T$, where I is the $N \times N$ identity matrix. Moreover the remaining eigenvalues $\lambda_m(c)$, have the property that for any $p > 0$, there exists a $c_0 > 0$ such that all $\lambda_m(c) < -p$. This condition simply means that the coupling leaves the diagonal invariant and can be made arbitrarily strong in the direction normal to the diagonal.

A new coordinate system (y, w) can be introduced by $z = Cw + Ey$, where the columns of C are orthogonal to E. In these coordinates (2.98) is equivalent to

$$\begin{aligned} w' &= B(c)w + F(w, y) = F(w, y) - \Omega(w, c) \\ y' &= \sum_1^n f_j(Cw + Ey) \end{aligned} \tag{2.99}$$

where F is a linear combination of the components of f. By the assumption on the eigenvalues $\lambda_m(c)$ this equation satisfies the conditions of proposition 2.9.3 with $M_0 = \{(z_1, z_2, \ldots, z_N) \in \mathbb{R}^{nN} : z_1 = z_2 = \ldots z_N\}$.

We can only expect $M_\epsilon = M_0$ when $f(x, x) = g(x, x)$. However since M_ϵ is within $\mathcal{O}(\epsilon)$ of M_0, the systems are synchronized in the sense of definition 2.5.1.

There is nothing special about linear couplings. Assume that a network of systems can be described by the equation

$$z' = f(z) + K(z, c) \tag{2.100}$$

where $K : \mathbb{R}^{nN} \to \mathbb{R}^{nN}$ is some coupling function. Let l is the codimension of the manifold M_0 in the phase space of the network. Assume that M_0 is a manifold invariant under the flow of $x' = K(x, c)$ for all values of c, and the neighborhood of M_0 can be smoothly foliated by l-dimensional leaves which are invariant under the flow of $x' = K(x, c)$. If this foliation provides a coordinate system in a neighborhood of M_0 then there is a natural way to write the system in the form of equation (2.90) in this neighborhood. In this case the function Ω will depend only on x and c. If $\Omega(x, c)$ satisfies the conditions of proposition 2.9.3, then we can conclude that synchronization occurs. This situation is illustrated schematically in figure 2.9.4.

Example 2.9.5 Consider the following Rössler system driven by a Lorenz system

$$\begin{aligned} x_1' &= \sigma(y_1 - x_1) & x_2' &= -y_2 - z_2 - k(x_2 - (x_1^2 + y_1^2)) \\ y_1' &= \rho x_1 - y_1 - x_1 z_1 & y_2' &= x_2 + a y_2 - k(y_2 - (y_1^2 + z_1^2)) \\ z_1' &= x_1 y_1 - \beta z_1 & z_2' &= b + z_2 x_2 - c z_2 - k(z_2 - (x_1^2 + z_1^2)) \end{aligned}$$

where all constants are chosen so that both systems are in the chaotic regime. In this case the manifold M_0 is a compact submanifold of the set

$$S = \{(x_1, y_1, z_1, x_2, y_2, z_2) \in \mathbb{R}^6 : x_2 = x_1^2 + y_1^2, y_2 = y_1^2 + z_1^2, z_2 = x_1^2 + z_1^2\}. \tag{2.101}$$

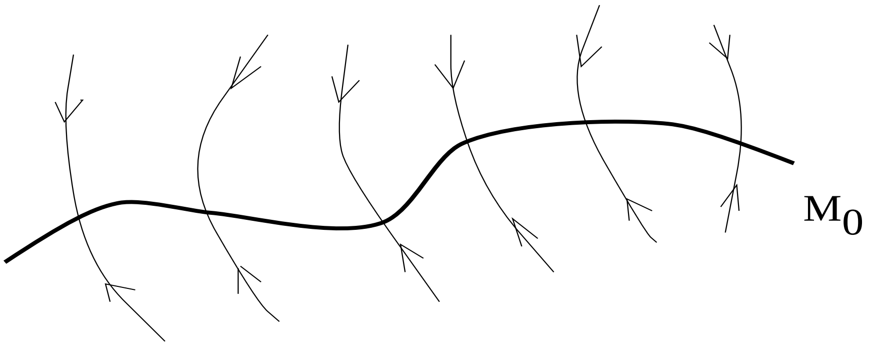

Figure 2.9: If the coupling leaves a foliation of a neighborhood of M_0 invariant, system (2.90) can be defined in a natural way.

For large values of k we therefore expect that orbits will lie in the vicinity of this manifold. Since the projections of the manifold S onto the coordinates (x_1, y_1, x_2), (y_1, z_1, z_2) and (x_1, z_1, z_2) are paraboloids, we can actually see how this synchronization manifold is approached. This is illustrated in figure 2.9.5 in which the (x_1, y_1, x_2) projections of a typical trajectory are shown at four different coupling values.

Example 2.9.6 The same approach can be used to study partially coupled systems. For instance consider the following pair of Lorenz systems coupled only through the y variable

$$\begin{aligned} \dot{x_1} &= \sigma(y_1 - x_1) & \dot{x_2} &= \sigma(y_2 - x_2) \\ \dot{y_1} &= \rho x_1 - y_1 - x_1 z_1 - c(y_1 - y_2) & \dot{y_2} &= \rho x_2 - y_2 - x_2 z_2 - c(y_2 - y_1) \\ \dot{z_1} &= -\beta z_1 + x_1 y_1 & \dot{z_2} &= -\beta z_2 + x_2 y_2 \end{aligned} \tag{2.102}$$

If we let $\eta = y_1 - y_2$, and $\chi = y_1 + y_2$, then

$$\epsilon\dot{\eta} = \epsilon[\rho(x_1 - x_2) - \eta - x_1 z_1 + x_2 z_2] - 2c\eta \tag{2.103}$$

and we can use geometric singular perturbation theory to conclude that the manifold $M_0 = \{(x_1, z_1, x_2, z_2, \eta, \chi) : \eta = 0\}$ persists for large coupling strengths. In the limit $\epsilon = 0$, the motion on the slow manifold is described by

$$\begin{aligned} \dot{x_1} &= \sigma(y_1 - x_1) & \dot{x_2} &= \sigma(y_2 - x_2) \\ \dot{\chi} &= \rho(x_1 + x_2) - \chi - x_1 z_1 - x_2 z_2 & & \\ \dot{z_1} &= -\beta z_1 + x_1 y_1 & \dot{z_2} &= -\beta z_2 + x_2 y_2 \end{aligned} \tag{2.104}$$

so that

$$\begin{aligned} \dot{x_1} - \dot{x_2} &= -\sigma(x_1 - x_2) \\ \dot{z_1} - \dot{z_2} &= -\beta(z_1 - z_2) + \frac{1}{2}\chi(x_1 - x_2) \end{aligned} \tag{2.105}$$

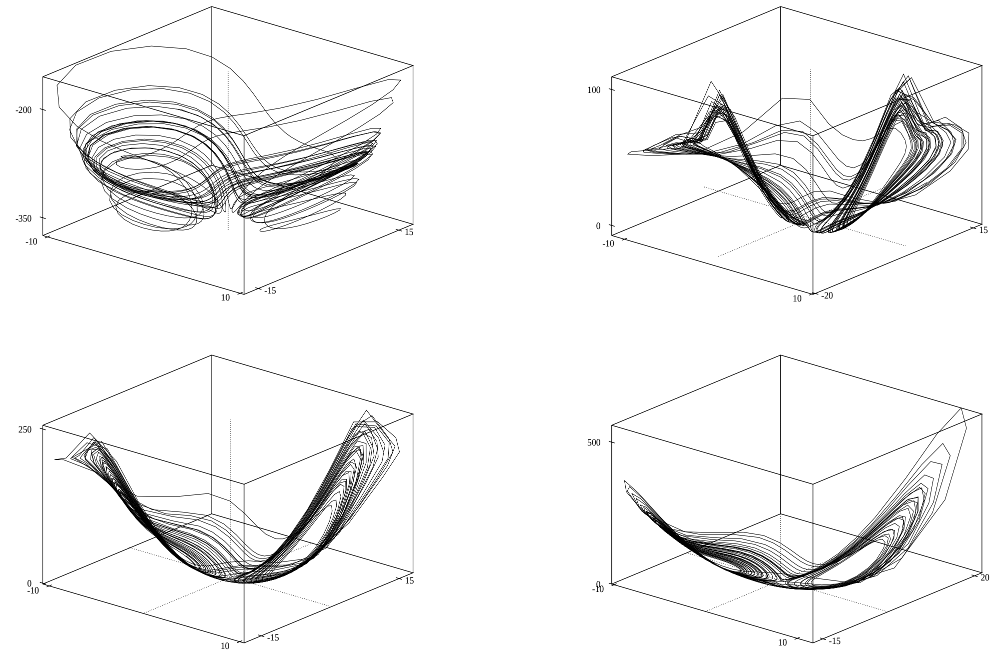

Figure 2.10: (x_1, y_1, x_2) projections of typical trajectories of the system (2.9.5) after transients die out. The four graphs correspond to coupling strengths of $k = 1$, $k = 50$, $k = 200$, and $k = 10000$ respectively.

If χ remains bounded, then both the differences $x_1 - x_2$, and $z_1 - z_2$ will decay. The trick used to show that the Lorenz system has an inflowing ellipsoid can be used for system (2.104) too. Consider the Lyapunov functional

$$V = r(x_1^2 + x_2^2) + \sigma\chi^2 + 2\sigma[(z_1 - 2r)^2 + (z_2 - 2r)^2] \tag{2.106}$$

so that

$$\dot{V} = -2\sigma[r(x_1^2 + x_2^2) - \chi^2 - 2\beta(z_1^2 + z_2^2) + 4r\beta(z_1 + z_2)] \tag{2.107}$$

The function V is positive outside of a sufficiently large ellipsoid E, and decays outside E, so that all trajectories of (2.104) enter E.

This shows that in the limit of infinite coupling the two systems synchronize. Moreover since equation (2.105) is stable under perturbations, it follows that the two systems will remain synchronized if we perturb from $\epsilon = 0$, and hence we can conclude that the systems are synchronized for large coupling strengths.

This example is somewhat simplified by the fact that that the two systems are identical. Partial coupling between non-identical systems may be approached in the same way. If the partially coupled system has a normally hyperbolic invariant manifold M_0 in the limit of infinite coupling, the idea is to show that the slow equations on M_0, have a locally attracting, normally hyperbolic manifold $N \subset M_0$ which has the properties of a synchronization manifold. This implies that for a large coupling c, the network will possess a synchronization manifold N_c. In the present example $M_0 = E \cap \{(x_1, y_1, z_1, x_2, y_2, z_2) \in \mathbb{R}^6 : y_1 = y_2\}$, and $N = E \cap \{(x_1, y_1, z_1, x_2, y_2, z_2) \in \mathbb{R}^6 : x_1 = x_2, y_1 = y_2, z_1 = z_2\}$.

A similar argument can be applied to a chain of n Lorenz systems coupled only through the x variable which will be examined in chapter 3

$$\begin{aligned} x_i' &= \sigma(y_i - x_i) + d_x \Delta x_i \\ y_i' &= r x_i - y_i - x_i z_i \\ z_i' &= -\beta z_i + x_i y_i \end{aligned} \tag{2.108}$$

where $\Delta x_i = x_{i-1} - 2x_i + x_{i+1}$ with the index i taken modulo n is the discrete Laplacian coupling so that periodic boundary conditions are assumed. As in the previous case, we define $\chi_{x_i} = x_{i+1 \mathrm{mod}\ n} + x_i$ and $\eta_{x_i} = x_{i+1 \mathrm{mod}\ n} - x_i$. In the limit $d_x \to \infty$, the manifold $S = \{\eta \in \mathbb{R}^n : \eta_{x_i} = 0 \text{ for all } 1 \leq i \leq n\}$ is a normally hyperbolic invariant manifold, as shown in [32]. The slow equations for the variables $\eta_{y_i} = y_{i+1 \mathrm{mod}\ n} - y_i$ and $\eta_{z_i} = z_{i+1 \mathrm{mod}\ n} - z_i$ take the form

$$\begin{bmatrix} \dot{\eta_{y_i}} \\ \dot{\eta_{z_i}} \end{bmatrix} = \begin{bmatrix} -1 & x(t) \\ -x(t) & -\beta \end{bmatrix} \begin{bmatrix} \eta_{y_i} \\ \eta_{z_i} \end{bmatrix} = A(t) \begin{bmatrix} \eta_{y_i} \\ \eta_{z_i} \end{bmatrix}. \tag{2.109}$$

Since the eigenvalues of the matrix

$$\frac{1}{2}[A^{\mathrm{T}}(t) + A(t)] = \begin{bmatrix} -1 & 0 \\ 0 & -\beta \end{bmatrix} \tag{2.110}$$

are both negative, it follows from a simple result about the stability of non-autonomous linear systems [34, p. 307], that the origin is stable fixed point of equation (2.110). It can be checked using Lyapunov functions that there is an inflowing subset of the synchronization manifold for the slow equations, and thus the finite ring (2.108) will synchronize for sufficiently large values of the coupling d_x.

For large, but finite values of d_x, the manifold S remains a stable, normally hyperbolic, invariant manifold due to the symmetry of the equations. Therefore $|x_i - x_j|$ will decrease exponentially for all i and j. A simple calculation shows that η_{y_i} and η_{z_i} must satisfy the following equation

$$\begin{bmatrix} \dot{\eta_{y_i}} \\ \dot{\eta_{z_i}} \end{bmatrix} = \begin{bmatrix} -1 & x(t) \\ -x(t) & -\beta \end{bmatrix} \begin{bmatrix} \eta_{y_i} \\ \eta_{z_i} \end{bmatrix} + \begin{bmatrix} (r + z_{i+1})\eta_{x_i} \\ y_{i+1}\eta_{x_i} \end{bmatrix}. \tag{2.111}$$

A direct application of Duhamel's formula now shows that the origin is an exponentially stable fixed point of these equations when η_{x_i} decays exponentially, and y_{i+1} and z_{i+1} remain bounded.

Remark 2.9.7 It is important to note that sometimes stable synchronization in partially coupled systems occurs only at intermediate couplings. This is illustrated in [32] and [71] where the state of identical synchrony in rings of partially coupled Rössler and Lorenz oscillators is shown to be stable only for an intermediate range of coupling strengths. As the coupling strength is increased past a critical value the network undergoes a *short-wavelength bifurcation* in which the shortest spatial wavevelength is the first to become unstable. This type of bifurcation is also known as *spatio-temporal shredding*. The stable synchronous behavior in such systems will remain undetected if they are only analyzed in the limit of infinite coupling strength.

2.10 Limitations of the Description of Synchronization in Terms of Invariant Manifolds

It is possible that two systems in a network are synchronized without the existence of a diffeomorphism from an open neighborhood of the attractor of one system to that of the other. In this case the description synchronization in terms of invariant manifolds is not applicable. In this section several such occurences will be discussed.

This situation may occur in a slightly heterogeneous network of diffusively coupled oscillators. If there exists a differentiable function f from the neighborhood of system x_i to the neighborhood of system x_j such that

$$|f(x_i(t)) - x_j(t)| < \epsilon \tag{2.112}$$

for all $t > 0$ then it can be said that system x_j is nearly synchronous to system x_i. In this situation there does not necessarily exist a synchronization manifold in the phase space of the network. Afraimovich, et. al. [72], [73], [76] have developed analytical techniques to show that for large couplings diffusively coupled inhomogeneous lattices of oscillators are nearly identically synchronized. These techniques are independent of the existence of invariant manifolds, and can thus be used to describe more general instances of synchronization. Note however that in section 2.9 it was shown that in the case of strong diffusive coupling in an inhomogeneous network the existence of a synchronization manifold can frequently be expected. It is not clear in what cases the network will be nearly synchronized without the existence of a synchronization manifold.

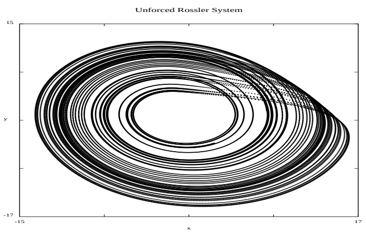

Figure 2.11: The projection of the attractor of the Rössler system (2.113) onto the (x, y) plane.

Perhaps even more important are the cases of phase locking and lag synchronization between chaotic phase-coherent systems. The attractor of the Rössler system

$$\begin{aligned} x' &= -\omega y - z \\ y' &= \omega x + ay \\ z' &= b + z(x - c) \end{aligned} \tag{2.113}$$

is shown in figure 2.10. An approximate frequency and phase of the of the attractor of this system can be defined naturally as ω and $\theta = \arctan \frac{y}{x}$ respectively.

Surprisingly, this system responds to a small periodic driving in a way very similar to periodically forced nonlinear phase oscillators. Let ω_0 and $\phi(t)$ be the frequency and phase of the periodic forcing. If ω_0 is close to ω and the forcing is sufficiently strong, then $|\theta(t) - \phi(t)| < \epsilon$ after transients die out[4].

Poincaré sections of the attractor at times $T_n = n\frac{2}{\omega_0}$ at three different amplitudes of the forcing are given in figure 2.10. When the coupling is of sufficient strength, $|\theta(T_n)) - \phi(T_n)| < \epsilon$ after transient die out. This explains why the points $\{x(T_n), y(T_n)\}_{n=N}^{\infty}$ in figure 2.10 lie in a wedge.

However if there existed a smooth functional relationship $\theta(T_n) = f(\phi(T_n))$ between the two phases, then the points $\{x(T_n), y(T_n)\}_{n=N}^{\infty}$ would lie on an intersection of the attractor with a smooth manifold. This does not appear to be the case in numerical and physical experiments, and it is therefore unlikely that this type of synchronization can be analyzed directly using invariant manifolds.

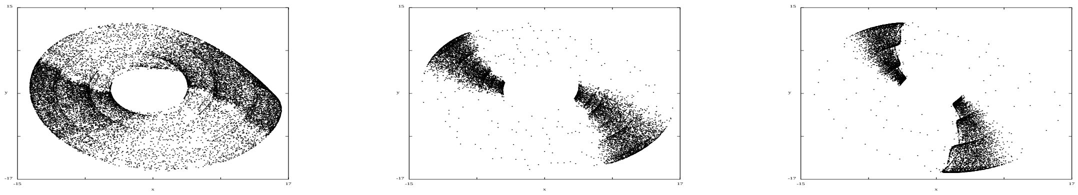

Figure 2.12: System (2.113) is phase locked to a periodically driving signal when the signal is of relatively small amplitude. As the amplitude of the signal is increased, the wedge in which $\{x(T_n), y(T_n)\}_{n=N}^{\infty}$ lies becomes slimmer, but this region does not appear to be an intersection of the attractor with a manifold.

It was shown numerically in [69] and experimentally in [70] that the transition to synchronization for a pair of diffusively, partially coupled phase-coherent systems x_1 and x_2 can be preceded by two bifurcations. First the two systems become phase locked in the sense of the preceding paragraphs. After the next bifurcation the two systems are *lag synchronized*, i.e. $x_1(t-\delta) = x_2(t)$. As the coupling is increased the delay between the two systems decreases, until finally $\delta = 0$, and the two systems are identically synchronized.

There clearly exists a function from the orbits of one system to that of the other in the case of lag synchronization $x_2(t) = D(x_1(t)) = x_1(t-\delta)$. An elementary theorem about the solutions of differential equations states that the solutions $x(t, x(0))$ of the system $x' = f(x)$ have a C^r dependence on the initial conditions $x(0)$ when $f \in C^r(\mathbb{R})$. This means that the function $D(x_0) = x(\delta, x_0)$ depends smoothly on x_0. Therefore if the coupling between the two systems x_1 and x_2 is unidirectional, then the map D is a diffeomorphism, and its graph is the synchronization manifold. As δ approaches 0, this synchronization manifold approaches the diagonal.

[4]The origin of the phase θ is assume to be shifted so that there is no constant phase difference between the two oscillators. In general this expression would be $|\theta_0 + \theta(t) - \phi(t)| < \epsilon$.

Remark 2.10.1 Both phase and lag synchronization are of great importance in biological applications. Neurons are frequently modeled as nonlinear phase oscillators, or by relaxation-oscillation equations. Experiments suggest that biological neurons are not exactly periodic. This non-periodicity is partly due to the random noise inherent in any physical systems, but some data analyses also suggest that the cause is deterministic [29]. The problem of phase locking and lag synchronization between systems with nonperioidic phase-coherent attractors is of direct relevance to this situation.

The definition of synchronization of two systems in terms of invariant manifolds 2.1.2 was introduced as a consequence of the requirement that there exist a diffeomorphism from an open neighborhood of the attractor of one system to an open neighborhood of the attractor of the second system. The following example shows that even when there exist a diffeomorphism from the attractor of one system to the attractor of the second it can not necessarily be extended to a neighborhood of the attractor.

Example 2.10.2 Consider the following system of equations

$$r' = \begin{bmatrix} -2 & 2\pi & 0 \\ -2\pi & -2 & 0 \\ 0 & 0 & -1 \end{bmatrix} r \qquad r \in \mathbb{R}^3 \tag{2.114}$$

$$\theta' = 1 \tag{2.115}$$

where $x_1 = (r_1 + 1)\cos 4\pi\theta$, $x_2 = (r_1 + 1)\sin 4\pi\theta$, $y_1 = r_2 + (r_1 + 1)\cos 4\pi\theta$, and $y_2 = r_3 + (r_1 + 1)\sin 4\pi\theta$. In these coordinates the system (2.115) may be viewed as composed of two coupled subsystems (x_1, x_2) and (y_1, y_2). The fundamental matrix solution of equation (2.115) is

$$X(t) = \begin{bmatrix} \cos 2\pi\theta & \sin 2\pi\theta & 0 \\ -\sin 2\pi\theta & \cos 2\pi\theta & 0 \\ 0 & 0 & 1 \end{bmatrix} \begin{bmatrix} e^{-2\theta} & 0 & 0 \\ 0 & e^{-2\theta} & 0 \\ 0 & 0 & e^{-\theta} \end{bmatrix} \tag{2.116}$$

Notice that the solution $r = 0$ is a stable periodic solution of the system (2.115). This periodic orbit Γ projects to a circle in both the x_1, x_2 and y_1, y_2 plane. Therefore we can say that there exists a diffeomorphism from the attractor $\Pi_1(\Gamma)$ of the first system to the attractor $\Pi_2(\Gamma)$ of the second. According to definition 2.1.2 system (y_1, y_2) is synchronized to system (x_1, x_2) if there exists a neighborhood of the attractor Γ to which this diffeomorphism can be extended. The graph of this diffeomorphism needs to be a two dimensional invariant manifold M such that both projections $\Pi_1(M)$ and $\Pi_2(M)$ are smooth. We show next that such a manifold does not exist in this case.

Consider the Poincaré section $P = \{\theta, r_1, r_2, r_3 \colon \theta = 1/2\}$. According to equation (2.116) the Poincaré map is given by

$$r_{n+1} = \begin{bmatrix} -e^{-1} & 0 & 0 \\ 0 & -e^{-1} & 0 \\ 0 & 0 & -e^{-\frac{1}{2}} \end{bmatrix} r_n. \tag{2.117}$$

Since all solutions of equation (2.116) intersect P transversally the intersection of P and any two dimensional invariant manifold M is a one dimensional submanifold of P.

If $M \cap P$ contains a point $p = (p_1, p_2, p_3)$ such that $p_3 \neq 0$, then it must contain all the forwards images of this point. Since the under the action of the map (2.117) the contraction is stronger in the (r_1, r_2) direction than in the r_3 direction, $M \cap P$ must be tangent to the r_3 axis at the origin. This means that the projection onto the (x_1, x_2) plane is not differentiable at the origin. Therefore any synchronization manifold must lie in the (r_1, r_2) plane.

By the definition of (2.117) all one dimensional invariant manifolds of the restriction of this map to the plane (r_1, r_2) are lines through the origin. The map (2.117), rotates these lines by an angle π. This implies that the invariant manifold M must be a Möbius band and therefore can not be the graph of a diffeomorphisms from $\mathbb{R}^2$ to $\mathbb{R}^2$.

It follows that the diffeomorphism from $\Pi_1(\Gamma)$ to $\Pi_2(\Gamma)$ cannot be extended to an open set containing $\Pi_1(\Gamma)$, and so the system (y_1, y_2) is not synchronized to (x_1, x_2) according to definition 2.1.2[5].

This situation is somewhat unsatisfactory since the two systems are clearly synchronized. Notice however that under a change of coordinates $\Phi(x_1, x_2, y_1, y_2) = (\tilde{x}_1, \tilde{x}_2, y_1, y_2)$ close to the identity the manifold

$$M_3 = \{(x_1, x_2, y_1, y_2) : x_1^2 + x_2^2 + y_1^2 = 1\}. \tag{2.118}$$

will project smoothly unto an open set in the $(\tilde{x}_1, \tilde{x}_2)$ plane. Since the contraction in the direction normal to M_3 is stronger than the contraction within M_3 it will be a synchronization manifold in these coordinates.

Another potential problem is the requrement of normal hyperbolicity of the synchronization manifold. Consider the system

$$r' = \begin{bmatrix} -1 & 0 & 0 \\ 0 & -1 & 0 \\ 0 & 0 & -1 \end{bmatrix} r \qquad r \in \mathbb{R}^3 \tag{2.119}$$

$$\theta' = 1 \tag{2.120}$$

where r and θ are the same as above. Since the contraction rates in all directions normal to the periodic orbit are the same, no two dimensional manifold containing the orbit can be normally hyperbolic. In this case the two systems remain synchronous under perturbation in spite of the fact that the attractor is not contained in a normally hyperbolic synchronization manifold.

Remark 2.10.3 These types of problems will not be encountered in the case of diffusive couplings discussed in section 2.9, Since most couplings found in the physical literature are of diffusive type, the problems that appear in the preceding example might not be very important.

2.11 Synchronization with Small Couplings

In the case of two coupled maps with hyperbolic compact attractors Λ_1 and Λ_2 neither of which is a fixed point, it is clear that the two maps can not be synchronized with an arbitrarily small C^1 coupling. This is due to the fact that $\Lambda_1 \times \Lambda_2$ is a hyperbolic attractor for the direct product of the

[5]It is not possible to construct an example in which all the two dimensional invariant manifolds containing the periodic orbit Γ are Möbius bands. This is due to the fact that (2.116) is a composition of a contraction and $S(t) \in$ SO(3) at each $t \in \mathbb{R}$. If all two dimensonal invariant manifolds are Möbius bands then $S(\frac{1}{2}) = -I$ which would imply that there exsts a path $S(t)$ from $S(0) = I$ to $-I$ in SO(3). This is impossible, since I and $-I$ are in two different path components of SO(3).

two uncoupled system. A small coupling can be viewed as a small perturbation of this product, and will hence have an attractor on which the dynamics are topologically conjugate to the dynamics of the uncoupled system on $\Lambda_1 \times \Lambda_2$.

The situation is somewhat diffrent in the case of flows. Even in the case of two hyperbolic systems, their direct product is no longer hyperbolic since it has *two* center directions. Notice that this is exactly the reason why two systems with attracting periodic orbits will generically be phase locked for small couplings as explained in example 1.1.5. The case of chaotic attractors is significantly different from this example, since there will be n unstable direction at ρ-almost all points on the attractor, where ρ is an invariant measure, and n is the number of positive Lyapunov exponents. Therefore the attractor of the direct product of the flows has $2n$ unstable directions, while the attractor of the identically synchronous state has n unstable directions at each point. In general, we don't expect the drop from $2n$ unstable directions to n unstable directions to occur for arbitrarily small perturbations of the system.

These ideas can also be expressed in terms of the dimension of the attractor. If ρ is an SRB measure then the Lyapunov dimension of the attractor of the product of the flows is $\dim_\Lambda \rho \times \rho = 2 \dim_\Lambda \rho$. It is not expected that a small perturbation of the flow will reduce this dimension by a factor of two.

The essential idea of the OGY method of controlling periodic orbits [68] may be used to synchronize two identical systems by a coupling that is arbitrarily small in the L^∞ norm. Consider discrete dynamical system $x_{n+1} = f(x_n)$ with a compact, uniformly hyperbolic attractor A. Assume moreover that typical orbits on A approach each other arbitrarily closely. There exists an $\epsilon > 0$ such that the stable and unstable manifolds of size ϵ, $W^s_{f,\epsilon}(x)$ and $W^u_{f,\epsilon}(x)$, are defined at each point on A. Let the response system be defined as

$$y_{n+1} = f(y_n) + g(x_n, y_n) \tag{2.121}$$

where

$$g(x_n, y_n) = \begin{cases} 0 & \text{if } d(f(x_n), f(y_n)) > \epsilon \\ \Pi_s^{f(x_n)}(f(y_n)) - f(y_n) & \text{otherwise} \end{cases} \tag{2.122}$$

where $\Pi_s^{x_n} : B_\epsilon(x_n) \to W^s_{f,\epsilon}(x_n)$ is the projection onto the stable manifold of x_n of the ϵ ball around x_n. Since all orbits come arbitrarily close to each other, eventually the orbit of the two systems will come close enough and the coupling function g will be non-zero. The effect of the coupling function is to place the subsystem onto the stable manifold of the orbit of the driving system. Once the response system is on this stable manifold $\Pi_s^{f(x_n)}(f(y_n)) = f(y_n)$, and thus $d(x_n, y_n) \to 0$ as $n \to \infty$ and the two systems synchronize identically at an exponential rate. In general this coupling will be only Hölder continuous, and it may not be small in the Hölder norm.

The following argument shows that this synchronization is persistent under perturbations. Assume that the driving system $x_{n+1} = f(x_n)$ is replaced by $x' = f_\delta(x)$ where f and f_δ are close in the C^1 topology, and the coupling function has the same form as in equation (2.122).

$$g(x_n, y_n) = \begin{cases} 0 & \text{if } d(f(x_n), f(y_n)) > \epsilon \\ \Pi_s^{f_\delta(x_n)}(f(y_n)) - f(y_n) & \text{otherwise} \end{cases} \tag{2.123}$$

Assume that typical orbits of the two systems still come within a distance ϵ of each other. By structural stability there exists a hyperbolic set Λ_δ uniformly close to Λ. Therefore there exists a constant $\eta > 0$ such that $d(f(x), f_\delta(x)) < \eta$ for all $x \in \Lambda_\delta$.

Assume that $d(f_\delta(x_n), f(y_n)) < \epsilon$, so that $d(x_{n+1}, y_{n+1}) < \epsilon$. If it can be shown that $d(x_{n+2}, y_{n+2}) < \epsilon$ the two systems will remain ϵ close by induction. Let θ be the minimum rate of contraction within the stable manifolds of the system $x' = f_\delta(x)$. Then we have the following inequalities

$$\begin{aligned} d(x_{n+2}, y_{n+2}) &\leq d(x_{n+2}, f_\delta(y_{n+1})) + d(f_\delta(y_{n+1}), f(y_{n+1}) + d(f(y_{n+1}), \Pi_s^{f_\delta}(f(y_{n+1}))) \\ &< \theta d(x_{n+1}, y_{n+1}) + 2\eta. \end{aligned} \tag{2.124}$$

If f and f_δ are sufficiently close, then $2\eta/(1-\theta) < \epsilon$ in which case equation (2.124) implies $d(x_{n+2}, y_{n+2}) < \epsilon$, and the synchronization is stable.

2.12 Concluding Remarks

In this chapter it was shown that the description of chaotic synchronization in terms of invariant manifolds provides a natural framework for the study of many types of synchronization which were considered separate and distinct in the physics literature. In particular it is shown that, from an abstract point of view, there is no essential difference between generalized and identical synchronization, or synchronization between unidirectionally and bidirectionally coupled systems.

Once the theory of invariant manifolds was introduced, it was also possible to give precise mathematical meaning to quantities such as conditional Lyapunov exponents used in the physical literature. Moreover, necessary and sufficient conditions for the persistence of synchronization under perturbations follow as direct corrolaries to theorems that provide conditions for the persistence of invariant manifolds.

Three different methods for the detection of synchronization were introduced. Each is applicable to a particular class of systems. If the coupling in a network of systems has certain symmetries, then the synchronization manifold can often be found as a fixed set of a particular symmetry group acting on the phase space of the network. In case the network may be split into a drive and response system, the synchronization manifold may be found as an invariant section of an extension. Finally, in many cases of diffusively coupled systems, geometric singular perturbation theory may be used to establish the existence of a synchronization manifold.

Although this chapter was mostly concerned with flows on $\mathbb{R}^n$, the theory of invariant manifolds carries over directly to maps and flows on arbitrary manifolds. Thus all the results discussed here can be extended to both of these situations with only minor modifications.

There is strong evidence that some interesting and important examples of chaotic synchronization can not be treated using this approach. It is possible that two systems are only approximately synchronized, or that their phase variables are approximately synchronized, without the existence of a synchronization manifold in the phase space. Some analytical tools have been developed to investigate such instances, however in general it is not even clear what definitions of chaotic synchronization are appropriate in such cases. One possible measure of the amount of synchronization between the systems could be an appropriate dimension of the attractor or an invariant measure on the attractor. It is expected that the dimension of the attractor in a network of n identical systems gradually decreases from $n \dim A$ to $\dim A$. A significant drop in the dimension could then be interpreted as an indication that some form of synchrony is present in the network.

Chapter 3

Stable Stationary States in Rings

3.1 Introduction

Chains and rings of diffusively coupled oscillators have a been a topic of research in a variety of contexts. The special case of coupled chaotic oscillators has received particular attention since the increased interest in synchronized chaotic systems. These types of systems are similar to lattices of coupled maps introduced in [80], however the present case of coupled flows in higher dimensions is more difficult to analyze.

In the present chapter the case of a ring of Lorenz systems in the chaotic regime interacting through a discrete Laplacian coupling will be studied numerically and analytically. The equations describing a chain of n such systems are

$$\begin{aligned} x_i' &= \sigma(y_i - x_i) + d_x \Delta x_i \\ y_i' &= r x_i - y_i - x_i z_i + d_y \Delta y_i \\ z_i' &= -\beta z_i + x_i y_i + d_z \Delta z_i \end{aligned} \tag{3.1}$$

where $\Delta x_i = x_{i-1} - 2x_i + x_{i+1}$ with the index i taken modulo n is the discrete Laplacian coupling. The coupling coefficients d_x, d_y, d_z determine the strength of the coupling and periodic boundary conditions are assumed. The same equations represent an infinite chain of Lorenz systems when $i \in \mathbb{Z}$. The constants are chosen as $\sigma = 10, r = 27$, and $\beta = 8/3$ so that each uncoupled oscillator is in the chaotic regime. These constants will remain fixed for the remainder of the discussion.

Since the coupling is diffusive, sufficiently large values of d_x, d_y, d_z will lead to the synchronization of the oscillators, as shown in section 2.9. We will be mostly concerned with the instance $d_x \neq 0, d_y = 0, d_z = 0$ since several of the computations are simpler in this case. This corresponds to partial coupling examined in example 2.9.6, where it was shown that for sufficiently large values of d_x any ring of finite size will be synchronized. Many physical couplings can be viewed as couplings in one variable of the model as shown in example 1.1.8 and [32].

In what follows we will examine what happens when d_x is large enough for the systems to interact in a nontrivial way. Numerical investigations indicate a variety of phenomena that can occur in this case: stable stationary states, "breathers" inside which the behavior appears to remain chaotic, phase locking between sites far removed in the ring, and, in the case $d_y \neq 0$ traveling waves on the ring. The subscript on d_x will be dropped since d_y and d_z will be set to 0.

Results about the synchronization of chains of chaotic systems that guarantee coherent behavior on a large scale in the chain require the coupling to grow proportionally to a power of the size of the chain [76], [75],[9]. From a physical viewpoint it is more interesting to examine large scale coherent behavior which occurs for a bounded value of coupling strengths independent of the size of the chain since it is often physically unreasonable to require the coupling strength to grow without bound. Following the steps one would use to analyze a nonlinear differential equation, we begin the study of this system by analyzing its stationary states. Exponentially stable stationary states are synchronized states according to the ideas of the previous section, since the fixed points are trivial r-normally hyperbolic synchronization manifolds.

It is first shown that in chains and rings in which the coupling has certain symmetries an abundance of fixed spatially periodic and aperiodic space can often be expected. In the remainder of the chapter we focus on the particular example of a ring of partially coupled Lorenz system (3.1). It is shown that a fixed, spatially periodic state can be found in rings of arbitrary size, for a fixed coupling constant d_x.

3.2 Numerical Experiments

Numerical experiments were performed on a Sun SuperSparc using the numerical integration program XPP. Several different integration methods were used to check the validity of the results. These included fixed and variable step Runge-Kutta methods of varying order and the gear method.

At very low values of the coupling constant d_x, the individual systems in the ring behaved as if they were uncoupled. As the coupling strength was increased the behavior of the ring became more coherent. Since the discrete Laplacian acts to synchronize neighboring systems in the ring, these results agree with our expectations. Some of the typical structures observed in these numerical experiments are discussed below.

3.2.1 Breathers

If some of the systems in the ring are nearly stationary, while others are undergoing oscillations we say that the oscillating systems form a breather. Since we are considering rings of finite size it is not expected that any system in the ring is stationary, unless the entire ring is stationary.

An example of a system with two breathers is shown in figure 3.2.1. It is interesting to note that in these states all of the variables undergo oscillations that are nearly periodic. Loosely speaking the motion of each individual system is trapped in a region close to one of the 'lobes" of the Lorenz attractor. No stable states in which all systems in the ring are trapped in the vicinity of only *one* "lobe" has been observed. Occurrences of nearly periodic behavior in lattices of chaotically bursting neurons have been observed numerically by M.I. Rabinovich, and collaborators [77].

Another interesting feature of breathers, which is also shared with other types of solutions of this system, is that frequently nonadjacent systems synchronize without synchronizing with the oscillators that lie between them. The synchrony is usually not exact, however this may be due to numerical errors in the calculations. Due to the many symmetries of the system this sometimes seems to be due to the stability of an invariant manifold corresponding to a partially synchronized state in the chain as discussed in section 2.5. In other cases the state does not appear to be symmetric, and it is unclear what the mechanism behind this synchronization is.

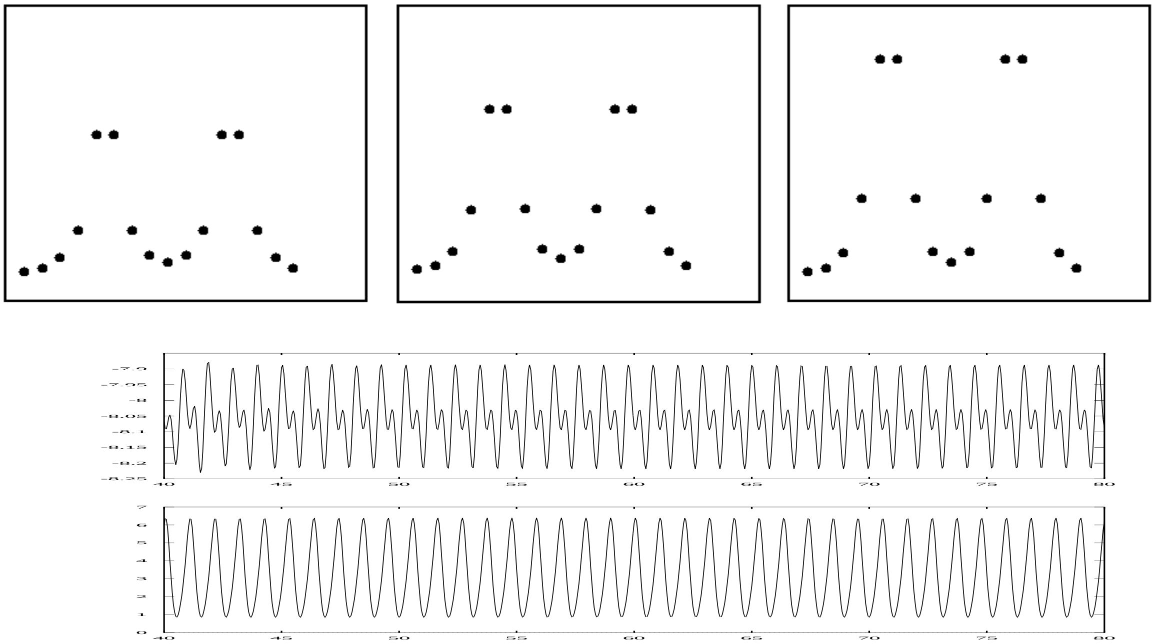

Figure 3.1: A stable state of two breathers in a ring of 16 Lorenz systems coupled through the x variable at $d_x = 15$. The first series of figures shows a snapshot of the x variables of the different systems at different points of one oscillation. In these figures, the position of the oscillator in the ring is given on the x-axis, while $x_i(t)$ is given on the y-axis. The timeseries of $x_1(t)$ and $x_5(t)$, which are nearly periodic, are given below.

It is important to note that some of the qualitative features of the dynamics remain unaffected by the size, or the coupling strength in the ring. Figure 3.2.1 shows typical timeseries of the x variable at four different coupling values in a ring of 32 oscillators. Note the smooth envelope and regularity of the oscillations, as well as the agreement of the timescales among the different timeseries. These general features remain unchanged as the number of systems in the ring is varied, as long as the coupling is below the synchronization threshold and above the value necessary for the appearance of coherent behavior.

3.2.2 Stable Stationary States

In numerical experiments with rings of 8 to 52 systems stable steady states were observed for a variety of initial conditions when the coupling constant $d_x > 10$. Typical stable fixed states are shown in figure 3.2.2.

For certain values of the coupling it appears that all initial conditions lead to one of the stationary states of the system. The basins of attraction of the stationary states seem to be intertwined in a complicated way in this case, as shown in figure 3.2.2. The same is true for other stable states of the system. Small changes in the initial values of the parameters, or even changes of the integrating

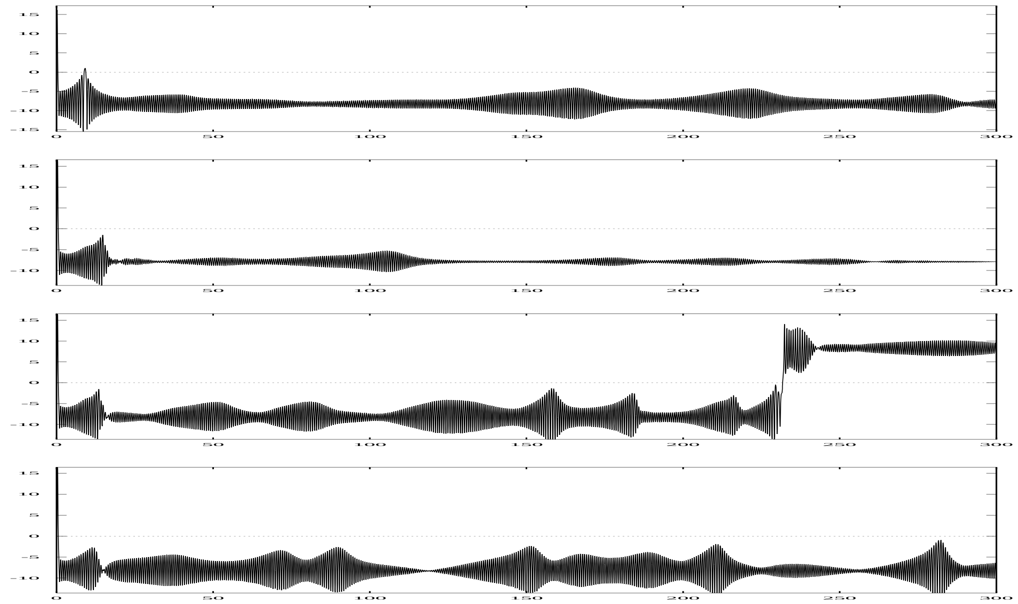

Figure 3.2: Typical timeseries of $x_{15}(t)$ at coupling strengths $d_x = 5, 15, 20, 25$ from top to bottom. Many features of the system remain similar at different coupling values. The oscillations have a smooth envelope, a feature that is typical to solutions for coupling strengths at which the network behaves coherently, but is not synchronized exactly. Even the transients that precede a stable fixed state have similar shapes.

methods can result in very different asymptotical behavior of the system. This situation is similar to that of attractors with riddled basins of attraction [50].

3.2.3 Traveling Pulses

Traveling pulses were observed in the ring only when $d_x \neq 0$ and $d_y \neq 0$. Figure 3.2.3 shows a typical pulse. This is not a pulse in the traditional sense since it oscillates as it propagates along the chain, and is thus not a fixed state in a moving coordinate frame. This can be seen in the timeseries in figure 3.2.3.

3.3 A General Framework for the Study of Steady States

The equations described in the preceding section are a special case of a lattice discrete or continuous time dynamical system

$$(u_j)' = F(\{u_j\}^s) \tag{3.2}$$

where $j \in \mathbb{Z}^D$, $u_j \in \mathbb{R}^p$ and $\{u_j\}^s = \{u_i : |i-j| \leq s\}$. In the following discussion we will use the convention that in u_i^k the subscript $i \in \mathbb{Z}$ denotes the position in the lattice, while the superscript

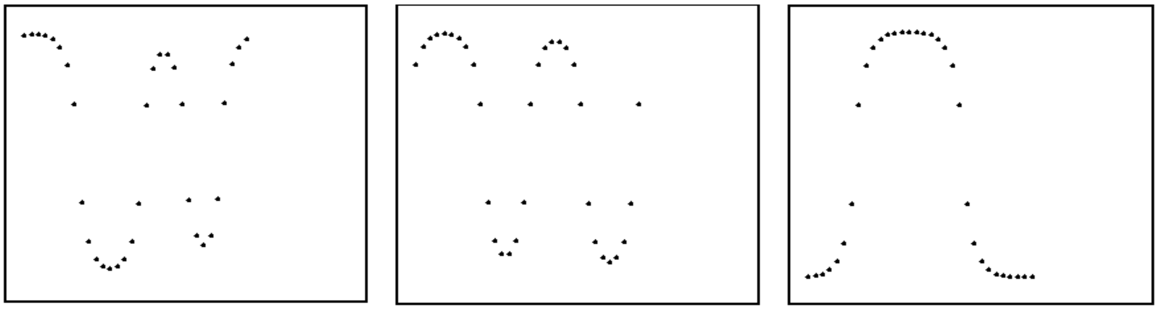

Figure 3.3: The system is very sensitive to initial conditions. The eventual stable state in a chain of 32 oscillators with $d_x = 40$ is shown. Only one initial condition $x_0(0)$ is different for each figure - it was incremented by 0.01. Very different states are reached. This suggests that the basins of attraction are intertwined in a complicated way. The stable states in these figures are typical, although fixed states with one "hump" are more common than states with more "humps".

$1 \leq k \leq p$ denotes the component of the vector u_i. Such systems have been studied by many authors [73], [80], [87] as discrete versions of partial differential equations of evolution type.

We will mainly be concerned with systems continuous in time with $D = 1$ and $s = 1$. These are simply chains of systems coupled to their nearest neighbors. The special case of *rings*, that is chains of finite size with periodic boundary condition will be the focus of our attention. A state in a ring of n systems corresponds to a state of period n in the spatial variable in an infinite chain.

A steady state of a chain given in (3.2) is determined by

$$F(\{u_j\}^s) = F(u_{j-1}, u_j, u_{j+1}) = 0 \tag{3.3}$$
$$F(\{u_j\}^s) = F(u_{j-1}, u_j, u_{j+1}) = u_j \tag{3.4}$$

in the continuous, respectively discrete case. We will study systems that satisfy the following condition:

Condition 1 If we write $F : \mathbb{R}^{3p} \to \mathbb{R}^p$ as $F(\chi, \eta, \zeta) = (F^1(\chi, \eta, \zeta),\ F^2(\chi, \eta, \zeta),\ \ldots,\ F^p(\chi, \eta, \zeta))$ then $\det \left[\frac{\partial F^i}{\partial \zeta^j}(\chi, \eta, \zeta)\right]_{i,j} \neq 0$.

Using the Implicit Function Theorem in the case of continuous time if $\det \left[\frac{\partial F^i}{\partial \zeta^j}(\chi, \eta, \zeta)\right]_{i,j} \neq 0$ for all values of χ, η, ζ then either there exists a point $(a, b, c) \in \mathbb{R}^{3p}$ such that $F(a, b, c) = 0$ and therefore a function $G(\eta, \chi)$ such that $F(\chi, \eta, G(\eta, \chi)) = 0$, or $F(\chi, \eta, \zeta) = 0$ has no solutions and there are no fixed points of (3.2). An equivalent argument holds in the case of discrete time. If such a function G exists and we define $u_{j+1} = G(u_j, u_{j-1})$, $x_j = u_j$ and $y_j = u_{j-1}$ this leads to the following dynamical system on $\mathbb{R}^{2p}$:

$$\begin{aligned} x_{j+1} &= G(x_j, y_j) \\ y_{j+1} &= x_j \end{aligned} \tag{3.5}$$

The steady states of (3.2) are given by the x-coordinates of the orbits of (3.5). In general, the function G may not be unique, in which case more than one system of the form (3.5) is needed to determine all the fixed points of the chain.

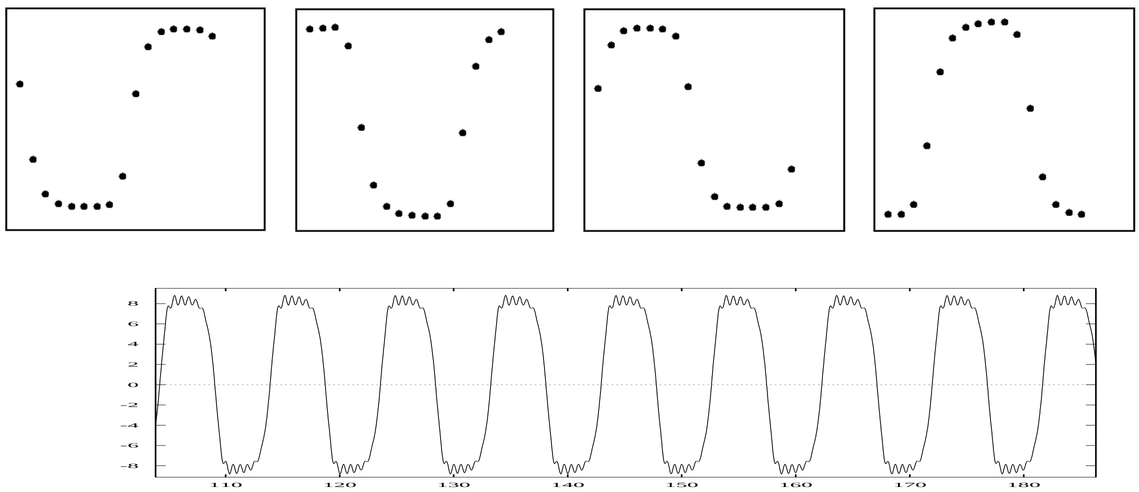

Figure 3.4: The wave when $d_x = d_y = 6$. This seems to be a globally stable solution of the equations.

Since the function G can assume any form, there is not much we can say about such systems in general. The subclass of chains described in the following definition will be easier to analyze

Definition 3.3.1 *A nearest neighbor coupling of a chain of systems is said to be* symmetric *if* $F(u_{j-1}, u_j,\, u_{j+1}) = F(u_{j+1}, u_j, u_{j-1})$.

This simply means that a system in the chain is coupled to its left and right neighbor in the same way. For example the discrete Laplacian coupling $\Delta u_j = u_{j-1} - 2u_j + u_{j+1}$ or the coupling $\Psi u_j = u_{j-1}u_{j+1} + u_j$ are both of this type. The stationary states of symmetrically coupled chains are related to a special class of dynamical systems:

Definition 3.3.2 *Given a diffeomorphism* $\Phi : \mathbb{R}^{2p} \to \mathbb{R}^{2p}$ *and an involution* $R : \mathbb{R}^{2p} \to \mathbb{R}^{2p}$ *such that the dimension of the fixed point set of* R *is* p *we say that* Φ *is* R-reversible *if*

$$R \circ \Phi = \Phi^{-1} \circ R \tag{3.6}$$

The dynamical system defined by $x_{i+1} = \Phi(x_i)$ *is also said to be R-reversible in this case.*

The relation between symmetrically coupled chains and reversible systems is given in the following

Theorem 3.3.3 *The fixed states of a symmetrically copuled chain of systems satisfying condition 1 correspond to the orbits of a dynamical system of the form (3.5) which is R-reversible and volume preserving. For such a system* $R(x, y) = (y, x)$, *with* $x, y \in \mathbb{R}^p$.

Proof: The arguments for the continuous and discrete case are virtually identical, so only the first will be given here. Equation (3.3) together with the assumption that the coupling is symmetric implies that

$$F(u_{j-1}, u_j, u_{j+1}) = F(u_{j+1}, u_j, u_{j-1}) = 0 \tag{3.7}$$

Therefore this leads to the recursion equations

$$u_{j+1} = G(u_j, u_{j-1}) \quad u_{j-1} = G(u_j, u_{j+1}) \tag{3.8}$$

and the two dynamical systems

$$\begin{aligned} x_{j+1} &= G(x_j, y_j) & \qquad z_{j-1} &= G(z_j, w_j) \\ y_{j+1} &= x_j & w_{j-1} &= z_j \end{aligned} \tag{3.9}$$

where $x_j = z_j = u_j$, $y_j = u_{j-1}$ and $w_j = u_{j+1}$. The action of these systems is shown in the diagram below.

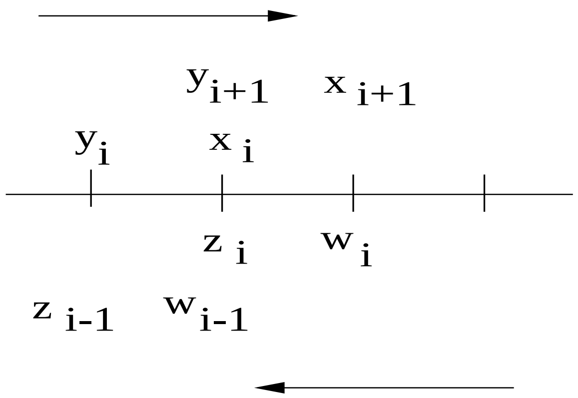

Figure 3.5: The action of the two systems in equation (3.9)

Let $R(x, y) = (y, x)$ and $\Phi(x, y) = (G(x, y), x)$ so that the dynamical systems in (3.9) is generated by Φ. By the definition of this diffeomorphism

$$\begin{aligned} R \circ \Phi \circ R \circ \Phi(x_i, y_i) &= R \circ \Phi(y_{i+1}, x_{i+1}) = R \circ \Phi(z_i, w_i) \\ &= R(z_{i-1}, w_{i-1}) = R(y_i, x_i) = (x_i, y_i) \end{aligned} \tag{3.10}$$

Since R is an involution with $\mathrm{Fix}(R) = \{(x, y) : x = y\}$ the diffeomorphism Φ and the dynamical system it induces on the plane are R-reversible.

To prove that the map Φ is volume preserving notice that

$$D\Phi = \begin{bmatrix} D_1G & D_2G \\ I & 0 \end{bmatrix} \tag{3.11}$$

By the definition of the function G we know that $F(\chi, \eta, G(\eta, \chi)) = 0$ so that differentiating with respect to χ leads to

$$D_1F + D_3FD_2G = 0 \tag{3.12}$$

D_3F is an invertible matrix by Condition 1, so that $D_2G = -D_1F(D_3F)^{-1}$. By assumption the system is symmetric so that $D_1F = D_3F$ at all points in $\mathbb{R}^{3p}$ and hence $D_2G = -I$. A direct calculation shows that

$$\begin{bmatrix} 0 & I \\ -I & 0 \end{bmatrix} \begin{bmatrix} D_1 G & -I \\ I & 0 \end{bmatrix} = \begin{bmatrix} I & 0 \\ -D_1 G & I \end{bmatrix}. \tag{3.13}$$

Since

$$\begin{vmatrix} 0 & I \\ -I & 0 \end{vmatrix} = \begin{vmatrix} I & 0 \\ -D_1 G & I \end{vmatrix} = 1 \tag{3.14}$$

it follows that $\det D\Phi = 1$ and the diffeomorphism Φ is volume preserving. $\diamondsuit$

R-reversible systems have many properties that facilitate their study. We will make use of several of these summarized in the following proposition adopted from [82]

Proposition 3.3.4 *Let R and Φ be as in Definition (3.3.2).*

1. *If $p \in Fix(R)$ and $\Phi^k(p) \in Fix(R)$, then $\Phi^{2k}(p) = p$. Such periodic points will be referred to as* symmetric periodic points[1]
2. *Let $p \in Fix(R)$ be a fixed point of Φ, then $R(W^u(p)) = W^s(p)$ and $R(W^s(p)) = W^u(p)$ so that if $q \in W^u(p) \cap Fix(R)$ then q is a homoclinic point.*
3. *If $p \in Fix(R)$ is a fixed point of Φ such that $W^u(p)$ intersects $Fix(R)$ transversally at a point q, then there exist infinitely many symmetric periodic points in any neighborhood of p.*

Not all periodic points of a reversible diffeomorphism are symmetric. The nonsymmetric periodic points occur in pairs since if p is a fixed point of Φ^k then so is $R(p)$ by reversibility.

Consider the spatial translation operator $S^k : \mathbb{R}^{nd} \to \mathbb{R}^{nd}$ and the inversion operator $J : \mathbb{R}^{nd} \to \mathbb{R}^{nd}$ defined on a state u in a ring of size n by $(S^k u)_j = u_{j+k \bmod n}$ and $(Ju)_j = u_{n-j \bmod n}$. If we imagine a ring of size n as a physical ring with nearest neighbors connected to each other the operator S^k rotates a state k steps, while J gives a mirror reflection of a state. From the definition of these two operators the following is immediate:

Proposition 3.3.5 *If $u = (u_j)$ is a fixed state in a ring of n systems symmetrically coupled to their nearest neighbors then both $S^k u$ and Ju are fixed states in the same ring. Moreover the stability of the states $S^k u$ and Ju is the same as the stability of u.*

Proof: It is clear that the proposition holds for S^k since by our assumption the coupling is homogeneous in the space variable. The evolution equation of the ring can be written as $u' = \mathcal{F}(u)$ where $u = (u_0, \ldots, u_{n-1})$ and $\mathcal{F}(u) = (F(u_{j-1 \bmod n}, u_j, u_{j+1 \bmod n})_{j=0}^{n-1} = (F(u_{n-1}, u_0, u_1)$ $, F(u_0, u_1, u_2)$ $, \ldots,$ $F(u_{n-2}, un-1, u_0))$. Using this notation it is immediate that

$$\begin{aligned} \mathcal{F}(Ju) &= (F(u_{n-j+1 \bmod n}, u_{n-j}, u_{n-j-1 \bmod n}))_{j=0}^{n-1} = \\ &= (F(u_{n-j-1 \bmod n}, u_{n-j}, u_{n-j+1 \bmod n}))_{j=0}^{n-1} = J\mathcal{F}(u) \end{aligned} \tag{3.15}$$

where the middle equality follows from the symmetry of the coupling. Differentiating both sides of this equation leads to:

$$D\mathcal{F}(Ju)J = JD\mathcal{F}(u) \tag{3.16}$$

[1] Note that this definition does not cover all periodic points whose orbits are mapped into themselves under R.

so that $D\mathcal{F}(Iu)$ and $D\mathcal{F}(u)$ are similar matrices and have the same eigenvalues. $\diamondsuit$

Let $O(x_0, x_1)$ and $R(O(x_0, x_1))$ be two orbits of period n of the system (**??**). These states correspond to steady states of the corresponding ring of size n. If the conditions of theorem 3.3.3 hold, the inversion operator J provides a connection between this pair of states.

Corollary 3.3.6 *The fixed states corresponding to $O(x_0, x_1)$ and $R(O(x_0, x_1))$ have the same stability.*

Proof: If we write $O(x_0, x_1) = ((x_0, x_1), (x_1, x_2), \ldots, (x_n, x_0))$ then $R(O(x_0, x_1)) = ((x_0, x_n), (x_n, x_{n-1}), \ldots, (x_1, x_0))$. If u is the fixed state of the ring corresponding $O(x_0, x_1)$ and v the fixed state corresponding to $R(O(x_0, x_1))$ then $Iu = v$. By proposition 3.3.5, u and v have the same stability. $\diamondsuit$

3.4 Steady States In the Case of Discrete Laplacian Coupling

For a chain of systems of the form $u' = f(u)$ coupled through a discrete Laplacian $\Delta u_j = (u_{j-1} - 2u_j + u_{j+1})$ the equation (3.2) takes the form

$$(u_j)' = f(u_j) + d(u_{j-1} - 2u_j + u_{j+1}) \tag{3.17}$$

and the dynamical system (3.5) takes the form

$$\begin{aligned} x_{i+1} &= -\frac{1}{d}f(x_i) - y_i + (2 + \frac{c}{d})x_i \\ y_{i+1} &= x_i \end{aligned} \tag{3.18}$$

where $c = 0$ in the case of continuous time and $c = 1$ in the case of discrete time. The following proposition follows immediately from these definitions

Proposition 3.4.1 *The fixed points of (3.18) are of the form $x_i = y_i = u_0$ where u_0 is any solution of the equation $f(u) = 0$ in the continuous time and $f(u) = u$ in the discrete time case. Thus all fixed points of (3.18) lie on $Fix(R) = \{(x, y) : x = y\}$ and are in 1-1 correspondence with the steady states of an uncoupled system in the chain.*

Proof: In the continuous time case if u_0 is a solution of $f(u) = 0$ and if $x_i = y_i = u_0$ then a direct computation shows that $x_{i+1} = y_{i+1} = x_i = y_i$. Conversely if (x_0, y_0) is a fixed point of equation (3.18) then another direct calculation shows that $f(x_0) = 0$. The same computations prove the proposition in the case of maps. $\diamondsuit$

The fixed points of (3.5) correspond to states of the chain that are constant in space and time and proposition 3.4.1 shows that the only such states $\{u_j\}_{j\in\mathbb{Z}}$ in the case of a discrete Laplacian coupling are given by $u_j = u_0$ for all $j \in \mathbb{Z}$ where u_0 is a fixed point of an uncoupled system of the chain $u' = f(u)$. Since the fixed points of (3.18) are $(u_0, u_0) \in \mathrm{Fix}(R)$[2] this allows us to make use

[2] A chain coupled by a discrete Laplacian is an instance of a chain that can be written as

$$(u_j)' = f(u_j) + g(u_{j-1}, u_j, u_{j+1}) \tag{3.19}$$

where $g(u_{j-1}, u_j, u_{j+1})$ vanishes on the linear submanifold of $\mathbb{R}^{3p}$ defined by $u_{j-1} = u_j = u_{j+1} = 0$. Notice that if some $u_0 \in \mathbb{R}^p$ satisfies $f(u_0) = 0$ in the continuous case or $f(u_0) = u_0$ in the discrete case then the state $\{u_j\}$ of (3.19) defined by $u_j = u_0$ for all $j \in \mathbb{Z}$ is a steady state of (3.19) by an argument identical to the one given in proposition 3.4.1. Moreover if the steady states of (3.19) can be expressed as orbits of (3.5), then the steady states $u_j = u_0$ will correspond to fixed points of the form (u_0, u_0) of (3.5). In this case the principles outlined in this section still apply.

of Proposition 3.3.4 .

Moreover we can apply Theorem 3.3.3 directly in this case to conclude that the map defining the fixed points is R-reversible and volume preserving.

Remark: It is interesting to note that if the fixed states of a chain of one dimensional systems are determined by a dynamical system of the form (3.18) on $\mathbb{R}^2$ and (x_0, y_0) is a fixed point of (3.18) then

$$D\Phi(x_0, y_0) = \begin{bmatrix} -\frac{1}{d}f'(x_0) + (2 + c/d) & 1 \\ -1 & 0 \end{bmatrix}. \tag{3.20}$$

The discriminant of the characteristic polynomial of $D\Phi(x_0, y_0)$ is

$$\sqrt{(-\frac{1}{d}f'(x_0) + 2 + c/d)^2 - 4}. \tag{3.21}$$

Since det $D\Phi(x_0, y_0) = 1$ we can conclude the following:

1. In the case of discrete time the eigenvalues of $D\Phi(x_0, y_0)$ are on the unit circle when $f'(x_0) > 1$ and $d > (f'(x_0) - 1)/4)$ or $f'(x_0) < 1$ and $d < (f'(x_0) - 1)/4)$.
2. In the case of continuous time, the eigenvalues of $D\Phi(x_0, y_0)$ are on the unit circle for sufficiently large *positive* d when $f'(x_0) > 0$ and for sufficiently large *negative* d when $f'(x_0) < 0$,

By a theorem going back to Birkhoff (see for example [85]) since Φ is area preserving, the dynamical system (3.18) will generically have infinitely many periodic orbits in any neighborhood of (x_0, y_0). Any such periodic orbit will correspond to a fixed state of (3.17) which is periodic in space, i.e. in the variable j.

The condition det $D\Phi(x_0, y_0) = 1$ is not sufficient to guarantee that $D\Phi(x_0, y_0)$ will have eigenvalues on the unit circle if (3.18) is not a dynamical system on the plane. Additional information needs to be considered to conclude the existence of such periodic orbits in this case.

Example 1: Consider a chain of systems whose dynamics is described by the tent map and which are coupled through a discrete Laplacian. This system can be written as $u'_j = f(u_j) + \Delta u_j$ with

$$f(u_j) = \begin{cases} 2u_j & \text{if } u_j < 1/2, \\ -2u_j + 2 & \text{if } u_j \geq 1/2. \end{cases} \tag{3.22}$$

The fixed states of this chain are the orbits of a homeomorphism of the plane given in (3.18) with $c = 1$.

Proposition 3.4.1 shows that the only fixed points of (3.18) are of the form (u_0, u_0) where u_0 is a solution of the equation $f(u) = u$, in this case (0,0) and (2/3, 2/3).

Since in this case the dynamical system (3.18) is linear in each of the two halves of the plane $x < 1/2$ and $x \geq 1/2$ the analysis of the dynamics around the fixed points is straightforward. In the region $x < 1/2$ the system can be written as:

$$\begin{bmatrix} x_{i+1} \\ y_{i+1} \end{bmatrix} = \begin{bmatrix} (2 - \frac{1}{d}) & -1 \\ 1 & 0 \end{bmatrix} \begin{bmatrix} x_i \\ y_i \end{bmatrix} \tag{3.23}$$

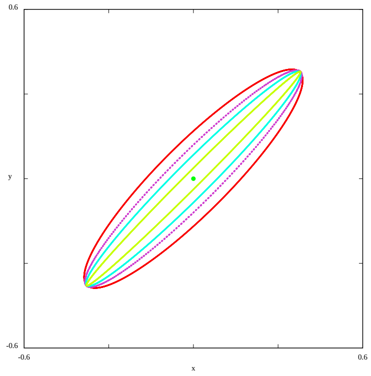

Figure 3.6: Invariant ellipses around (0,0) describing the fixed states in a chain of tent maps. As d increases the ellipses approach the diagonal.

By the previous remark, if $d > (f'(0) - 1)/4 = 1/4$ then the origin is an elliptic point. In this case the matrix in (3.23) has eigenvalues

$$\lambda_{\pm} = 1 - \frac{1}{2d} \pm \frac{1}{2}\sqrt{(\frac{1}{d} - 2)^2 - 4} \tag{3.24}$$

which lie on the unit circle in $\mathbb{C}$. Therefore if $d > 1/4$ the orbits of points around the origin lie on ellipses and are rotated by an angle

$$\theta = \arctan \frac{\sqrt{(4 - \frac{1}{d} - 2)^2}}{2 - \frac{1}{d}} \tag{3.25}$$

in each iteration. Since the system is R-reversible these ellipses must have their major axis on the diagonal $x = y$. If θ is irrational then this orbits correspond to quasiperiodic fixed states in the original chain of tent maps. If θ is rational these states are periodic fixed states in the chain or, equivalently, fixed states in a ring of size determined by the period of the points in the orbit.

As d increases $\lambda_{\pm} \to 1$ along the unit circle in $\mathbb{C}$. This means that the invariant ellipses around the origin become more and more eccentric and come closer to the diagonal $x = y$ as d increases. Therefore the fixed states in the chain of tent maps described by orbits lying on these invariant ellipses also approach the diagonal $u_i = u_j$ in the state space of the infinite chain of systems[3]

[3]Although not directly relevant to the present discussion, notice that the discrete Laplacian coupling will tend to synchronize a chain of continuous time dynamical systems since its spectrum lies in the interval $(-4, 0)$, i.e. in the

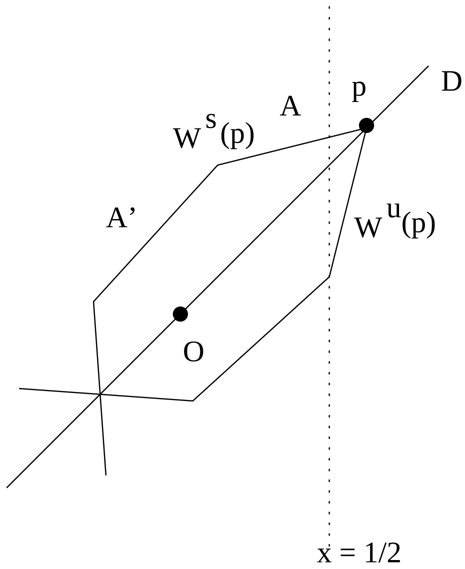

Figure 3.7: The invariant circles around (0,0) give way to complicated behavior close to (1/2, 1/2) due to the transversal intersection of $W^u(2/3, 2/3)$ and $W^s(2/3, 2/3)$.

Also as d increases the values of d that correspond to rational rotation angles θ lead to orbits of increasingly large periods, and therefore given a ring of fixed size N there is a value d_0 such that there are no stationary states in the ring close to the state $u_j = 0$ for all i.

The fixed states of the chain corresponding to these orbits are not stable. If $\hat{u} = \{\hat{u}_j\}_{j \in \mathbb{Z}}$ is a fixed state in the chain such that $\hat{u}_j < 1/2$ for all j then around this state the dynamics of the chain are described by:

$$u_j' = 2u_j + d\Delta u_j \tag{3.26}$$

The spectrum of the operator $2 + d\Delta$ is the interval $[2 - 4d, 2]$ and so $\hat{u}$ is not stable.

Besides these invariant ellipses, this system will also typically have infinitely many periodic orbits, and will exhibit complicated behavior, as the following argument shows. A simple calculation shows that the point $p = (2/3, 2/3)$ is hyperbolic for all values $d > 0$. Since the dynamics is piecewise linear the stable and unstable manifold can be calculated explicitly. $W^u(p)$ will consist of a ray contained in the half plane $x > 1/2$ and a second more complicated part which is constructed as follows. The first section of $W^u(p)$ is a line A, as shown in figure 3.4. The part of A contained in the half plane $x < 1/2$ is rotated along the invariant ellipses around the origin to the line A' under forward iteration. The subsequent images of A' are lines that are rotated further. Therefore $f^{n_0}(A')$ intersects the diagonal D for some n_0. Whenever the angle of this intersection is not a right angle $W^u(p)$ will intersect $W^s(p)$ transversely since by proposition 3.3.4 the stable manifold is the reflection of the unstable manifold through the diagonal $W^u(p)$. This shows that complicated

left half of $\mathbb{C}$ [9]. However since for large coupling values the spectrum of $d\Delta$ is outside the unit circle, such coupling will generally act to desynchronize a chain of discrete time systems. It is interesting to note that despite this, the stationary states discussed in the present example become more synchronous as d is increased.

dynamics of (3.18) can be expected and implies the existence of infinitely many periodic as well as spatially chaotic states in the chain of tent maps.

Example 2: We can apply the general ideas discussed in the previous sections to the case of rings, that is finite chains with periodic boundary conditions. The ring of Lorenz systems described in (3.1) will be considered and proposition 3.3.4 and a modification of an argument found in [82] will be used to show that for any value of d steady states exist for infinitely many values of n, where n is the size of the ring.

After setting the right–hand side of equations (3.1) to 0 and using the second and third equation in (3.1) to eliminate the variables y_i and z_i the following equation for a fixed state $\hat{\mathbf{v}} = \{\hat{x}_i, \hat{y}_i, \hat{z}_i\}_{i=-\infty}^{\infty}$ is obtained

$$\sigma(\hat{x}_i - \frac{\beta r \hat{x}_i}{\beta + (\hat{x}_i)^2}) - d(\hat{x}_{i-1} - 2\hat{x}_i + \hat{x}_{i+1}) = 0 \tag{3.27}$$

$$\hat{y}_i = \frac{\beta r \hat{x}_i}{\beta + (\hat{x}_i)^2} \tag{3.28}$$

$$\hat{z}_i = \frac{r(\hat{x}_i)^2}{\beta + (\hat{x}_i)^2}. \tag{3.29}$$

Equation (3.27) defines the following dynamical system on the plane

$$\begin{bmatrix} x_{i+1} \\ y_{i+1} \end{bmatrix} = F\left(\begin{bmatrix} x_i \\ y_i \end{bmatrix}\right) = \begin{bmatrix} \frac{\sigma}{d}(x_i - \frac{\beta r x_i}{\beta + (x_i)^2}) + 2x_i - y_i \\ x_i \end{bmatrix} \tag{3.30}$$

Orbits of period n of this system are in 1–1 correspondence with the steady states in the ring of n Lorenz systems. As in the previous example all fixed points (x_0, y_0) of (3.30) lie on $\text{Fix}(R)$ and $x_0 = y_0 = u_0$ where u_0 is a root of $f(u) = \sigma(u - \frac{\beta r u}{\beta + (u)^2})$. The fixed points are therefore (0,0) and $(\pm\sqrt{\beta(r-1)}, \pm\sqrt{\beta(r-1)}) = (\pm 8.32\dot{6}, \pm 8.32\dot{6})$.

To proceed we need the following definition from [82]

Definition 3.4.2 *A compact region H in the plane is called* overflowing *in the y-direction for a function F if the image of any point $(x_0, y_0) \in int(H)$ lies strictly above the line $y = y_0$. In other words the y-coordinate function is a strict Lyapunov function for points in the interior of H.*

Notice that any point in the interior of H either leaves H or is asymptotic to a periodic point on the boundary of H.

Theorem 3.4.3 *The map (3.30) has a homoclinic point and infinitely many periodic points for all $0 < d \leq 20$.*

Proof: Let p denote the fixed point $(-\sqrt{\beta(r-1)}, -\sqrt{\beta(r-1)})$ of (3.30), G the line $y = -\sqrt{\beta(r-1)}$ with $x > -\sqrt{\beta(r-1)}$, and $D = \{(x,y) : x = y\}$ the diagonal in $\mathbb{R}^2$. The image of the triangular region W bounded by D and G lies between the two cubics

$$F(D) = \{(x,y) : x = \frac{\sigma}{d}(y - \frac{\beta r y}{\beta + y^2}) + y\} \tag{3.31}$$

$$F(G) = \{(x,y) : x = \frac{\sigma}{d}(y - \frac{\beta r y}{\beta + y^2}) + 2y + \sqrt{\beta(r-1)}\} \tag{3.32}$$

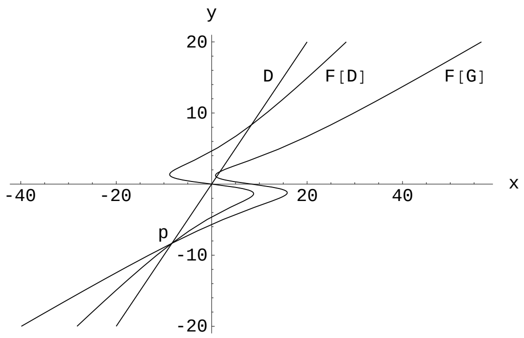

Figure 3.8: The region H is bounded by the two cubics $F(D)$ and $F(G)$ and D. The figure on the left W corresponds to the case $d = 20$. For $d > 20 + \epsilon$ these curves do not bound a compact region.

Consider the region $F(W) \cap W = H$ depicted in figure 3.8. Let $(x_0, y_0) \in \text{int}(H)$ and consider the vertical line segment l passing through (x_0, y_0) and connecting G and D. The image of l is a horizontal line segment connecting $F(G)$ and $F(D)$ contained in the line $y = x_0$. Any point of this line segment lies above (x_0, y_0). Therefore H is overflowing in the y direction.

Since $F(H)-$ int(H) and H lie on opposite sides of D, any point in H must have an iterate which either lies on D or crosses D. A direct calculation shows that one branch of $W^u(p)$ enters H. Since H is overflowing in the y direction, $W^u(p)$ must either cross D or be asymptotic to the fixed point $(0, 0)$ creating a saddle-saddle connection. The second possibility can be excluded as follows:

The eigenvector of the linearization of F around (0,0) corresponding to the stable direction is $\mathbf{v}_1 = (1, -\frac{d}{d-130+2\sqrt{65^2-d}})$. The vector $\mathbf{v}_2 = (1, \frac{d-260}{d})$ is tangent to $F(D)$ at (0,0). A direct computation shows that for $0 < d < 20$ the vector $\mathbf{v}_1$ points to the left of $\mathbf{v}_2$ and so the tangent to $W^s(0, 0)$ at (0,0) does not point into H. This excludes the possibility that $W^u(p)$ is asymptotic to (0,0).

By proposition 3.3.4 the fact that $W^u(p)$ meets D implies the existence of a homoclinic point.

Numerical investigations suggest that the theorem remains true for arbitrarily large values of d, although a more subtle argument is needed to prove this.

By proposition 3.3.4 in the case of R-reversible systems an infinite number of periodic points exists whenever $W^u(p)$ crosses D transversely at a homoclinic point. If this point of intersection is not transverse then a transverse intersection of $W^u(p)$ and D can be produced nearby by an argument given in [82], p. 261. $\diamondsuit$

A priori one can not expect that any of the steady states corresponding to these periodic orbits are stable. Numerical investigations show that not only are they stable, but their basins of attraction occupy a large portion of phase space. Further numerical experiments suggest that their basins of attraction are intertwined in a complicated way so that even the choice of integration method can lead to different steady states. In what follows we analyze the stability of the periodic fixed states.

3.5 Stability of the steady states

In the previous sections it has been shown that periodic fixed states can be expected to exist in chains of symmetrically coupled systems, and it is now time to examine when such states will be

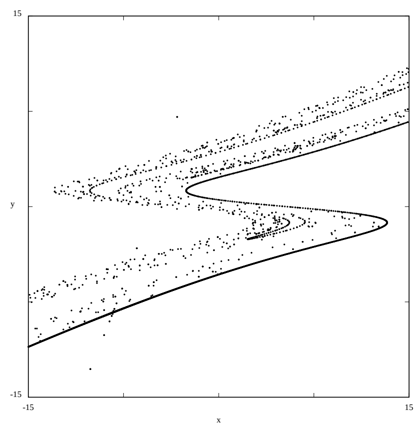

Figure 3.9: A numerical approximation of the manifold $W^u(p)$ is shown on the right. The complex structure of the manifold suggests complicated behavior on some invariant set of points.

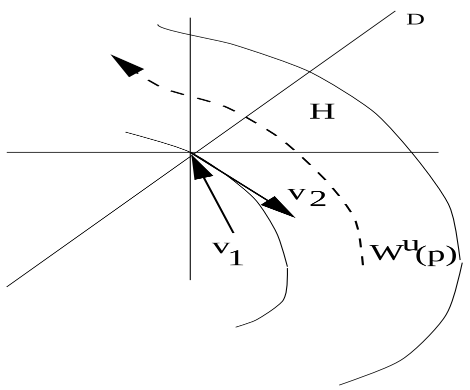

Figure 3.10: If $W^u(p)$ coincides with the stable manifold of the origin then v_1 must be tangent to $W^u(p)$ at the origin. Since v_1 points outside of H this is impossible.

stable. The study of stable fixed states in a chain of oscillators is not new. They are described in [83], [78] as instances of oscillator death in a chain of neural oscillators, in [75] as synchronous states of phase lock loops, and conditions for the stability of complex stationary states in general lattices are given in [74]. The situation presented here is different in that an explicit periodic stationary state is analyzed in a case where the methods from the theory of parabolic partial differential equations used in [83] are not applicable, and the conditions proposoed in [74] cannot be verified.

In the following sections we will concentrate on the specific example of a ring of Lorenz systems coupled in the x variable discussed in example 2 of the last section. However the ideas presented can be applied to any chain of symmetrically coupled systems for which condition 1 holds.

The linearization of each of the Lorenz equations around a point $\hat{\mathbf{v}}_{\mathbf{i}} = (\hat{x}_i, \hat{y}_i, \hat{z}_i)$ when $d = 0$ is

$$D_{\hat{\mathbf{v}}_{\mathbf{i}}} f = \begin{bmatrix} -\sigma & \sigma & 0 \\ r - \hat{z}_i & -1 & -\hat{x}_i \\ \hat{y}_i & \hat{x}_i & -b \end{bmatrix} \tag{3.33}$$

and hence linearizing the entire ring around the steady state $\hat{\mathbf{v}} = (\hat{\mathbf{v}}_{\mathbf{i}})_{i=1}^{n} = (\hat{x}_1, \hat{y}_1, \hat{z}_1, \dots, \hat{x}_n, \hat{y}_n, \hat{z}_n)$ leads to

$$D_{\hat{\mathbf{v}}} F = \begin{bmatrix} D_{\hat{\mathbf{v}}_{\mathbf{1}}} f - 2\Gamma & \Gamma & 0 & \dots & 0 & \Gamma \\ \Gamma & D_{\hat{\mathbf{v}}_{\mathbf{2}}} f - 2\Gamma & \Gamma & \dots & 0 & 0 \\ \dots & \dots & \dots & \dots & \dots & \dots \\ \Gamma & 0 & 0 & \dots & \Gamma & D_{\hat{\mathbf{v}}_{\mathbf{n}}} f - 2\Gamma \end{bmatrix} \tag{3.34}$$

where the matrix Γ is defined as:

$$\Gamma = \begin{bmatrix} d & 0 & 0 \\ 0 & 0 & 0 \\ 0 & 0 & 0 \end{bmatrix} \tag{3.35}$$

We were unable to compute the eigenvalues of this matrix analytically and in particular cases numerical methods were used to determine the stability of the system.

Even if some of the fixed states in a ring of n systems are stable it can not be concluded that stable equilibria exist in arbitrarily long rings of such systems. If a stable fixed state is viewed as a special case of synchronization, it could be guessed from results in Afraimovich and Lin [76] that the coupling necessary to have stable steady states in longer rings increases as a power of the size of the ring. It has already been argued that this is not realistic from a physical viewpoint.

In what follows we address the existence of asymptotically stable fixed states. If $\hat{\mathbf{v}}$ is a fixed state in a ring of n oscillators then repeating these values K times to obtain $\hat{\mathbf{v}}^{(K)} = \{\hat{\mathbf{v}}, \hat{\mathbf{v}}, \dots, \hat{\mathbf{v}}\}$ produces a steady state in a chain of Kn oscillators. We refer to such a state as the *K-multiple* of the steady state $\hat{\mathbf{v}}$. We will derive conditions under which all K-multiples of a stable steady state are themselves stable and demonstrate that these conditions hold in a particular case.

The linearization around the steady state $\hat{\mathbf{v}}^{(K)}$ leads to the following stability matrix:

$$D_{\hat{\mathbf{v}}^{(K)}} F = \begin{bmatrix} M & E_d & 0 & \dots & 0 & E_u \\ E_u & M & E_d & \dots & 0 & 0 \\ \dots & \dots & \dots & \dots & \dots & \dots \\ E_d & 0 & 0 & \dots & E_u & M \end{bmatrix}$$

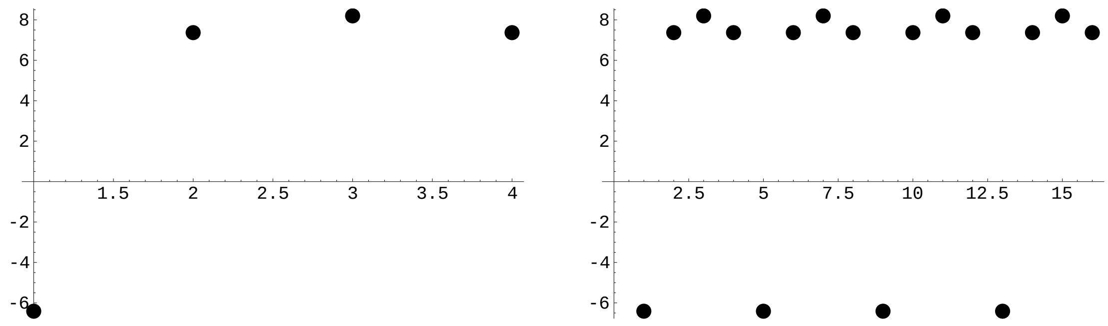

Figure 3.11: The fixed state that will be used as an example, and its 4-multiple.

where

$$M = \begin{bmatrix} D_{\hat{\mathbf{v}}_1} f - 2\Gamma & \Gamma & 0 & \dots & 0 & 0 \\ \Gamma & D_{\hat{\mathbf{v}}_2} f - 2\Gamma & \Gamma & \dots & 0 & 0 \\ \cdots & \cdots & \cdots & \cdots & \cdots & \cdots \\ 0 & 0 & 0 & \dots & \Gamma & D_{\hat{\mathbf{v}}_n} f - 2\Gamma \end{bmatrix}$$

and E is an $3n \times 3n$ matrix of the form

$$E_u = \begin{bmatrix} 0 & \dots & \Gamma \\ \cdots & \cdots & \cdots \\ 0 & \dots & 0 \end{bmatrix} \qquad E_d = \begin{bmatrix} 0 & \dots & 0 \\ \cdots & \cdots & \cdots \\ \Gamma & \dots & 0 \end{bmatrix}$$

In general it is impossible to compute the spectrum of this $3Kn \times 3Kn$ matrix. However in the present instance Bloch wave theory, also known as Floquet theory, provides a way of expressing the eigenfunctions of a larger system with a periodic dependency as the eigenfunctions of a smaller system. This reduction is usually accompanied by the introduction of an additional parameter into the equations. Here the Bloch wave approach will be used to reduce the problem of computing the eigenvalues of the $3Kn \times 3Kn$ matrix $D_{\hat{\mathbf{v}}^{(K)}}$ for arbitrary K to the computation of the eigenvalues of an $3n \times 3n$ matrix dependent on a parameter t.

Let $\mathbf{e} = (\Psi(j), \Phi(j), \eta(j))_{j=1}^{Kn} = (\Psi(1), \Phi(1), \eta(1), \dots, \Psi(Kn), \Phi(Kn), \eta(Kn))$ where

$$\begin{aligned} \Psi(j) &= \exp\left(\frac{2\pi i q}{nK} j\right) \tilde{\Psi}_q(j) \\ \Phi(j) &= \exp\left(\frac{2\pi i q}{nK} j\right) \tilde{\Phi}_q(j) \\ \eta(j) &= \exp\left(\frac{2\pi i q}{nK} j\right) \tilde{\eta}_q(j) \end{aligned} \tag{3.36}$$

for $1 \leq q \leq Kn$ and $\tilde{\Psi}_q, \tilde{\Phi}_q, \tilde{\eta}_q$ are assumed to be n-periodic. We will show that the vector $\mathbf{e}$ is an eigenvector of $D_{\hat{\mathbf{v}}^{(K)}}$ whenever the vector

$$\mathbf{i} = (\tilde{\Psi}(j), \tilde{\Phi}(j), \tilde{\eta}(j))_{j=1}^{n} \tag{3.37}$$

is an eigenvector of a particular $3n \times 3n$ matrix derived from $D_{\hat{\mathbf{v}}(K)}$. A direct calculation leads to:

$$
\begin{aligned}
[D_{\hat{\mathbf{v}}(K)}F]\,\mathbf{e}\,(3j) =& e^{\frac{2\pi iq}{nK}j}(de^{\frac{2\pi iq}{nK}}\tilde{\Psi}_q(j+1 \bmod n) + de^{-\frac{2\pi iq}{nK}}\tilde{\Psi}_q(j-1 \bmod n) - \\
& 2\tilde{\Psi}_q(j) + v_1(j)\tilde{\Psi}_q(j) + w_1(j)\tilde{\Phi}_q(j) + u_1(j)\tilde{\eta}_q(j)) \\
[D_{\hat{\mathbf{v}}(K)}F]\,\mathbf{e}\,(3j+1) =& e^{\frac{2\pi iq}{nK}j}(v_2(j)\tilde{\Psi}_q(j) + w_2(j)\tilde{\Phi}_q(j) + u_2(j)\tilde{\eta}_q(j)) \\
[D_{\hat{\mathbf{v}}(K)}F]\,\mathbf{e}\,(3j+2) =& e^{\frac{2\pi iq}{nK}j}(v_3(j)\tilde{\Psi}_q(j) + w_3(j)\tilde{\Phi}_q(j) + u_3(j)\tilde{\eta}_q(j))
\end{aligned}
\tag{3.38}
$$

for $1 \leq j \leq Kn$. Here $v_i(j), w_i(j), u_i(j)$ are given by equation (3.33) as

$$
\begin{bmatrix} v_1(j) & w_1(j) & u_1(j) \\ v_2(j) & w_2(j) & u_2(j) \\ v_3(j) & w_3(j) & u_3(j) \end{bmatrix} = \begin{bmatrix} -\sigma & \sigma & 0 \\ r - \hat{z}_{j \bmod n} & -1 & -\hat{x}_{j \bmod n} \\ \hat{y}_{j \bmod n} & \hat{x}_{j \bmod n} & -b \end{bmatrix}
$$

and are thus n-periodic.

We want to check when $\mathbf{e}$ is an eigenvector of $D_{\hat{\mathbf{v}}(K)}$ and so we set $D_{\hat{\mathbf{v}}(K)}\mathbf{e} = \lambda\mathbf{e}$. Using the expressions obtained in (3.38) we get

$$
\begin{aligned}
&\exp\left(\frac{2\pi iq}{nK}j\right)\left(de^{\frac{2\pi iq}{nK}}\tilde{\Psi}_q(j+1 \bmod n) + de^{-\frac{2\pi iq}{nK}}\tilde{\Psi}_q(j-1 \bmod n) - \right. \\
&2\tilde{\Psi}_q(j) + v_1(j)\tilde{\Psi}_q(j) + w_1(j)\tilde{\Phi}_q(j) + u_1(j)\tilde{\eta}_q(j),\;\; v_2(j)\tilde{\Psi}_q(j) + w_2(j)\tilde{\Phi}_q(j) + u_2(j)\tilde{\eta}_q(j), \\
&\left. v_3(j)\tilde{\Psi}_q(j) + w_3(j)\tilde{\Phi}_q(j) + u_3(j)\tilde{\eta}_q(j)\right)_{j=1}^{Kn} = \lambda \exp\left(\frac{2\pi iq}{nK}j\right)\left(\tilde{\Psi}_q(j), \tilde{\Phi}_q(j), \tilde{\eta}_q(j)\right)_{j=1}^{Kn}.
\end{aligned}
\tag{3.39}
$$

Since all the functions on the right hand side of (3.39) are n-periodic we can express equation (3.39) as $\mathcal{D}(q)\mathbf{i} = \lambda\mathbf{i}$ where $\mathbf{i}$ is defined in equation (3.37) and

$$
\mathcal{D}(q) = \begin{bmatrix} D_{\hat{\mathbf{v}}_1}f - 2\Gamma & E(q)^+ & 0 & \dots & 0 & E(q)^- \\ E(q)^- & D_{\hat{\mathbf{v}}_2}f - 2\Gamma & E(q)^+ & \dots & 0 & 0 \\ \dots & \dots & \dots & \dots & \dots & \dots \\ E(q)^+ & 0 & 0 & \dots & E(q)^- & D_{\hat{\mathbf{v}}_n}f - 2\Gamma \end{bmatrix}
\tag{3.40}
$$

where the matrices $E(q)^{\pm}$ are defined as:

$$
E(q)^{\pm} = \begin{bmatrix} de^{\pm\frac{2\pi iq}{nK}} & 0 & 0 \\ 0 & 0 & 0 \\ 0 & 0 & 0 \end{bmatrix}
\tag{3.41}
$$

This implies that the eigenvalues of $D_{\hat{\mathbf{v}}(K)}F$ are the same as the eigenvalues of the $3n \times 3n$ matrices $\mathcal{D}(q)$ for $1 \leq q \leq Kn$.

The $3n \times 3n$ matrix $\mathcal{D}(q)$ is easier to handle than the $3nK \times 3nK$ matrix $D_{\hat{\mathbf{v}}(K)}F$. The same idea can be applied to reduce the problem of determining the stability of the K-multiple of a stable state in a ring of oscillators to the problem of determining the eigenvalues of a matrix of type (3.40).

3.6 Stability of fixed states in arbitrarily large rings

To conclude that any K-multiple of a stable fixed state $\mathbf{v}_0$ of a ring of n oscillator is stable it is sufficient to show that the eigenvalues of the matrix $\mathcal{D}(q)$ have negative real part for all values of q

and K. To simplify the calculations we can replace the argument $q \in \mathbb{Z}$ by a continuous parameter $t \in \mathbb{R}$ by replacing the matrices $E(q)^{\pm}$ with the matrices

$$E_t^{\pm} = \begin{bmatrix} de^{\pm it} & 0 & 0 \\ 0 & 0 & 0 \\ 0 & 0 & 0 \end{bmatrix}$$

in the expression for $\mathcal{D}$. If we can show that $\mathcal{D}(t)$ has eigenvalues with negative real part for all $t \in \mathbb{R}$ then the same is true for $\mathcal{D}(q)$ for any values of K and q in $\mathbb{Z}$. This eliminates the dependence on the size of the ring, Kn.

Sufficient conditions for all eigenvalues of $\mathcal{D}(t)$ to be in the left half of the complex plane will be obtained as a consequence of the following lemma and a convergence criterion for the Newton-Raphson method. We first prove the following lemmas about the class of matrices of type (3.40) which come from the Bloch wave reduction of $K - multiples$ in systems of arbitrary size coupled through one variable.

Lemma 3.6.1 *Assume A is an $(n+m) \times (n+m)$ matrix of the form*

$$A = \begin{bmatrix} B & D^{+} & 0 & \dots & 0 \\ D^{-} & & & & \\ 0 & & C & & \\ \vdots & & & & \\ 0 & & & & \end{bmatrix} \tag{3.42}$$

where B and C are arbitrary $n \times n$, respectively $m \times m$ matrices and $D^{\pm}$ are $n \times n$ matrices of the form

$$D^{\pm} = \begin{bmatrix} d_{\pm} & 0 & \dots & 0 \\ 0 & 0 & \dots & 0 \\ \dots & \dots & \dots & \dots \\ 0 & 0 & \dots & 0 \end{bmatrix}. \tag{3.43}$$

Writing the determinant of A as

$$\det A = \sum_{\sigma} sgn\, \sigma \prod_{i=1}^{m+n} a_{i,\sigma(i)} \tag{3.44}$$

then if $a_{1,\sigma(1)} = a_{1,n+1} = d_{+}$ then

$$\prod_{i=2}^{M+n} a_{i,\sigma(i)} \neq 0 \tag{3.45}$$

only if $a_{n+1,\sigma(n+1)} = a_{n+1,1} = d_{-}$.

This lemma simply states that the only nonzero products in (3.44) containing d_{+} as a factor necessarily contain d_{-} as a factor. Notice that since we can interchange rows and columns when calculating determinants the opposite is also true: nonzero products containing d_- as a factor necessarily contain d_+ as a factor.

Proof: Writing the matrix A as

$$A = \begin{bmatrix} b_{1,1} & b_{1,2} & \dots & b_{1,n} & d_+ & 0 & \dots \\ b_{2,1} & b_{2,2} & \dots & b_{2,n} & 0 & 0 & \dots \\ \dots & \dots & \dots & \dots & \dots & \dots & \dots \\ d_- & 0 & \dots & 0 & & & \\ 0 & 0 & \dots & 0 & & & \\ \vdots & \vdots & \vdots & \vdots & & \mathrm{C} & \\ 0 & 0 & 0 & 0 & & & \end{bmatrix}. \tag{3.46}$$

If $a_{n+1,\sigma(n+1)} = a_{n+1,1} = d_+$ and $\sigma(i) = 1$ for some $2 \leq i \leq n$ another $n-1$ nonzero factors in the product (3.45) need to be chosen from columns 2 through n. However, barring rows 1 and i which were already used, there are only $n-2$ rows remaining which have nonzero entries in these columns. This shows that factors $a_{2,\sigma(2)}, a_{3,\sigma(3)}, \dots, a_{n,\sigma(n)}$ must come from columns 2 through n. Since the rows 1 through n are now exhausted, the only nonzero element remaining in column 1 is d_-. This proves the lemma. $\diamondsuit$

Lemma 3.6.2 *The characteristic polynomial of the $Km \times Km$ matrix*

$$A = \begin{bmatrix} M_1 & E(t)^+ & 0 & \dots & 0 & 0 & 0 \\ E(t)^- & M_2 & E(t)^+ & \dots & 0 & 0 & 0 \\ \dots & \dots & \dots & \dots & \dots & \dots & \dots \\ 0 & 0 & 0 & \dots & E(t)^- & M_{K-1} & E(t)^+ \\ 0 & 0 & 0 & \dots & 0 & E(t)^- & M_K \end{bmatrix}$$

where M_i are arbitrary $m \times m$ matrices and $E(t)^\pm$ are $m \times m$ matrices defined as

$$E(t)^\pm = \begin{bmatrix} de^{\pm it} & 0 & \dots & 0 \\ 0 & 0 & \dots & 0 \\ \dots & \dots & \dots & \dots \\ 0 & 0 & \dots & 0 \end{bmatrix}$$

does not depend on t.

Proof: Define the matrix $C = A - \lambda I$. We need to show that the determinant of C is independent of t. The proof is by induction on K. When $K = 1$ the matrix C is itself t independent so the statement is trivial. The cofactors of the entries $c_{1,j}$ for $1 \leq j \leq m$ are of the form

$$\begin{bmatrix} c_{2,1} & \dots & \hat{c}_{2,j} & \dots & c_{1,m} & 0 & \dots & 0 \\ \dots & \dots & \dots & \dots & \dots & \dots & \dots & \dots \\ c_{m,1} & \dots & \hat{c}_{m,j} & \dots & c_{m,m} & 0 & \dots & 0 \\ de^{-it} & 0 & \dots & \dots & 0 & & & \\ 0 & 0 & \dots & \dots & 0 & & & \\ \vdots & \vdots & \vdots & \vdots & \vdots & & \mathrm{M} & \\ 0 & 0 & 0 & 0 & 0 & & & \end{bmatrix} \tag{3.47}$$

where the hat signifies the omission of that particular column. Since the columns and rows can be interchanged when the determinant is computed lemma 3.6.1 implies that any product in (3.44) containing de^{-it} as a factor also contains $c_{1,n+1} = 0$ as a factor and is thus zero. Lemma 3.6.1 also implies that any nonzero product containing $c_{1,n+1} = de^{it}$ as a factor necessarily contains $c_{1,n+1} = de^{-it}$ as a factor and so does not depend on t either. Since this exhausts all possible cofactors of the nonzero elements of the first row the lemma is proved. $\diamondsuit$

The preceding two lemmas lead to the following.

Lemma 3.6.3 *Let $E(t)^{\pm}$ be as in the previous lemma. The characteristic polynomial of a $Km \times Km$ matrix*

$$B = \begin{bmatrix} M_1 & E(t)^+ & 0 & \dots & 0 & 0 & E(t)^- \\ E(t)^- & M_2 & E(t)^+ & \dots 0 & & 0 & 0 \\ \dots & \dots & \dots & \dots & \dots & \dots & \\ 0 & 0 & 0 & \dots & E(t)^- & M_{K-1} & E(t)^+ \\ E(t)^+ & 0 & 0 & \dots & 0 & E(t)^- & M_K \end{bmatrix}$$

is of the form

$$p_M(t,\lambda) = \sum_{i=0}^{(K-1)m} (\alpha_i + \beta_i \cos Kt)\lambda^i + \sum_{i=(K-1)m+1}^{Km} \alpha_i \lambda^i. \tag{3.48}$$

In particular, notice that the matrix $\mathcal{D}(t)$ is of this type.

Proof: We need to show that the determinant of $C = B - \lambda I$ is of the form (3.48). Definition (3.44) will again be used for the determinant. We now have three cases:

Case 1: Assume that for σ in the product in (3.44) we have $1 \leq \sigma(1) \leq m$. Since the next $m-1$ rows have zero entries in all but the first m columns this particular product will be zero unless it contains $c_{j,1}$ as a factor for some $1 \leq j \leq m$. This excludes the possibility that either $c_{1,(K-1)m+1} = de^{-it}$ or $c_{(K-1)m+1,1} = de^{it}$ appear as factors. If we fix $\sigma(1), \dots, \sigma(m)$, the part of the sum (3.44) corresponding to all such permutations σ is equal to

$$c_{1,\sigma(1)} \cdots c_{m,\sigma(m)} \begin{vmatrix} M_2 & E(t)^+ & 0 & \dots & 0 & 0 & 0 \\ E(t)^- & M_3 & E(t)^+ & \dots 0 & & 0 & 0 \\ \dots & \dots & \dots & \dots & \dots & \dots & \\ 0 & 0 & 0 & \dots & E(t)^- & M_{K-1} & E(t)^+ \\ 0 & 0 & 0 & \dots & 0 & E(t)^- & M_K \end{vmatrix} \tag{3.49}$$

by cofactor expansion. By lemma 3.6.2 these summands will not depend on t.

Case 2: Assume that $\sigma(1) = m+1$ so that the first factor in the product in (3.44) is $c_{1,m+1} = de^{it}$. Then the elements $c_{2,\sigma(2)}, \dots, c_{m,\sigma(m)}$ must come from the matrix

$$\tilde{C} = \begin{bmatrix} c_{2,2} & \dots & c_{2,m} \\ c_{3,2} & \dots & c_{3,m} \\ \dots & \dots & \dots \\ c_{m,2} & \dots & c_{m,m} \end{bmatrix}$$

by an argument identical to the one given in the second paragraph of lemma (3.6.1). The only nonzero factors that can be chosen from column 1 are therefore $c_{m+1,\sigma(m+1)} = c_{m+1,1} = de^{-it}$ and $c_{(K-1)m+1,\sigma(K-1)m+1} = c_{(K-1)m+1,1} = de^{it}$. We therefore have the following two subcases:

Case 2a: If $c_{m+1,1} = de^{-it}$ is chosen it cancels the term $c_{1,m+1} = de^{it}$ that was chosen as the first factor in the product. In this case we are again in the situation of lemma 3.6.2 using Laplace expansion as in case 1, and so this product will not depend on t.

The contributions to the characteristic polynomial from Case 1 and 2a are time independent and therefore enter the term $\sum_{i=(K-1)m+1}^{Km} \alpha_i \lambda^i$ in (3.48). The remainder of the lemma follows from induction.

Case 2b: If the assumptions of Case 2 hold and $c_{(K-1)m+1,\sigma((K-1)m+1)} = c_{(K-1)m+1,1} = de^{it}$ then if a permutation σ leads to a nonzero product in (3.44) it must satisfy $\sigma(jm+1) = (j+1)m+1$ for all $j < K-1$. This simply means that any nonzero product of this kind contains all the entries $c_{jm+1,(j+1)m+1} = de^{it}$ as factors. This assertion is proved as follows:

The factor $c_{1,m+1}$ is contained in the product by assumption. Assume that $\sigma(lm+1) = (l+1)m+1$ for all $l < j$. It will be shown that in this case $\sigma(jm+1) = (jm+1)m+1$ which will complete the induction argument.

By assumption the $\sigma((j-1)m+1) = jm+1$. The only nonzero elements in columns $jm+2, \ldots (j+1)m$ come from the submatrix

$$\begin{bmatrix} c_{jm+2,jm+2} & \cdots & c_{jm+2,(j+1)m} \\ c_{jm+3,jm+2} & \cdots & c_{jm+3,(j+1)m} \\ \cdots & \cdots & \cdots \\ c_{(j+1)m,jm+2} & \cdots & c_{(j+1)m,(j+1)m} \end{bmatrix}$$

and since an entry from row $jm+1$ has already been chosen, the coefficients $c_{jm+2,\sigma(jm+2)}, \ldots, c_{(j+1)m,\sigma((j+1)m)}$ must all come from this submatrix. The only nonzero entries remaining on row $jm+1$ are $c_{jm+1,(j-1)m+1} = de^{-it}$ and $c_{jm+1,(j+1)m+1} = de^{it}$. By the induction hypothesis we can exclude the first possibility and we are left to conclude that $c_{jm+1,(j+1)m+1} = de^{it}$ for any $1 < j < K$ is a coefficient in any nonzero product in the case 2b.

This shows that any permutation σ of the type described in Case 2b contributes a factor $\gamma_\sigma e^{Kit} r(\lambda)$ to the characteristic polynomial (3.48).

Case 3: The only remaining nonzero entry in row 1 of matrix C is $c_{1,(K-1)m+1} = de^{-it}$. An argument identical to the one presented in case 2 shows that any permutation σ leading to a nonzero summand in (3.44) must satisfy either $c_{(K-1)m+1,\sigma((K-1)m+1)} = c_{(K-1)m+1,1} = de^{it}$ or $c_{(K-1)m+1,\sigma((K-1)m+1)} = c_{(K-1)m+1,(K-2)m+1} = de^{-it}$ which again leads to two subcases:

Case 3a: If $c_{(K-1)m+1,\sigma((K-1)m+1)} = de^{it}$ the situation is virtually identical to case 2a. Laplace expansion and lemma 3.6.2 show that the contributions to the characteristic polynomial are independent of t.

Case 3b: If $c_{(K-1)m+1,\sigma((K-1)m+1)} = de^{-it}$ the situation is similar to case 2b. A parallel argument shows that all the terms de^{-it} in the matrix must be coefficients in any nonzero product. Moreover due to the properties of the matrix, to each product $\gamma_\sigma e^{Kit} r(\lambda)$ from case 2b corresponds a product $\gamma_\sigma e^{-Kit} r(\lambda)$ from this case. Since these are the only time dependent contributions to the characteristic polynomial the lemma is proved. $\diamondsuit$

3.7 An Example

This section describes a computer assisted proof that any K-multiple of a particular stable fixed state in a ring of four Lorenz system is stable. The proof involves the use of interval arithmetic and the following theorems about the convergence of the Newton-Raphson-Kantorovich method. The computations were performed using Mathematica's implementation of interval arithmetic. The code used to perform the computation is given in appendix B.

Theorem 3.7.1 *Let $f(z)$ be a complex analytic function and assume $f(z_0)f'(z_0) \neq 0$ for some z_0. Define $h_0 = -f(z_0)/f'(z_0)$, the disc $K_0 = \{z : |z - z_0| \leq |h_0|\}$ and $M = \max_{K_0} |f''(z)|$. If $2|h_0|M \leq |f'(z_0)|$ then there is exactly one root of f in the closed disc K_0.*

Theorem 3.7.2 (Kantorovich's Convergence Theorem) *Given a twice differentiable function $f : \mathbb{R}^n \to \mathbb{R}^n$ which is nonsingular at a point $x_0 = (x_1^0, x_2^0, \ldots, x_n^0)$ let $[\Gamma_{ik}] = [\frac{\partial f_i}{\partial x_k}(x_0)]^{-1}$. Let A, B, C be positive real numbers such that*

$$\max_i \sum_{k=1}^{n} |\Gamma_{ik}| \leq A \qquad \max_i \sum_{k=1}^{n} |\Gamma_{ik} f_k(x_0)| \leq B \qquad C \leq \frac{1}{2AB}. \tag{3.50}$$

Define the region $R = \{x \in \mathbb{R}^n : \max_i |x_i - x_i^0| \leq (AC)^{-1}(1 - \sqrt{1 - 2ABC})\}$. If

$$\max_{x \in R} \sum_{j=1}^{n} \sum_{k=1}^{n} \left| \frac{\partial^2 f_i}{\partial x_j \partial x_k} \right| \leq C \qquad i = 1, \ldots, n \tag{3.51}$$

then the equation $f(x) = 0$ has a solution in R.

The argument will proceed as follows: First a steady state of the ring is found using interval arithmetic. Next it is shown that the polynomial $p_{\mathcal{D}}(\lambda, t)$ of this steady state has roots with negative real part at $t = \frac{\pi}{4}$. Finally it is proved that $p_{\mathcal{D}}(\lambda, t)$ does not have roots on the imaginary axis for any $t \in \mathbb{R}$. Since the roots of a polynomial depend continuously on its coefficients this implies that the roots of $p_{\mathcal{D}}(\lambda, t)$ cannot cross into right half of $\mathbb{C}$. By the results of section 3.6 this implies that all K-multiples of the fixed state under consideration must be stable.

In the following intervals of numbers will be denoted with overbars to distinguish them from real numbers, and make the notation less cumbersome. For instance $\bar{\lambda}$ denotes an interval and the interval $[3.16524, 3.16533]$ is denoted $\overline{3.165}$.

Numerical investigations with the program XPP show that a stable state in a chain of four oscillators coupled with $d = 1.5$ occurs close to $\hat{\mathbf{x}} = (\hat{x}_1, \hat{x}_2, \hat{x}_3, \hat{x}_4) =$ (-6.4114408, 7.3696656, 8.1984129, 7.3696656). Notice that the orbit of (3.30) describing this state is not symmetric in the sense of proposition 3.3.4 although it is mapped into itself under R. This numerically obtained solution is used as an initial guess in Mathematica's implementation of Newton's method to determine the roots x_a^i of the set of equations

$$\sigma(x_i - \frac{\beta r x_i}{\beta + (x_i)^2}) - 1.5(x_{(i-1) \bmod 4+1} - 2x_i + x_{(i+1) \bmod 4+1}) \qquad i = 1, 2, 3, 4. \tag{3.52}$$

Although Mathematica can be instructed to find roots to an arbitrary precision, so far only floating point arithmetic was used so that none of the results are rigorous yet.

At this point all the quantities in the computations are redefined as intervals rather than floating point numbers and theorem 3.7.2 is applied to find an interval around each x_a^i in which the roots of equation (3.52) must lie. These bounds are now rigorous.

In sections 3.5 and 3.6 it was shown that a fixed state and all of its K-multiples are stable if the polynomial $p_{\mathcal{D}}(\lambda, t)$ corresponding to that state has roots with negative real part for all $t \in [0, \pi/2]$. Using interval arithmetic it is shown that

$$\begin{aligned}\bar{p}_{\mathcal{D}}(\lambda,t) =&\overline{3.61524} \times 10^{12} - \overline{5.02753} \times 10^{7} \cos 4t + (\overline{9.49583} \times 10^{11} - \overline{1.33199} \times 10^{7} \cos 4t)\, \lambda + \\ &(\overline{2.67802} \times 10^{11} - \overline{4.94338} \times 10^{6} \cos 4t)\, \lambda^2 + (\overline{4.90382} \times 10^{10} - \overline{771725} \cos 4t)\, \lambda^3 + \\ &(\overline{7.551} \times 10^{9} - \overline{144880} \cos 4t)\, \lambda^4 + (\overline{9.81388} \times 10^{8} - \overline{13673.3} \cos 4t)\lambda^5 + \\ &(\overline{1.03403} \times 10^{8} - \overline{1560.66} \cos 4t)\lambda^6 + (\overline{9.39525} \times 10^{6} - \overline{74.25} \cos 4t)\lambda^7 + \\ &(\overline{703005} - \overline{5.0625} \cos 4t)\lambda^8 + \overline{42026.7}\, \lambda^9 + \overline{2023.92}\, \lambda^{10} + \overline{66.6667}\lambda^{11} + \lambda^{12}\end{aligned} \tag{3.53}$$

for the fixed state under consideration.

In the next step the roots of the polynomial $\bar{p}_{\mathcal{D}}(\lambda, \frac{\pi}{2})$ are found. To employ Mathematica's implementation of Newton's method we need a polynomial with coefficients that are floating point numbers rather than intervals.Floating point numbers inside the intervals which determine the coefficients of the polynomial $\bar{p}_{\mathcal{D}}(\lambda, \frac{\pi}{2})$ can be chosen to define a polynomial $p^a_{\mathcal{D}}(\lambda, \frac{\pi}{2})$ which approximates $p_{\mathcal{D}}(\lambda, \frac{\pi}{2})$. The roots of $\{r^a_i\}_{i=1}^{12}$ of $p^a_{\mathcal{D}}(\lambda, \frac{\pi}{2})$ are now found using Newton's method.

Defining the roots $\{r^a_i\}_{i=1}^{12}$ theorem 3.7.1 can be employed next to provide complex intervals[4] inside which the roots of $\bar{p}_{\mathcal{D}}(\lambda, \frac{\pi}{2})$ must lie. The 4 real roots and 4 complex pairs obtained by this procedure are given in the table below.

$\overline{-18.481}$	$\overline{-0.2463 \pm i9.769}$
$\overline{-17.173}$	$\overline{-0.1961 \pm i9.317}$
$\overline{-15.437}$	$\overline{-0.1345 \pm i9.164}$
$\overline{-14.238}$	$\overline{-0.09054 \pm i8.622}$

Since interval arithmetic was used in these calculations, these estiamtes are now rigorous. The remainder of the argument shows that these roots will not cross the imaginary axis as t varies.

By lemma 3.6.3 the characteristic polynomial $p_{\mathcal{D}}(\lambda, t)$ takes the following form when evaluated on the imaginary axis:

$$\begin{aligned}p_{\mathcal{D}}(i\mu, t) &= \sum_{j=0, j \text{ even}}^{12} (\alpha_j + \beta_j \cos 4t)\mu^j(-1)^{\frac{j}{2}} + i \sum_{j=1, j \text{ odd}}^{11} (\alpha_j + \beta_j \cos 4t)\mu^j(-1)^{\frac{j-1}{2}} = \\ &= p^{\mathrm{R}}_{\mathcal{D}}(\mu, t) + i p^{\mathrm{I}}_{\mathcal{D}}(\mu, t)\end{aligned}$$

Since the roots of $p_{\mathcal{D}}(\lambda, t)$ depend continuously on the parameter t, if $p_{\mathcal{D}}(\lambda, t)$ has roots with positive real part for some t_1 then there must exist a t_0 such that $p_{\mathcal{D}}(\lambda, t_0)$ has a root on the imaginary axis. In other words there must exist a μ_0 such that

$$p^{\mathrm{R}}_{\mathcal{D}}(\mu_0, t_0) = p^{\mathrm{I}}_{\mathcal{D}}(\mu_0, t_0) = 0. \tag{3.54}$$

We will use interval arithmetic to show that this cannot happen. The polynomial $p_{\mathcal{D}}(\lambda, t)$ is split into a real and complex part to avoid using complex interval arithmetic in the numerical calculations since complex interval arithmetic leads to much rougher estimates than real interval arithmetic.

[4]There are several ways in which complex intervals can be defined. In this case we use regions of the form $\bar{z} = \bar{x} + i\bar{y}$ where $\bar{x}$ and $\bar{y}$ are real intervals. These are simply rectangular regions in $\mathbb{C}$.

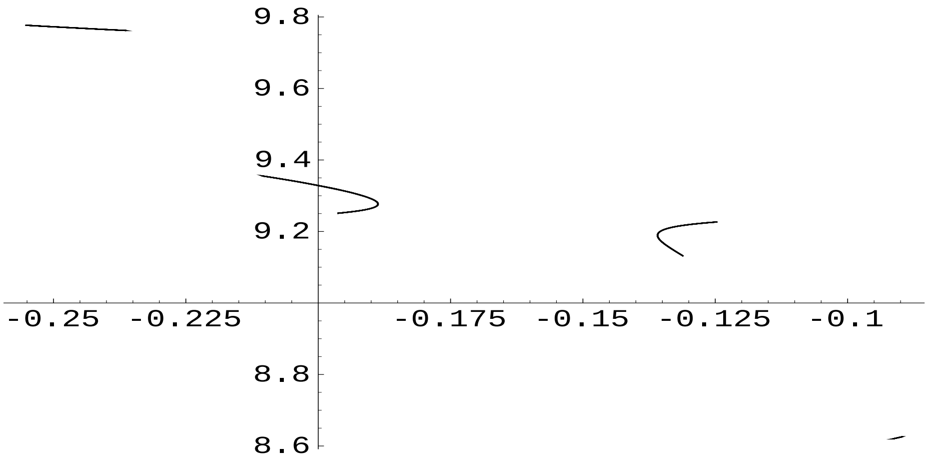

Figure 3.12: A numerical computation of the paths that the 8 complex eigenvalues with smallest real part trace out as t varies. Only one eigenvalue in the complex conjugate pair is shown. Notice the small trace of the eigenvalue with the least negative real part.

By Grešgorin's theorem the eigenvalues of the matrix $\mathcal{D}(t)$ lie in the union of discs $C_i = \{z : |z - \mathcal{D}_{ii}| < R_i\}$ where $\mathcal{D}_{ij}$ are the entries in the matrix $\mathcal{D}(t)$ and $R_i = \sum_{j=1, j\neq i}^{12} |\mathcal{D}_{ij}|$. A direct computation shows that the intersection of $\cup_{i=1}^{12} C_i$ with the imaginary axis is contained in the interval $[-17i, 17i]$ and it is therefore sufficient to show that $p_{\mathcal{D}}^{\mathrm{R}}(\mu, t_0)$ and $p_{\mathcal{D}}^{\mathrm{I}}(\mu, t_0)$ are not zero simultaneously for any value of t and $\mu \in [-17, 17]$.

Since the coefficients of $\bar{p}_{\mathcal{D}}(\lambda, t)$ are $\frac{\pi}{2}$ periodic in t, it is sufficient to show that (3.54) is not satisfied for any $\lambda \in [-17, 17]$ and $t \in [0, \frac{\pi}{2}]$. This is shown by subdividing these intervals into a sufficient number of subintervals $\bar{\mu}_n$ and $\bar{t}_m$ so that $[-17, 17] \subset \cup_{i=1}^{N} \bar{\mu}_n$ and $[0, \frac{\pi}{2}] \subset \cup_{m=1}^{M} \bar{t}_m$ with the property that the intervals $\bar{p}_{\mathcal{D}}^{\mathrm{R}}(\bar{\mu}_n, \bar{t}_m)$ and $\bar{p}_{\mathcal{D}}^{\mathrm{I}}(\bar{\mu}_n, \bar{t}_m)$ do not contain zero simultaneously for any given pair of subintervals $\bar{\mu}_n$ and $\bar{t}_m$. Therefore the roots of $p_{\mathcal{D}}(\lambda, t)$ stay in the left half plane for all $t \in \mathbb{R}$ and all K-multiples of the fixed state under consideration are also stable.

3.8 Another Criterion for Stability

The following method can sometimes be used to check directly how far a particular eigenvalue moves. Although this method frequently works for regular numerical calculations, it does not give sufficiently sharp bounds for interval arithmetic calculations. The eigenvalues of the matrix $\mathcal{D}(0)$ can be used as a first guess for the eigenvalues of $\mathcal{D}(t)$ for any other t. If the eigenvalues of $\mathcal{D}(t)$ don't move too far as t is varied and the other conditions of theorem 3.7.1 hold, applying the Newton-Raphson method with such an initial guess will give eigenvalues of $\mathcal{D}(t)$. The following corollary to theorem 3.7.1 and lemma 3.6.3 gives a precise meaning to these notions.

Corollary 3.8.1 *Let λ_k^0 be an eigenvalue of the matrix $\mathcal{D}(0)$. Define*

$$A_k = \sum_{i=0}^{3n} \alpha_i (\lambda_k^0)^i \qquad B_k = \sum_{i=0}^{3n} \beta_i (\lambda_k^0)^i \tag{3.55}$$

$$A_k' = \sum_{i=0}^{3n} i\alpha_i (\lambda_k^0)^{i-1} \qquad B_k' = \sum_{i=0}^{3n} i\beta_i (\lambda_k^0)^{i-1} \tag{3.56}$$

where α_i and $\beta_i$are as in lemma (3.6.3). Also define the disc $D_k = \{z : |z - \lambda_k^0| \leq |r_k|\}$ with radius $r_k = \frac{|A_k|+|B_k|}{|A_k'|-|B_k'|}$ and

$$M_k = \max_{t\in\mathbb{R},\lambda\in D_k} \left| \frac{\partial^2 p_{\mathcal{D}}(t,\lambda)}{\partial\lambda^2} \right|.$$

Then if $|A_k'| > |B_k'|$ and

$$2M_k \frac{|A_k| + |B_k|}{(|A_k'| - |B_k'|)^2} \leq 1 \tag{3.57}$$

and the disc D_k is contained in the left half of the complex plane then the matrix $\mathcal{D}(t)$ has one eigenvalue inside D_k for all t.

Proof: First notice that $\frac{\partial p_{\mathcal{D}}}{\partial\lambda} = \sum_{i=1}^{3n} i(\alpha_i + \beta_i \cos nt)\lambda^{i-1}$. Following the notation of theorem 3.7.1 this implies that

$$|h_k| = \left| \frac{p_{\mathcal{D}}(\lambda_k^0, t)}{\frac{\partial p_{\mathcal{D}}}{\partial\lambda}(\lambda_k^0, t)} \right| = \left| \frac{A_k + B_k \cos nt}{A_k' + B_k' \cos nt} \right| \leq \frac{|A_k| + |B_k|}{|A_k'| - |B_k'|} = r_k$$

when $|A_k'| > |B_k'|$. It follows that

$$M_k^0 = \max_{t\in\mathbb{R},\{z:|z-\lambda_k^0|\leq h_k\}} |\frac{\partial^2 p_{\mathcal{D}}}{\partial\lambda^2}(t,\lambda)| \leq \max_{t\in\mathbb{R},\lambda\in D_k} |\frac{\partial^2 p_{\mathcal{D}}}{\partial\lambda^2}(t,\lambda)| = M_k$$

A similar comparison leads to

$$\left| \frac{h_k}{\frac{\partial p_{\mathcal{D}}}{\partial\lambda}(\lambda_k^0, t)} \right| \leq \frac{|A_k| + |B_k|}{(|A_k'| - |B_k'|)^2}$$

so that if the assumption of the corollary holds we have

$$2\left| \frac{h_k}{\frac{\partial p_{\mathcal{D}}}{\partial\lambda}(\lambda_k^0, t)} \right| M_k^0 \leq 2M_k \frac{|A_k| + |B_k|}{(|A_k'| - |B_k'|)^2} \leq 1.$$

Since all these estimates are independent of t we can use theorem 3.7.1 to conclude that for every t the matrix $\mathcal{D}(t)$ has one root in the disc D_k which is by assumption in the left half of $\mathbb{C}$. $\diamondsuit$

Appendix A

Interval Arithmetic

Due to the physical restrictions of digital computing devices, all numerical computations are subject to roundoff error. This type of error is a consequence of the fact that numbers in a numerical calculation need to be approximated, or rounded off to fit within an allocated memory space. The errors that are produced by rounding off at each point of the calculation may accumulate in an unpredictable way, and thus the final result of a numerical computation may be far from the solution it is meant to approximate.

Even innocuous looking calculations may lead to severe roundoff errors.

Example A.0.2 Consider the following function proposed in [89], and analyzed in [90]

$$f(x,y) = 333.75y^6 + x^2(11x^2y^2 - y^6 - 121y^4 - 2) + 5.5y^8 + \frac{x}{2y} \tag{A.1}$$

Running a FORTRAN program to evaluate this expression at $x = 77617$ and $y = 33096$ single, double and extended precision, gives the following result

$$f(77617, 33096) \approx 6.33825 \times 10^{29} \qquad \text{single precision} \tag{A.2}$$

$$f(77617, 33096) \approx 1.1726039400532 \qquad \text{double precision} \tag{A.3}$$

$$f(77617, 33096) \approx 1.172603940053178631858834904520183 8 \qquad \text{extended precision} \tag{A.4}$$

A superficial examination of these results might suggest that the first result is wrong, while the second two correctly approximate the solution to at least 14 digits. However this is wrong since using interval arithmetic we can show that the correct result lies in

$$\begin{aligned}&[-0.827396059946821368141165095479816292005,\\ &\ -0.827396059946821368141165095479816291986]\end{aligned} \tag{A.5}$$

One way to monitor the accumulation of errors in numerical computations is the use of interval arithmetic. The idea behind this approach is simple: use intervals, rather then floating point numbers in computations. The usual binary operations $+, -, \times$ and $/$ may be defined on two intervals

$A = [a_1, a_2]$, and $B = [b_1, b_2]$ with $0 \notin B$ as follows

$$A + B = [a_1 + b_1, a_2 + b_2] \tag{A.6}$$
$$A - B = [a_1 - b_2, a_2 - b_1] \tag{A.7}$$
$$A \times B = [\min\{a_1b_1, a_1b_2, a_2b_1, a_2b_2\}, \max\{a_1b_1, a_1b_2, a_2b_1, a_2b_2\}] \tag{A.8}$$
$$A/B = [a_1, a_2] \times [1/b_2, 1/b_1]. \tag{A.9}$$

Similarly, any unary operator r on $\mathbb{R}$ can be extended to a unary operator on intervals by the following definition

$$r(X) = [\min_{x\in X} r(x), \max_{x\in X} r(x)] \tag{A.10}$$

The point of these definitions is that if $x \in X$, then $r(x) \in r(X)$, and similarly for the binary operations. This means that if we know an *approximation* to x, by using interval arithmetic we can find an interval in which $r(x)$ must lie.

When implementing these ideas care needs to be taken about the roundoff error that accumulates at the endpoints of the intervals used in the computations. This problem is resolved by using an interval rounding operation $\updownarrow$ which satisfies $X \subseteq \updownarrow X$, so that

$$r(x) \in r(X) \subseteq \updownarrow r(X) \tag{A.11}$$

and similarly for the binary operations defined in A.6.

If interval arithmetic is implemented in conjunction with an interval rounding operation $\updownarrow$, then it can be used to give *rigorous* estimates on the numerical values of functions that are constructed using the unary and binary operations defined on intervals.

All computations in chapter 3 were done using the interval arithmetic implementation of the software package Mathematica. Since some of the estimates are rather delicate, the calculations are done using intervals bounded by floating point numbers of very high precision. This was facilitated by the fact that Mathematica provides an environment in which floating point numbers, and hence intervals, of arbitrary precision can be used. When we say that the results obtained using interval arithmetic calculations are rigorous we assume that Mathematica reliably rounds these numbers. We also implicitly assume that the computer on which the calculations are performed conforms to IEEE floating point arithmetic standards.

Appendix B

Commented Code

The precision of the computation is set to sufficienly many digits for our purposes.

```
$MaxExtraPrecision = 10000
```

```
10000
```

```
$MinPrecision = 30
```

```
30
```

First we define a function and then we evaluate the different quantities for finding the box in which the solution lies.

```
ss = 10; bbb = 8 / 3; rrr = 27; ddd = 15 / 10;
```

The following function defines the fixed points in a chain of Lorenz equations.

```
x =.; y =.; z =.; s =.; b =.; rr =.; d =.
```

```
f[y_, x_, z_] = s * (x - (b * rr * x / (b + x^2))) - d * ( y - 2 * x + z)
```

$$s\left(x-\frac{b\,rr\,x}{b+x^2}\right)-d\,(-2\,x+y+z)$$

This function is without for the approximation of roots.

```
g[x_] = ss * (x - (bbb * rrr * x / (bbb + x^2)));
```

```
vars = {dd, aa, bb, cc, dd, aa};
```

Now we define the equations to find the roots to arbitrary precision. The output of the numerical simulations in XPP are used as initial guesses.

```
y1 = -6.4114408; y2 = 7.3696656; y3 = 8.1984129;  y4 = 7.3696656;
```

```
eqns = Table [ g[ vars[[ll + 1]] ] -
    ddd * (vars[[ll]] - 2 * vars[[ll + 1]] + vars[[ll + 2]]) == 0,
  {ll, 1, 4}];
```

```
aa =.; bb =.; cc =.; dd =.
```

Next we use these initial guesses to find the roots numerically. Kantorovich's Convergence Theorem will then be used to prove that the actual roots lie in a neighborhood of the roots that were computer numerically.

```
FindRoot[eqns, {aa, y1 - .1, y1 + .1}, {bb, y2 - .1, y2 + .1},
 {cc, y3 - .1, y3 + .1}, {dd, y4 - .1, y4 + .1}, WorkingPrecision -> 200,
 AccuracyGoal -> 40]

{aa →
  -6.41144895962609063033378992115043930980442556925220301120559935349677
    62078949762773535313218 90, bb →
  7.36967467926028811921120949733204156498618252799635571046602532793152 5
   7729866482251033402083677, cc →
  8.19842278174062083622079772643505125193255586829734718815990285085732 5
   0291363702658608188452422, dd →
  7.36967467926028811921120949733204156498618252799635571046602532793151 8
   9530924246929305218849158}

init = {aa, bb, cc, dd} /. %;

F[x_, y_, z_, w_] = {f[w, x, y], f[x, y, z], f[y, z, w], f[z, w, x]};
```

Now all the parameters are defined as intervals, so that interval arithmetic can be used in Kantorovich's theorem.

```
s = Interval[10]; b = Interval[N[8 / 3]]; rr = Interval[27];
d = Interval[15 / 10];

Feval = F[x1, x2, x3, x4];

x1 = Interval[init[[1]]]; x2 = Interval[init[[2]]];
x3 = Interval[init[[3]]];  x4 = Interval[init[[4]]];

f1 = D[f[x, y, z], x];

f2[y_] = D[f[x, y, z], y];

f3 = D[f[x, y, z], z];

M[x_, y_, z_, w_] =
{{f2[x], f3, 0, f1}, {f1, f2[y], f3, 0}, {0, f1, f2[z], f3},
{f3, 0, f1, f2[w]}};

Meval = M[x1, x2, x3, x4];

G = Inverse[M[x1, x2, x3, x4]];
```

The constants A, B and CC are defined as in Kantorovich's Theorem. The quantity 1/(A*CC) * (1 − Sqrt[1 − 2 A B CC) gives the maximum size of the box around each root. The extended precision used here will be essential in the second part of the calculations.

```
r[i_] := Sum[ Abs[G[[i, k]]], {k, 1, 4}];

q[i_] := Sum[ Abs[G[[i, k]] * Feval[[k]]], {k, 1, 4}]

A = Interval[Max[r[1], r[2], r[3], r[4]]];
```

```
A = Interval[Max[r[1], r[2], r[3], r[4]]];

B = Interval[Max[ q[1], q[2], q[3], q[4]]];

1 / (2 * A * B )

Interval[{2.812308362736921293080353669 41×10^29,
  2.812308362736921293080353669 46×10^29 }]

CC = Interval[10];

1 / (A * CC) * (1 - Sqrt[1 - 2 * A * B * CC])

Interval[{3.512765819222400629009824812 0×10^-29,
  3.512765819222400629009824812 2×10^-29 }]
```

If we can check the other estimates of Kantorovich’s Theorem, then 5 x 10^(−29) can be used as the size of the box in which the roots are guaranteed to lie. Since the second derivatives of f_i with respect to x_i are the only non−zero second derivatives, it is sufficient to check that each of them is less than CC = 10 in absolute value at all points in the rectangular region R around each root (see theorem 3.7.2).

```
box = Interval[{-5 * 10 ^ (-29), 5 * 10 ^ (-29)}];

xx1 = x1 + box; xx2 = x2 + box;
xx3 = x3 + box; xx4 = x4 + box;

D2f[y_] = D[f[x, y, z], {y, 2}];

D2f[xx1]

Interval[{3.644224259045301830154854448 1,
  3.644224259045301830154854452 3}]

D2f[xx2]

Interval[{-2.656844179221995648020980527 86,
  -2.656844179221995648020980525 27}]

D2f[xx3]

Interval[{-2.048540450746366134007135360 22,
  -2.048540450746366134007135358 45}]
```

```
D2f[xx4]

Interval[{-2.65684417922199564802098052786,
  -2.65684417922199564802098052527}]
```

This shows that the right hand side of equation (3.53) is less than CC so that the Kantorovich theorem can be applied

Now we use the above approximations to find the characteristic polynomial

First we define the matrix D(t) of equation (3.41).

```
g[x_] = -Interval[10]
   (x - Interval[27] * (x / ((Interval[3 / 8]) * x^2 + Interval[1])));

s = 10; rr = 27; b = 8 / 3; d = 15 / 10;

z = rr * x^2 / (b + x^2);

y = rr * x / (1 + x^2 / b);

M[x_] = {{-s, s, 0}, {rr - z, -1, -x}, {y, x, -b}};

dat2 = {xx1, xx2, xx3, xx4};

Mdat2 = Table [If[ IntegerPart[(i - 1) / 3] == IntegerPart[(j - 1) / 3],
    M[dat2[[IntegerPart[(i - 1) / 3] + 1]]][[Mod[i - 1, 3] + 1,
      Mod[j - 1, 3] + 1]], 0],
   {i, 1, 12},
   {j, 1, 12}];

Lapexp = Table[Switch[i - j, 0, If[Mod[i - 1, 3] == 0, -2, 0],
    3, If[Mod[i - 1, 3] == 0, Exp[-I * t], 0], -3,
    If[Mod[i - 1, 3] == 0, Exp[ I * t], 0], _, 0], {i, 12},
   {j, 12}];

Lapexp[[1, 10]] = Exp[-I * t]; Lapexp[[10, 1]] = Exp[I * t];

MMexp = Mdat2 + d * Lapexp;
```

The matrix MMexp is exactly the matrix D(t) of equation (3.41). Next we calculate its characteristic polynomial. Since this is a 12 x 12 matrix, and the calculations involve interval arithmetic, Laplace expansion was used to reduce the problem to a simpler one.

```
L = MMexp - x * IdentityMatrix[12];
```

```
poly[x_, t_] = Collect[ Det[L[[{1, 2, 3}, {1, 2, 3}]]] *
    Det[L[[Range[4, 12], Range[4, 12]]]] - d * Exp[I * t] *
(L[[2, 1]] * Det[L[[Range[3, 12], Join [{2, 3}, Range[5, 12]]]]] -
      L[[2, 2]] *
       Det[L[[Range[3, 12], Join [{1, 3}, Range[5, 12]]]]] +
L[[2, 3]] * Det[L[[Range[3, 12], Join [{1, 2}, Range[5, 12]]]]]) -
d * Exp[-I * t] *
(L[[2, 1]] * Det[L[[Range[3, 12], Join [Range[2, 9], {11, 12}]]]] -
      L[[2, 2]] *
       Det[L[[Range[3, 12], Join [{1}, Range[3, 9], {11, 12}]]]] +
L[[2, 3]] * Det[
        L[[Range[3, 12], Join [{1, 2}, Range[4, 9], {11, 12}]]]]),
  x];
```

Next we find the approximate eigenvalues of the matrix at t = Pi/4 and use the theorem for the proof of convergence of Newton's Method (Theorem 3.7.1) again to show that these are close to the real eigenvalues.

```
dat = {init[[1]], init[[2]], init[[3]], init[[4]]};

Mdat = Table [If[ IntegerPart[(i - 1) / 3] == IntegerPart[(j - 1) / 3],
   M[dat[[IntegerPart[(i - 1) / 3] + 1]]][[Mod[i - 1, 3] + 1,
     Mod[j - 1, 3] + 1]], 0],
  {i, 1, 12},
  {j, 1, 12}];

MMe = Mdat + d * Lapexp;

p[x_, t_] = Collect[Det[MMe - IdentityMatrix[12] * x], x];
```

Here we set the time at which we are taking the evaluation

```
t0 = Pi / 4;

NSolve[p[x, t0] == 0, x, 16]

Solve::precsm : Requested precision 16 is smaller than
   $MinPrecision. Using $MinPrecision instead.

{{x → -18.04851457073983489059505},
 {x → -17.85276301082035742023899},
 {x → -14.84351653534664076641148},
 {x → -14.58678139981675285800251},
 {x → -0.236280433991687957594723 - 9.762133833916483712969365 I},
 {x → -0.236280433991687957594723 + 9.762133833916483712969365 I},
 {x → -0.21061402735642356995119 - 9.35543612222739675259584 I},
 {x → -0.21061402735642356995119 + 9.35543612222739675259584 I},
 {x → -0.13104809857289500694540 - 9.13125586929224329215367 I},
 {x → -0.13104809857289500694540 + 9.13125586929224329215367 I},
 {x → -0.089603015050533831218001 - 8.625996722981923747236634 I},
 {x → -0.089603015050533831218001 + 8.625996722981923747236634 I}}
```

These are the approximate eigenvalues at t= Pi/4. The real parts are all negative. Next we use theorem 3.7.1 to show rigorously that there is a rectangle around each of these approximate roots which must contain a real root.

```
roots = x /. %;

General::spell1 : Possible spelling error: new symbol
   name "roots" is similar to existing symbol "Roots".

pp[x_, t_] = D[p[x, t], x];
polyp[x_, t_] = D[poly[x, t], x];
polypp[x_, t_] = D[polyp[x, t], x];
polyppp[x_, t_] = D[polypp[x, t], x];
```

Next we define the function hh which is equivalent to the function h in theorem 3.7.1. We need this function to verify that the roots that we obtained are actual roots. The function that will actually be used is the function hh below. Some manipulation of the equations was necessary to put them in a form appropriate for our purposes. In particular cf, cfp, cfpp, and cfppp denote the coefficients of the characteristic polynomial and its first three derivatives respectively.

```
h[i_] := Abs[poly[roots[[i]], t0]] / Abs[polyp[roots[[i]], t0]]
cff = CoefficientList[poly[x, 0], x];
cfb = Coefficient[
  ExpToTrig[CoefficientList[poly[x, t], x]], Cos[4 * t]];
cfa = cff - cfb;
cf = cff - cfb + cfb * Cos[4 * t0];
cfpf = CoefficientList[polyp[x, 0], x];
cfpb = Coefficient[
  ExpToTrig[CoefficientList[polyp[x, t], x]], Cos[4 * t]];
cfpa = cfpf - cfpb;
cfp = cfpf - cfpb + cfpb * Cos[4 * t0];
cfppf = CoefficientList[polypp[x, 0], x];
cfppb = Coefficient[
  ExpToTrig[CoefficientList[polypp[x, t], x]], Cos[4 * t]];
cfpp = cfppf - cfppb + cfppb * Cos[4 * t0];
cfppch[t_] := cfppf - cfppb + cfppb * Cos[4 * t];
cfppp = CoefficientList[polyppp[x, Pi], x];
powers[x_] = {1, x, x^2, x^3,
  x^4, x^5, x^6, x^7, x^8, x^9, x^10, x^11, x^12};
powersp[x_] =
 {1, x, x^2, x^3, x^4, x^5, x^6, x^7, x^8, x^9, x^10, x^11};
powerspp[x_] =
 {1, x, x^2, x^3, x^4, x^5, x^6, x^7, x^8, x^9, x^10};
powersppp[x_] =
 {1, x, x^2, x^3, x^4, x^5, x^6, x^7, x^8, x^9};
chr[z_] := Re[powerspp[z]];
chi[z_] := Im[powerspp[z]];
rl[i_] := Re[powers[roots[[i]]]];
rlp[i_] := Re[powersp[roots[[i]]]];
rlpp[i_] := Re[powerspp[roots[[i]]]];
rlppp[i_] := Re[powersppp[roots[[i]]]];
img[i_] := Im[powers[roots[[i]]]];
imgp[i_] := Im[powersp[roots[[i]]]];
imgpp[i_] := Im[powerspp[roots[[i]]]];
imgppp[i_] := Im[powersppp[roots[[i]]]];
ABS[i_] := Sqrt[(rl[i] . cf)^2 + (img[i] . cf)^2]
ABSP[i_] := Sqrt[(rlp[i] . cfp)^2 + (imgp[i] . cfp)^2]
ABSPP[i_] := Sqrt[(rlpp[i] . cfpp)^2 + (imgpp[i] . cfpp)^2]
hh[i_] := ABS[i] / ABSP[i]
rts[i_] := Re[roots[[i]]] + Interval[{-Max[hh[i]], Max[hh[i]]}] +
  I * (Im[roots[[i]]] + Interval[{-Max[hh[i]], Max[hh[i]]}])
ABSPPch[z_, t_] :=
 Sqrt[(chr[z] . cfppch[t])^2 + (chi[z] . cfppch[t])^2]
```

The value of hh determines the box in which the root is located. We now need to verify the inequalities
in theorem 3.7.1. to show that the root really lies in this box. The functions rll.., imll give the real, respectively imaginary part of the powers of the roots. ABSPP2 denotes the value of the second derivative in the rectangle K_0. By theorem 3.7.1, it is sufficient that chk[i] <1 for all roots rts_i.

```
While[(int = int + 0.1) < Pi / 2,
tt = Interval[{int - 0.1, int}];
cf2 =
  cff - cfb + cfb * Cos[4.000000000000000000000000000000000000000000000 * tt];
cfeven = Table[cf2[[i]] * (-1) ^ ((i - 1) / 2), {i, 1, 13, 2}];
cfodd = Table[cf2[[i]] * (-1) ^ ((i - 2) / 2), {i, 2, 12, 2}];
poly1 =.; poly2 =.;
poly1[x_] := cfeven . powerseven[x];
poly2[x_] := cfodd . powersodd[x];
f = -17;
While[(f = f + 0.001) < -11,
If[Sign[Min[poly2[Interval[{f, f + 0.001}]]]] =!=
     Sign[Max[poly2[Interval[{f, f + 0.001}]]]] &&
    Sign[Min[poly1[Interval[{f, f + 0.001}]]]] =!=
     Sign[Max[poly1[Interval[{f, f + 0.001}]]]],
Print[Interval[{f, f + 0.001}]]]]]

int = 0;

While[(int = int + 0.1) < Pi / 2,
tt = Interval[{int - 0.1, int}];
cf2 =
  cff - cfb + cfb * Cos[4.000000000000000000000000000000000000000000000 * tt];
cfeven = Table[cf2[[i]] * (-1) ^ ((i - 1) / 2), {i, 1, 13, 2}];
cfodd = Table[cf2[[i]] * (-1) ^ ((i - 2) / 2), {i, 2, 12, 2}];
poly1 =.; poly2 =.;
poly1[x_] := cfeven . powerseven[x];
poly2[x_] := cfodd . powersodd[x];
f = -7;
While[(f = f + 0.001) < -0,
If[Sign[Min[poly2[Interval[{f, f + 0.001}]]]] =!=
     Sign[Max[poly2[Interval[{f, f + 0.001}]]]] &&
    Sign[Min[poly1[Interval[{f, f + 0.001}]]]] =!=
     Sign[Max[poly1[Interval[{f, f + 0.001}]]]],
Print[Interval[{f, f + 0.001}]]]]]

int = 0;

While[(int = int + 0.05) < Pi / 2 + 0.05,
tt = Interval[{int - 0.05, int}];
cf2 =
  cff - cfb + cfb * Cos[4.000000000000000000000000000000000000000000000 * tt];
cfeven = Table[cf2[[i]] * (-1) ^ ((i - 1) / 2), {i, 1, 13, 2}];
cfodd = Table[cf2[[i]] * (-1) ^ ((i - 2) / 2), {i, 2, 12, 2}];
poly1 =.; poly2 =.;
poly1[x_] := cfeven . powerseven[x];
poly2[x_] := cfodd . powersodd[x];
f = -8.3;
While[(f = f + 0.0001) < -7,
If[Sign[Min[poly2[Interval[{f, f + 0.0001}]]]] =!=
     Sign[Max[poly2[Interval[{f, f + 0.0001}]]]] &&
    Sign[Min[poly1[Interval[{f, f + 0.0001}]]]] =!=
     Sign[Max[poly1[Interval[{f, f + 0.0001}]]]],
Print[Interval[{f, f + 0.0001}]]]]]
```

These three computations show that there are no roots in the intervals [−17, −11] and [−8.3,0]. These are the quickest compuations since all the roots are relatively far from these intervals, and thus a coarse subdivision of the intervals is sufficient. Next we check the interval [−11, 8.3]. We start with [−11, −10.2].

```
int = 0;

While[(int = int + 0.01) < Pi / 2 + 0.01,
tt = Interval[{int - 0.01, int}];
cf2 =
  cff - cfb + cfb * Cos[4.000000000000000000000000000000000000000000000 * tt];
cfeven = Table[cf2[[i]] * (-1) ^ ((i - 1) / 2), {i, 1, 13, 2}];
cfodd = Table[cf2[[i]] * (-1) ^ ((i - 2) / 2), {i, 2, 12, 2}];
poly1 =.; poly2 =.;
poly1[x_] := cfeven . powerseven[x];
poly2[x_] := cfodd . powersodd[x];
f = -11;
While[(f = f + 0.000001) < -9.28,
If[Sign[Min[poly2[Interval[{f, f + 0.000001}]]]] =!=
     Sign[Max[poly2[Interval[{f, f + 0.000001}]]]] &&
    Sign[Min[poly1[Interval[{f, f + 0.000001}]]]] =!=
     Sign[Max[poly1[Interval[{f, f + 0.000001}]]]],
Print[Interval[{f, f + 0.000001}]]]]]
```

There is another rough spot in [−9.28, −9.2], and an even finer subdivision is needed.

```
int = 0;

While[(int = int + 0.01) < Pi / 2 + 0.01,
tt = Interval[{int - 0.01, int}];
cf2 =
  cff - cfb + cfb * Cos[4.000000000000000000000000000000000000000000000 * tt];
cfeven = Table[cf2[[i]] * (-1) ^ ((i - 1) / 2), {i, 1, 13, 2}];
cfodd = Table[cf2[[i]] * (-1) ^ ((i - 2) / 2), {i, 2, 12, 2}];
poly1 =.; poly2 =.;
poly1[x_] := cfeven . powerseven[x];
poly2[x_] := cfodd . powersodd[x];
f = -9.28;
While[(f = f + 0.0000001) < -9.2,
If[Sign[Min[poly2[Interval[{f, f + 0.0000001}]]]] =!=
     Sign[Max[poly2[Interval[{f, f + 0.0000001}]]]] &&
    Sign[Min[poly1[Interval[{f, f + 0.0000001}]]]] =!=
     Sign[Max[poly1[Interval[{f, f + 0.0000001}]]]],
Print[int]; Print[Interval[{f, f + 0.0000001}]]; Break[]]]]
```

We check the interval [−9.2,−8.3] next. This completes the calculations.

```
int = 0;
```

```
While[(int = int + 0.01) < Pi / 2 + 0.01,
Print[int];
tt = Interval[{int - 0.01, int}];
cf2 =
  cff - cfb + cfb * Cos[4.000000000000000000000000000000000000000000000 * tt];
cfeven = Table[cf2[[i]] * (-1) ^ ((i - 1) / 2), {i, 1, 13, 2}];
cfodd = Table[cf2[[i]] * (-1) ^ ((i - 2) / 2), {i, 2, 12, 2}];
poly1 =.; poly2 =.;
poly1[x_] := cfeven . powerseven[x];
poly2[x_] := cfodd . powersodd[x];
f = -9.2;
While[(f = f + 0.000001) < -8.3,
If[Sign[Min[poly2[Interval[{f, f + 0.000001}]]]] =!=
     Sign[Max[poly2[Interval[{f, f + 0.000001}]]]] &&
    Sign[Min[poly1[Interval[{f, f + 0.000001}]]]] =!=
     Sign[Max[poly1[Interval[{f, f + 0.000001}]]]],
Print[int]; Print[Interval[{f, f + 0.000001}]]; Break[]]]];
```

Bibliography

[1] V.S. Afraimovich, N.N. Verichev, and M.I. Rabinovich, "Stochastic Synchronization of Oscillations in Dissipative Systems," Radio Phys. and Quantum Electron. **29,** 747 – 751 (1986).

[2] H. Fujisaka and T. Yamada, "Stability Theory of Synchronized Motion in Coupled Oscillator Systems," Prog. Theor. Phys. **69,** 32 – 47 (1983).

[3] M. Hasler, Yu. Maistrenko and O. Popovych, "Simple Example of Partial Synchronization of Chaotic Systems," Phys. Rev. E **58,** 6843 – 6846 (1998).

[4] L.M. Pecora and T.L. Carroll, "Synchronization in Chaotic Systems," Phys. Rev. Lett. **64,** 821 – 824 (1990).

[5] L.M. Pecora and T.L. Carroll, "Driving Systems with Chaotic Signals", Phys. Rev. A **44,** 2374 – 2383 (1992).

[6] M.M. Sushchik, N.F. Rulkov, and H.D.I. Abarbanel, "Robustness and Stability of Synchronized Chaos: An Illustrative Model", IEEE Trans. Circ. and Sys. I, **44,** 867–873 (1997).

[7] H.D.I. Abarbanel, N.F. Rulkov, and M. Sushchik, "Generalized Synchronization of Chaos: The Auxiliary Approach," Phys. Rev. E **53,** 4528 – 4535 (1996).

[8] L. Kocarev and U. Parlitz, "Generalized Synchronization, Predictability, and Equivalence of Unidirectionally coupled dynamical systems," Phys. Rev. Lett. **76,** 1816 –1819 (1996).

[9] J. Hale, "Diffusive Coupling, Dissipation, and Synchronization," J. Dyn. and Diff. Eq. **9,** 1 – 52 (1997).

[10] T. Ushio, "Chaotic Synchronization and Controlling Chaos Based on Contraction Mappings," Phys. Lett. A **198,** 14 – 22 (1995).

[11] M.G. Rosenblum, A.S. Pikovsky, and J. Kurths, "Phase Synchronization of Chaotic Oscillators," Phys. Rev. Lett. **76,** 1804 – 1807 (1996).

[12] L.O. Chua and M. Itoh, "Chaos Synchronization in Chua's Circuit," J. Circ. Syst. Comput. **3,** 93 – 108 (1993).

[13] R. Roy and K. S. Thornburg Jr., in press.

[14] R. E. Mirollo and S. H. Strogatz, "Synchronization of Pulse-Coupled Biological Oscillators," SIAM J. Appl. Math. **50,** 1645 – 1662 (1990).

[15] S. Watanabe, H.S.J. van der Zant, S.H. Strogatz, and T.P. Orlando, preprint (1995).

[16] R. Huerta, M. Bazhenov, and M.I. Rabinovich, "Clusters of Synchronization and Bistability in Lattices of Chaotic Neurons," Europhy. Lett. **43,** 719–724 (1998).

[17] A. Maybhate and R.E. Amritkar, "Use of Synchronization and Adaptive Control in Parameter Estimation from a Time Series," Phys. Rev. E **59,** 284 – 293 (1999).

[18] K. Pyragas "Continuous Control of Chaos by Self-Controlling Feedback," Phys. Lett A **170,** 421 – 428 (1992).

[19] K. Pyragas, "Predictable Chaos in Slightly Perturbed Unpredictable Chaotic Systems," Phys. Lett. A **181,** 203 – 210 (1993).

[20] C. Tresser, P. Worfolk, and H. Bass,"Master Slave Synchronization From the Point of View of Global Dynamics," Chaos **5,** 693 – 699 (1995).

[21] L.M. Pecora, et al. "Fundamentals of Synchronization in Chatoic Systems, Concepts and Applications," Chaos **7,** 520 –543 (1997).

[22] K.M. Short,"Steps Toward Unmasking Secure Communications," Int. J. Bifurcations Chaos **4,** 959 (1994).

[23] Blekhman, I.I. *Synchronization in Science and Engineering,* Nauka (1981).

[24] G.B. Ermentrout, "$n : m$ Phase-Locking of Weakly Coupled Oscillators," J. Math. Biology **12** 327 – 342 (1981).

[25] A. Katok and B.Hassleblatt, *Introduction to the Modern Theory of Dynamical Systems,* Cambridge Press (1997).

[26] N.F. Rulkov,"Images of Synchronized Chaos: Experiments with Circuits," Chaos **6,** 262 – 278 (1996).

[27] A.S. Pikovsky, et. al. "Phase Synchronization of Chaotic Oscillators by External Driving," Physica D **104,** 219 – 238 (1997).

[28] A.S. Pikovsky, et. al. "Phase Synchronization of Chaotic Oscillations in Terms of Periodic Orbits," Chaos **7,** 680 – 687 (1997).

[29] H.D.I. Abarbanel, et. al. "Synchronized Action of Synaptically Coupled Chaotic Neurons," Neural Comp. **8,** 1567 – 1602 (1996).

[30] R.C. Elson, et. al. "Synchronous Behavior of Two Coupled Biological Neurons," to appear in Phys. Rev. Lett. (1998).

[31] C. Tresser, P. Worfolk, and H. Bass, "Master-Slave Synchronization from the Point of View of Global Dynamics," Chaos **5,** 693–699 (1995).

[32] J.F. Heagy, T.L. Carroll and L.M. Pecora, "Synchronous Chaos in Coupled Oscillator Systems," Phys. Rev. E **50,** 1874 – 1885 (1994).

[33] C. Sparrow, *The Lorenz Equations: Bifurcations, Chaos, and Strange Attractors,* Springer-Verlag (1982).

[34] W. Hahn,*Stability of Motion,* Springer Verlag (1967).

[35] I.U. Bronstein and A. Ya. Kopanskii, *Smooth Invariant Manifolds and Normal Forms,* World Scientific (1994).

[36] S. Wiggins, *Normally Hyperbolic Invariant Manifolds in Dynamical Systems,* Springer–Verlag, (1994).

[37] M. Spivak, *A Comprehensive Introduction to Differntial Geometry,* Publish or Perish, Inc. (1979).

[38] N. Fenichel, "Persistence and Smoothness of Invariant Manifolds for Flows," Indiana Univ. Math. J. bf 21, 193 – 226 (1971).

[39] N. Fenichel, "Asymptotic Stability with Rate Conditions," Indiana Univ. Math. J. **23,** 1109 – 1137 (1974).

[40] N. Fenichel, "Asymptotic Stability with Rate Conditions II," Indiana Univ. Math. J. **26,** 87 –93 (1974).

[41] N. Fenichel, "Geometric Singular Perturbation Theory for Ordinary Differential Equations," J. Diff. Eqn. **31,** 53–98 (1979).

[42] R. Sacker, "A Perturbation Theorem for Invariant Manifolds and Hölder Continuity," J. Math. Mech. **18,** 705 – 762 (1969).

[43] J. Jarnik and J.Kurzweil, "On Invariant Sets and Invariant Manifolds of Differential Systems," J. Diff. Eq. **6,** 247 – 263 (1969).

[44] R. Mañé,"Persistent Manifolds are Normally Hyperbolic," Trans. Am. Math. Soc. **246,** 261–283 (1978).

[45] R. Abraham, J.E. Marsden, and T. Ratiu, *Manifolds, Tensor Analysis, and Applications,* Addison-Wesley Publishing Co. (1983).

[46] S-N. Chow, and W. Liu, "Synchronization, Stability and Normal Hyperbolicity," Resenhas IME-USP **3,** 139–158 (1997).

[47] K. Josić, "Invariant Manifolds and Synchronization of Coupled Dynamical Systems", Phys. Rev. Lett. **80** 3053–3057 (1998).

[48] J.R. Terry, et. al., "Synchronization of Chaos in an Array of Three Lasers," to appear in Phys. Rev. E.

[49] J.R. Terry, private communication.

[50] P.Ashwin, J. Buescu, and I. Stewart, "From Attractor to Chaotic Saddle: a Tale of Transverse Instability," Nonlinearity **9,** 703 – 737 (1996).

[51] P. Ashwin, J. Buescu, and I. Stewart "Bubbling of Attractors and Synchronisation of Chaotic Oscillators," Phys. Lett. A **193,** 126 – 139 (1994).

[52] B. Hunt, and E. Ott, "Optimal Periodic Orbits of Chaotic Systems," Phys. Rev. Lett. **76,** 2254–2258 (1996).

[53] B. Hunt, and E. Ott, "Optimal Periodic Orbits of Chaotic Systems Occur at Low Period," Phys. Rev. E **54,** 328–337 (1996).

[54] B. Hunt, private communication.

[55] G. Baker, J.A. Blackburn, and J.H.T. Smith, "Intermittent Synchronization in a Pair of Copuled Chaotic Pendula," Phys. Rev. Lett. **81,** 554 - 558 (1998).

[56] A. Stefanski, et. al. "Torus On-Off Intermittency in Coupled Lorenz Systems," Phys. Rev. E **57,** 1175 – 1178 (1998).

[57] D. Gauthier, and J. Bienfang, "Intermittent Loss of Synchronization in Coupled Chaotic Oscillators: Toward a New Criterion for High-Quality Synchronization," Phys. Rev. Lett. **77,** 1751 – 1754 (1996).

[58] R. Brown, and F. Rulkov, "Synchronization of Chaotic Systems: Transversal Stability of Trajectories in Invariant Manifolds," Chaos **7,** 395 – 413 (1996).

[59] J. Hale *Ordinary Differential Equations,* Robert E. Krieger Publishing Co. (1969).

[60] J. Blakely, et. al. "Bursting and Synchronization Criteria in Coupled Oscillators," to appear in Phys. Rev. Lett. (1999).

[61] B. Hunt, E. Ott, and J. Yorke, "Differentiable Generalized Synchronization of Chaos," Phys. Rev. E. **55,** 4029 – 4034 (1997).

[62] J.L. Kaplan, J. Mallet-Paret, and J. Yorke, "The Lyapunov Dimension of a Nowhere Differentiable Torus," Ergod. Th. & Dynam. Sys. **4,** 261–281 (1984).

[63] A. Delshams, R. de la Llave, and T. M. Seara, "A Geometric Approach to the Existence of Orbits with Unbounded Energy in the Generic Periodic Perturbations by a Potential of Generic Geodesic Flow of $\mathbb{T}^2$," preprint.

[64] M.W. Hirsch, C.C. Pugh, and M. Shub, *Invariant Manifolds,* Lecture Notes in Mathematics, vol. **583,** Springer Verlag (1977).

[65] I.U. Bronštein, *Extensions of Minimal Transformation Groups,* Sijthoff & Noordhoff (1979).

[66] I.U. Bronshteyn, private communication.

[67] U. Parlitz, L. Junge, and Lj. Kocarev, "Subharmonic Entrainment of Unstable Periodic Orbits and Generalized Synchronization," Phys. Rev. Lett. **79** 3158 – 3161 (1997).

[68] E. Ott, C. Grebogi, and J. Yorke, "Controlling Chaos," Phys. Rev. Lett. **64,** 1196 – 1199 (1990).

[69] M.G. Rosenblum, A.S. Pikovsky, and J. Kurths, "From Phase to Lag Synchronisation in Coupled Chaotic Oscillators," Phys. Rev. Lett. **78,** 4193 – 4196 (1997).

[70] D.Y. Tang, et. al. "Stages of Chaotic Synchronization," Chaos **8,** 697 – 701 (1998).

[71] L.M. Pecora, "Synchronous Conditions and Desynchronizing Patterns in Coupled Limit-Cycle and Chaotic Systems," Phys. Rev. E **58,** 347 – 359 (1998).

[72] V.S. Afraimovich, S-N. Chow, and J.K. Hale "Synchronization in Lattices of Coupled Oscillators," Physica D **103,** 442 –451 (1997).

[73] V.S. Afraimovich, S-N Chow, "Topological Spatial Chaos and Homoclinic Points of $\mathbb{Z}^d$-Actions in Lattice Dynamical Systems," Japan J. of Ind. and Appl. Math **12,** 367–383 (1995).

[74] V.S. Afraimovich, S-N Chow, "Hyperbolic Homoclinic Point of $\mathbb{Z}^d$-Actions in Lattice Dynamical Systems," Int. J. of Bif. and Chaos" **6,** 1059 – 1075 (1996).

[75] V.S. Afraimovich, et. al. *Stability, Structures and Chaos in Nonlinear Synchronization Networks*, World Scientific (1994).

[76] V.S. Afraimovich and W-W. Lin, "Synchronization in Lattices of Coupled Oscillators with Neumann/Periodic Boundary Conditions," preprint

[77] M.I. Rabinovich, private communication (1999).

[78] D.G. Aronson, G.B. Ermentrout and N. Kopell, "Amplitude Response of Coupled Oscillators," Physica D **41,** 403–449 (1990).

[79] L. Bunimovich, "Coupled map lattices: one step forward and two steps back," Physica D **86,** 248–255 (1995).

[80] L. Bunimovich and Ya.G. Sinai, "Space-time Chaos in Coupled Map Lattices," Nonlinearity **1** 491–516 (1988).

[81] A.N. Carvalho, H.M. Rodrigues, and T. Dlotko, "Upper Semicontinuity of Attractors and Synchronization," J. of Math. Anal. and App. **218** (1997).

[82] R.L. Devaney, "Homoclinic Bifurcations and the Area-Conserving Hénon Mapping," J. Diff. Eq. **51** 254 -266 (1984).

[83] G.B. Ermentrout and N. Kopell, "Oscillator Death in Systems of Coupled Neural Oscillators," SIAM J. Appl. Math. **50,** 125–146 (1990).

[84] R.A. Horn and C.R. Johnson, *Matrix Analysis*, Cambridge University Press, 1985.

[85] J. Moser, "Proof of a Generalized Form of a Fixed Point Theorem Due to G.D. Birkhoff," preprint.

[86] A.M. Ostrowski, *Solutions of Equations and Systems of Equations*, Academic Press (1960).

[87] D.R. Orendovici, Ya. B. Pesin, Chaos in Traveling Waves of Lattice Systems of Unbounded Media, preprint.

[88] C.K.R.T. Jones, "Geometric Singural Perturbation Theory," Lecture Notes in Mathematics, vol. **1609,** 44 – 118 (1994).

[89] S.M. Rump, *Reliability in Computing: The Role of Interval Methods in Scientific Computing,* Academic Press (1988).

[90] A.P. Leclerc, "Should We be Concerned about Roundoff Error?", WWW address: *http://stono.cs.cofc.edu/ leclerc/math_tech_HTML/math_tech_HTML.html* (1996).

Vita

Krešimir Josić was born on November 24, 1971 in Pula, Croatia. Soon thereafter he was taken on a tour of Europe that included longer stops at Zagreb and Berlin. The fun ended with the beginning of the Reagan era, when he was forced to start attending school. Somehow he never managed to extricate himself from the predicament of being a student ever since. He finished high school in Barrington, R.I. and graduated from the University of Texas at Austin with a B.Sc. degrees in mathematics and physics, and was conducting graduate studies at The Pennsylvania State University from 1994 until 1999. He was rescued from the doldrums of State College in 1998, by a bold move of his advisor.

Krešo is fond of music, theater, film, and good food. He has also been known to torment people in his immediate vicinity by playing the bass.